POLITECNICO DI TORINO

Master Degree course in Engineering and Management

Techno-Economic Analysis of the Valorization of Products Obtained by Low-Temperature Pyrolysis

Advisor:
Prof. Eng. Paolo Maria Tronville
Co-advisor:
Prof. Eng. Murilo Daniel de Mello Innocentini

Thesis of:
Sveva Loddo

Academic Year: 2025-2026

Abstract

The increasing need for sustainable waste management has increased interest in the valorization of agro-industrial residues. A wide range of biomass are available, including forestry and agricultural residues and food-processing wastes such as coconut husk, pine wood chips, orange peel, ginger residues, sugarcane bagasse, green coffee and coffee cherry husk. Within this context, this thesis focuses on spent coffee grounds (SCGs) due to their large accessibility and favorable chemical composition. Using an integrated experimental and techno-economic approach, this work explores the pyrolysis of SCGs as a route for the production of bio-oil, with biochar obtained as a valuable byproduct. Pyrolysis experiments were carried out to determine mass balances and products yields, and they showed bio-oil and biochar yield of approximately 37% and 30%, respectively. The bio-oil was chemically characterized through antioxidant activity, total phenolic content, pH measurement, thermogravimetric analysis, and chromatographic analysis. In particular, the chemical characterization revealed an interesting mixture of compounds, including organic acids (acetic, formic, and butyric acid), ketones and esters (acetone, ethyl acetate, diacetyl), furanic and sugar-derived compounds (furfural and levoglucosan), phenolic compounds (phenol, guaiacol, ethyl guaiacol, ethylphenol, catechol, syringol, and isovanillin), and nitrogen-containing species such as caffeine. These compounds have applications as industrial solvents, chemical intermediates, antioxidants, flavoring agents, and bio-based platform chemicals. These experimental results put the base for the techno-economic analysis, which was developed to evaluate the feasibility of the process under two valorization scenarios. The baseline scenario considers the direct commercialization of bulk bio-oil, along with the obtained biochar; on the other hand, the more advanced scenario identifies and evaluates each single compound composing the bio-oil, alongside with the biochar. The economic performance was assessed using indicators such as unit production cost, profit per kilogram of product, operating margin, and payback period. Results show that the economic performance of the process is strongly dependent on the chosen valorization strategy. Regarding the baseline scenario, profitability remains limited, with profit values of approximately 0.83 €/kg, consistent with typical bio-oil market margins. In contrast, the more advanced scenario yields an estimated profit of about 4.35 €/kg, placing the process within the lower-to-middle range of bio-based specialty chemical markets. A common CAPEX of approximately 3201.00€ was assumed for both scenarios, as both configurations are based on the same laboratory-scale pyrolysis unit and differ only in the downstream valorization strategy. OPEX amounts to 203.00 €/year for Scenario A and 373.00 €/year for Scenario B, resulting in unit production costs of 0.13 €/kg and 0.24 €/kg, respectively. Although Scenario B is

associated with higher operating and production costs, these are offset by significantly higher product value, leading to an improved economic performance. Overall, this study demonstrates that the process of pyrolysis of SCGs represents a viable waste-to-value path when coupled with chemical valorization startegies. The advanced scenario is intended as an economic tool, supporting the potential interest in further investments in downstream separation and upgrading technologies.

Contents

List of Figures

List of Tables

Nomenclature

Symbols

m_B	Initial mass of dried biomass fed to the reactor (kg)
m_C	Mass of biochar collected (kg)
m_O	Mass of bio-oil obtained after condensation (kg)
m_G	Mass of non-condensable gases (kg)
m_F	Generic mass of product fraction used for yield calculations (kg)
Y_{oil}	Bio-oil yield on dry biomass basis (wt%)
Y_{char}	Biochar yield on dry biomass basis (wt%)
Y_{gas}	Non-condensable gas yield on dry biomass basis (wt%)
T_{pyr}	Pyrolysis temperature (°C)
t_{res}	Residence time in the reactor (min)
t_{batch}	Operating time per batch (h batch^{-1})
$M_{SCG,annual}$	Annual amount of spent coffee grounds processed (kg yr^{-1})
C_{CAPEX}	Capital expenditure (€)
C_{OPEX}	Annual operating expenditure (€ yr^{-1})
R	Annual revenue (€ yr^{-1})
Π	Annual profit (€ yr^{-1})
OM	Operating margin (%)
PBP	Payback period (yr)
UPC	Unit production cost (€ kg^{-1})
Π_{unit}	Profit per unit of product (€ kg^{-1})
P_{oil}	Crude bio-oil selling price (€ kg^{-1})
P_{char}	Biochar selling price (€ kg^{-1})
P_j	Selling price of product j (€ kg^{-1})
P_{el}	Electricity price (€ kWh^{-1})
C_{maint}	Maintenance cost factor (% of CAPEX)
f_{inst}	Installation cost factor (% of equipment cost)
f_{ind}	Indirect cost factor (% of installed cost)

Acronyms

SCG	Spent Coffee Grounds
TEA	Techno-Economic Analysis
GC/MS	Gas Chromatography–Mass Spectrometry
TGA	Thermogravimetric Analysis
DTG	Derivative Thermogravimetric Analysis
CAPEX	Capital Expenditure
OPEX	Operating Expenditure
DPPH	2,2-diphenyl-1-picrylhydrazyl
GAE	Gallic Acid Equivalents
TRL	Technology Readiness Level

Chapter 1

Introduction

The interest in the valorization of agro-industrial residues has increased due to the growing need for sustainable resource management and the shift to a circular economy (Pereira et al., 2022; Pongsiriyakul et al., 2024; Barahmand et al., 2025). Every year, food processing and consumption activities produce large amounts of organic waste, which presents both economic and environmental problems with regard to resource inefficiency, greenhouse gas emissions, and disposal (AlMallahi et al., 2023). In this regard, turning biomass residues into energy carriers and value-added products has become a viable way to cut waste and recover energy and useful materials (Segers et al., 2024; Mujtaba et al., 2023; Ferrari et al., 2025).

Among agro-industrial residues, spent coffee grounds represent a particularly relevant waste stream due to the widespread consumption of coffee worldwide (Tamilselvan et al., 2024; Bartolucci et al., 2024; Al Balushi et al., 2025). According to estimates, several million tons of spent coffee grounds are produced each year (Thoppil and Zein, 2021; Al Balushi et al., 2025), mostly as a result of coffee brewing operations in homes, cafes, and businesses. Despite their high organic and carbon content, these residues are usually burned or dumped in landfills, which causes environmental problems. Consequently, spent coffee grounds are becoming more and more popular as a possible feedstock for biochemical and thermochemical conversion processes (Dari et al., 2025; Choe, 2025; Vardon et al., 2013; Pereira et al., 2022).

Pyrolysis is a thermochemical conversion process that breaks down biomass in an oxygen-limited environment to produce a gaseous fraction, a solid carbon-rich residue called biochar, and a liquid fraction known as bio-oil (Figueiredo et al., 2017; Jones et al., 2013; Jerzak et al., 2024; Ferrari et al., 2025). Pyrolysis has advantages over other conversion methods, including feedstock flexibility and the ability to generate several products at once (Pattiya, 2018; Bridgwater, 2012). Pyrolysis of spent coffee grounds has been thoroughly studied in the literature, primarily concentrating on product yields, chemical composition, and process optimization under various operating conditions (Krause et al., 2019; Primaz et al., 2018; AlMallahi et al., 2023; Jerzak et al., 2024). Bio-oil obtained from biomass pyrolysis is a complex mixture of oxygenated organic compounds and has been studied primarily as a renewable energy carrier and, to a lesser extent, as a source of chemicals (Pereira et al., 2022; Gracia-Vitoria et al., 2023;

Machado et al., 2022). Similarly, because of its porous structure and high carbon content, biochar has been extensively investigated for use in agriculture and environmental remediation (Mohammadalizadeh et al., 2025; Nascimento et al., 2023; Pereira et al., 2022; Li et al., 2017).

The majority of contributions have concentrated on laboratory-scale characterization and process optimization, despite the fact that many studies have examined the chemical and physical characteristics of products obtained from the pyrolysis of spent coffee grounds (Matrapazi and Zabaniotou, 2020). Evaluations that consider biochar solely as a by-product or neglect its potential economic contribution may lead to incomplete conclusions regarding the overall viability of the system (Segers et al., 2024; Rogers and Brammer, 2012; Jones et al., 2013; Barahmand et al., 2025). In this regard, this dissertation combines experimental characterization with a preliminary techno-economic evaluation to provide an integrated assessment of spent coffee grounds pyrolysis. The primary product of the study is bio-oil, but biochar is also taken into account as a useful co-product that improves the process's economic performance. The bio-oil and biochar fractions are characterized chemically, and an economic model is created to project expenses, income, and key performance indicators under various conditions.

Structure of the thesis

The thesis is structured as follows:

- **Chapter 2** presents a review of the relevant literature, focusing on the valorization of spent coffee grounds, pyrolysis processes, and the main properties the pyrolysis products.
- **Chapter 3** describes the materials and methods adopted in this study, including the pyrolysis experiments, analytical techniques for chemical characterization, and the methodological framework for the economic assessment.
- **Chapter 4** presents the results of the experimental analyses, including the chemical characterization of bio-oil and biochar.
- **Chapter 5** presents the techno-economic evaluation and the assessment of different economic scenarios.
- **Chapter 6** summarizes the main findings of the study, discusses the overall implications of the results, and outlines limitations and perspectives for future research.

Chapter 2

Literature Review

The objective of the following literature review is to provide a comprehensive overview of current research on biomass pyrolysis and related thermochemical conversion technologies. The review aims to identify the main scientific trends, experimental approaches, and process parameters that influence product distribution and quality. Particular attention has been given to studies focusing on the characterization of biomass feedstocks, the optimization of operational conditions, and the valorization of pyrolysis products such as bio-oil, biochar, and syngas.

The chapter is organized into the following sections:

- Section 2.1 describes the research methodology applied;
- Section 2.2 presents the findings related to pyrolysis types;
- Section 2.3 presents the findings related to biomass type and moisture content;
- Section 2.4 presents the findings related to spent coffee grounds as a biomass feedstock;
- Section 2.5 presents the findings related to products and yields;
- Section 2.6 presents the findings related to the influence of process parameters;
- Section 2.7 presents the findings related to alternative thermochemical pathways;
- Section 2.8 presents findings related to separation and purification techniques.

2.1 Research Approach

The first objective was to define an initial query focused on biomass pyrolysis and liquid product valorization. Starting from this general query, the analysis was expanded to cover different technological aspects, allowing the identification of specific papers addressing each area of interest. Thus, the first element to be set in the search strategy was the term “liquid smoke”, along with its common synonym “wood vinegar”, both referring to condensable products obtained from biomass pyrolysis. However, this alone was not sufficient to narrow the focus to studies specifically related to fast pyrolysis. To better target this context, additional terms were included. Table 2.1 summarizes the preliminary searches performed in Scopus using individual and combined keywords, aimed at assessing the relevance and frequency of each term within the research topic:

Table 2.1: Preliminary keyword searches in Scopus (September 2025).

Search term	**Results found**
“liquid smoke”	6421
“wood vinegar”	734
“fast pyrolysis”	10106
“biomass conversion”	55498
“food flavor”	35862
“aroma”	47539

The individual keywords yielded a large number of results, confirming the broad scientific interest in these topics. However, none of these terms alone could isolate publications specifically addressing the topic of interest. Based on these considerations, the final query was defined as follows:

(“liquid smoke” OR “wood vinegar”) AND (“fast pyrolysis” OR “biomass conversion”) AND (“food flavor” OR “aroma”)

This search led to 53 publications on Scopus (09/2025), from which 21 papers were selected after a detailed review of titles, abstracts, and conclusions. This set of studies provided a comprehensive overview of the current research landscape on the production and characterization of liquid smoke and bio-oil from biomass pyrolysis. However, to better contextualize these findings to the specific feedstock of interest, spent coffee grounds (SCGs), the scope of the analysis was further refined. A new query was therefore developed by integrating the previous search terms with those referring to coffee-based biomasses, specifically “coffee waste” and “coffee grounds”:

(“liquid smoke” OR “wood vinegar”) AND (“fast pyrolysis” OR “biomass conversion”) AND (“food flavor” OR “aroma”) AND (“coffee waste” OR “coffee grounds”)

This additional filter narrowed the search to five publications directly focused on coffee pyrolysis and its liquid products. Since this limited number of studies was not sufficient to capture all relevant scientific

contribution, the reference lists and citations of the five papers were examined to identify additional studies addressing related topics.

The second key element to be included in the search concerns the condensation and collection systems used for the recovery of bio-oil and liquid smoke fractions. To capture this aspect, several keywords were tested individually on Scopus to evaluate their scientific relevance and frequency. Table 2.2 summarizes the number of publications found for each search term.

Table 2.2: Initial keywords search on condensation and collection systems (Scopus, September 2025).

Search term	**Results found**
“fractional condensation”	17578
“staged condensation”	1368
“spray column condenser”	436
“heat exchanger condenser”	11
“liquid collection system”	161444
“fast pyrolysis”	10106
“phenols”	323400
“biomass conversion”	55498
“bio-oil”	493184
“liquid smoke”	6421
“acetic acid”	271887
“yield”	2422231
“wood vinegar”	734

Based on these results, the following query was formulated to specifically target studies related to fractional condensation, staged condensation, and condenser design in biomass fast pyrolysis:

> *(“fractional condensation” OR “staged condensation” OR “spray column condenser” OR “heat exchanger condenser” OR “liquid collection system”) AND (“fast pyrolysis” AND “biomass conversion”) AND (“bio-oil” OR “liquid smoke” OR “phenols” OR “acetic acid” OR “yield” OR "wood vinegar")*

This search led to 134 publications on Scopus (09/2025). From these, 19 papers were selected for in-depth analysis, based on their relevance to process optimization and product quality. Starting from these two specific queries, a final dataset was formulated as a basis for investigating bio-oil and liquid smoke production, condensation behavior, and potential applications. The selection process also included cross-referencing: several additional studies were identified through citations within the chosen papers. This approach allowed the inclusion of key experimental and review articles that were not

retrieved by the initial queries but were highly relevant to the objectives of this study.

2.2 Pyrolysis

The current climate change and the continuous rise in global energy demand have accelerated the search for sustainable and renewable energy sources. Conventional fossil fuels, which still account for nearly 80% of the global energy supply, are not only finite but also responsible for a significant share of greenhouse gas emissions, reaching approximately 37.4 billion tons of CO_2in 2023. The use of these resources calls for immediate transition toward cleaner and renewable alternatives. Biomass has emerged as a promising substitute due to its abundance, carbon-neutral nature, and its capacity to be converted into valuable energy carriers and chemical products (Pereira et al., 2022; Jerzak et al., 2024). Thanks to its structure, it represents a suitable feedstock for thermochemical conversion processes such as combustion, gasification, and pyrolysis.(Jones et al., 2013). Pyrolysis represents a more controlled pathway for biomass conversion, in contrast with direct combustion, that releases most of the energy as heat. Pyrolysis converts the input into liquid, solid and geseous fractions, which can be further upgraded into value-added products. (Pattiya, 2018; Bridgwater, 2012; Jerzak et al., 2024).

Pyrolysis, derived from the Greek words pyro (fire) and lysis (separation), refers to the thermal decomposition of organic material in the absence of oxygen (Jones et al., 2013). During this process, biomass is heated to moderate or high temperatures, typically between 300 and 700 ℃, causing its structure to break down into smaller compounds (Pattiya, 2018). The general process of biomass pyrolysis is illustrated in Figure 2.1. Biomass feedstock is fed into the pyrolysis reactor. Inside the reactor, the material is thermally decomposed in the absence of oxygen, at controlled temperatures and heating rates. The process leads to the formation of three main products: a solid fraction (biochar), a liquid condensate (bio-oil), and a gaseous fraction (non-condensable gas) (Bridgwater, 2012). These products are then separated through a condensation and gas collection system.

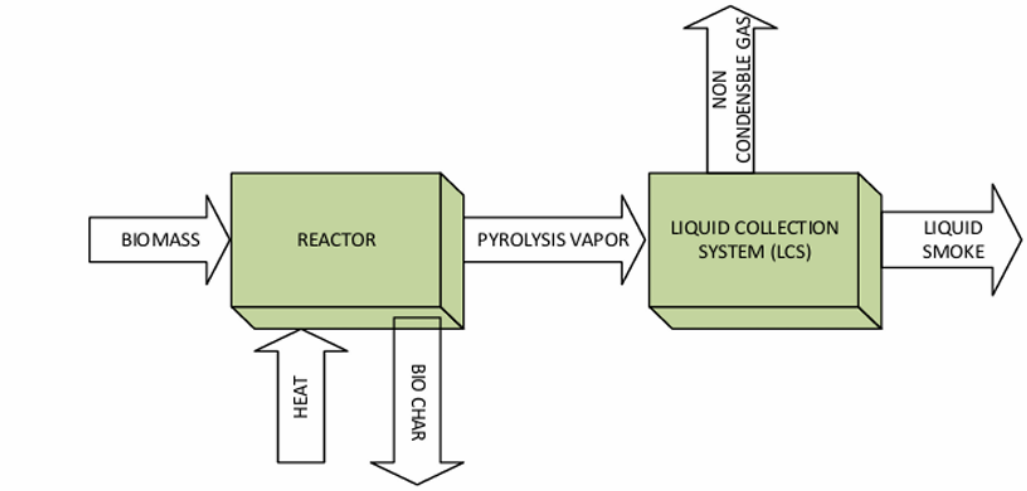

Figure 2.1: Schematic diagram of the pyrolysis process. Credit: Abdullah, N. A. et al.

The relative proportion of these products strongly depends on the process conditions, particularly temperature, heating rate, and vapor residence time, as well as on feedstock properties such as particle size, moisture, and composition (Eke et al., 2020; Westerhof et al., 2007; Westerhof et al., 2011; Liu

et al., 2025). Among these products, bio-oil has attracted the most attention due to its potential as a renewable liquid fuel and a source of value-added chemicals (Pereira et al., 2022; Gracia-Vitoria et al., 2023). Biochar, on the other hand, is increasingly recognized for its environmental benefits: it enhances soil fertility, sequesters carbon, and can serve as a precursor for catalysts and adsorbents (Pereira et al., 2022; Li et al., 2017). Non-condensable gas contributes additional energy recovery, either for electricity generation or to sustain the pyrolysis process itself. The pyrolysis process is highly flexible and can be tuned to favor the production of either solid, liquid, or gaseous fractions depending on the operating conditions (Jones et al., 2013; Jerzak et al., 2024; Jerzak et al., 2024). This has led to several distinct classifications: slow, fast, and flash pyrolysis (Pattiya, 2018; Bridgwater, 2012). Each of them is characterized by specific ranges of heating rates, temperatures, and residence times.

In recent years, the scientific interest in biomass pyrolysis has grown significantly, and this explains the growth in research activity. According to Scopus data, the number of publications has increased steadily from around 2000 in 2010 to nearly 16,000 in 2025 (Figure 2.2). This highlights the key role of pyrolysis in the field of renewable energy research and sustainable material conversion. Geographically, China contributes more than 55,000 documents, followed by the United States, India, and South Korea (Figure 2.3). The dominance of Asian countries, followed by American and European countries, shows the increasing international interest and dedication to pyrolysis research.

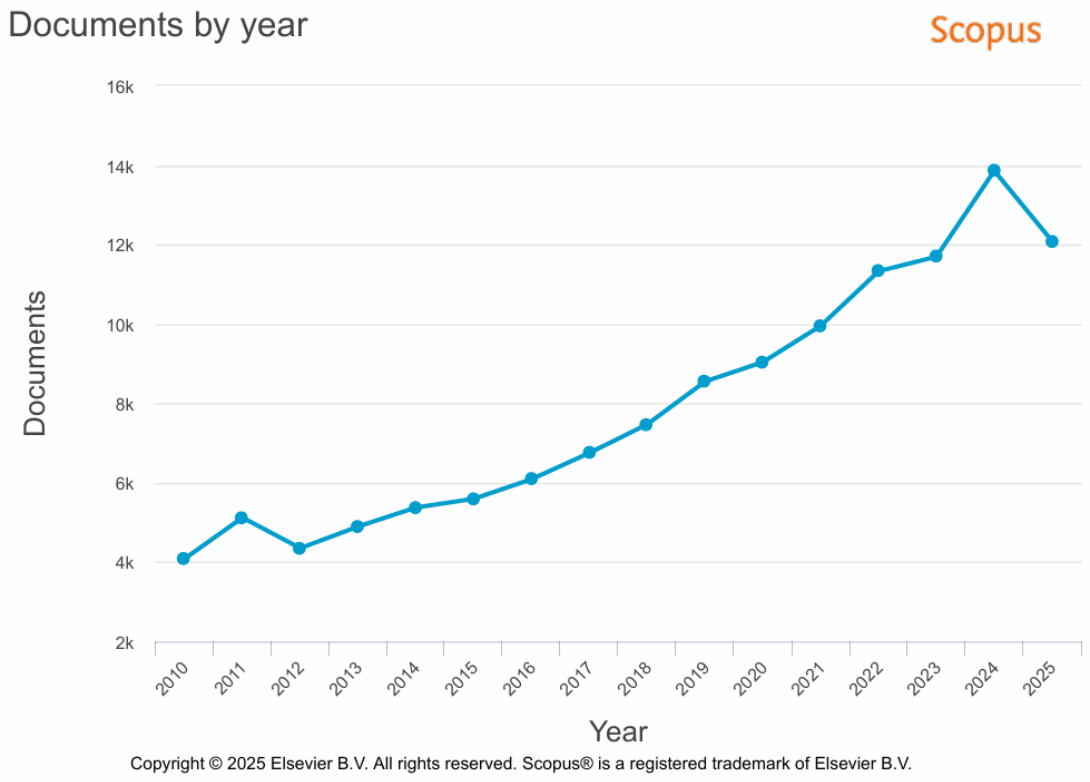

Figure 2.2: Annual number of publications on biomass pyrolysis from 2010 to 2025 (Scopus Data).

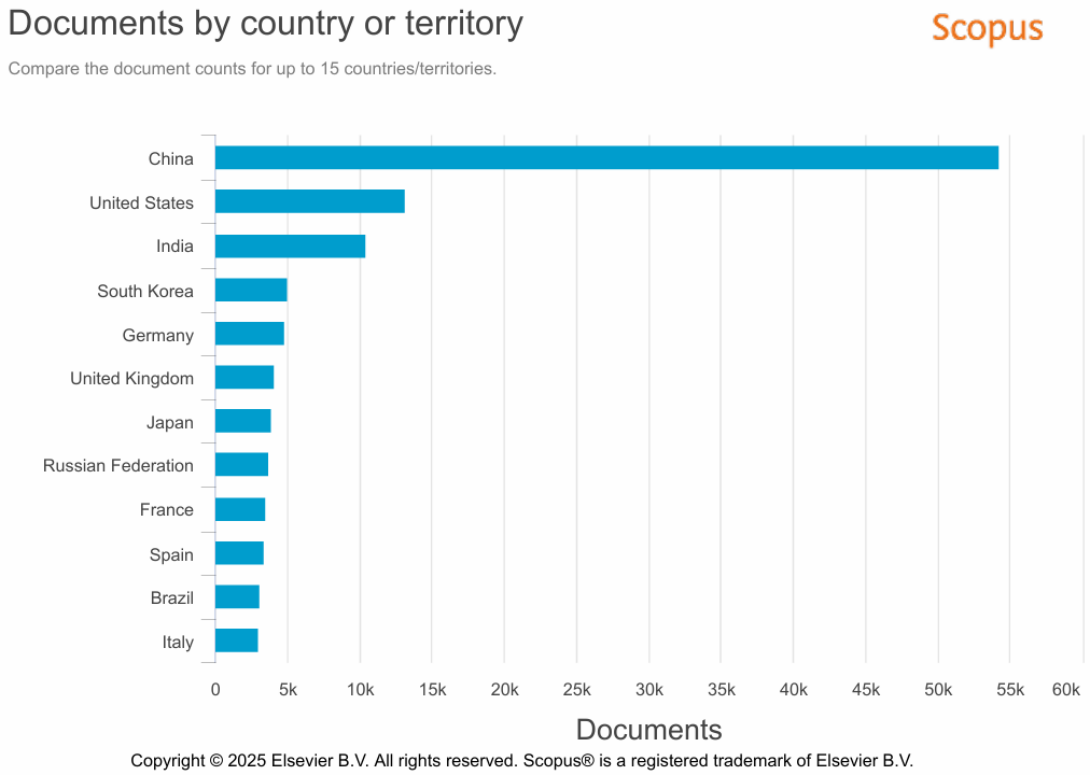

Figure 2.3: Distribution of publications by country (Scopus data).

The following sections present a comprehensive overview of the three main pyrolysis types, slow, fast, and flash pyrolysis, highlighting their fundamental mechanisms, operational parameters, and product distributions.

2.2.1 Slow Pyrolysis

Slow pyrolysis is the oldest and most established thermochemical conversion technique, dating back to the early 1900s when wood was processed for 24 hours to produce methanol, acetic acid, and charcoal (Ronsse et al., 2015; Pereira et al., 2022). It operates under moderate temperatures and very low heating rates, providing sufficient residence time for complete thermal decomposition of biomass (Segers et al., 2024; Jerzak et al., 2024). Typically, the process is carried out between 300 and 650 °C, with heating rates below 1 °C/s (commonly 5–20 °C/min) and solid residence times ranging from several minutes to multiple hours or even days, depending on reactor configuration and feedstock characteristics (Mujtaba et al., 2023; Nhuchhen et al., 2014).

In addition, slow pyrolysis tolerates relatively large particle sizes (0.075–19 mm) and elevated moisture content, allowing for the direct use of raw or minimally pretreated biomass (Segers et al., 2024; Nhuchhen et al., 2014). These operating conditions promote the formation of solid carbonaceous residue while minimizing the production of liquid and gaseous fractions. As a result, char is the dominant product, while wood vinegar and non-condensable gases are recovered as by-products (Segers et al., 2024; Setter et al., 2020; Ouattara et al., 2023). In general the distribution of products in slow pyrolysis strongly depends on feedstock composition, temperature, and residence time. Typical yields fall within the ranges shown in Figure 2.4 (Mujtaba et al., 2023; Ronsse et al., 2015; Pereira et al., 2022), with approximately 30–40 wt% of solid biochar, 20–35 wt% of condensable liquids, and 15–25 wt% of non-condensable gases. The relatively high solid fraction reflects the incomplete devolatilization of biomass and the prevalence of polymerization and condensation reactions at lower heating rates.

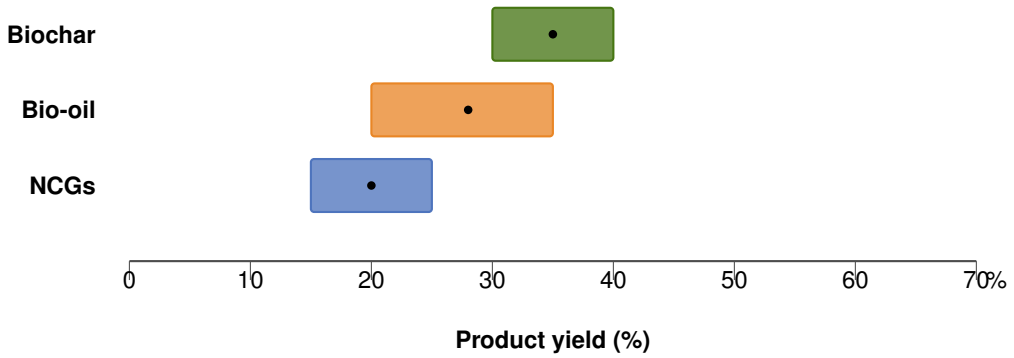

Figure 2.4: Slow pyrolysis — typical yield ranges and operating conditions. Biochar: 30–40%, Bio-oil: 20–35%, Non-condensable gas: 15–25%. The process takes place at moderate temperatures (300–650 °C), with low heating rates (below 1 °C s^{-1} or 5–20 °C min^{-1}) and long solid residence times ranging from several minutes to hours or even days. These mild conditions promote secondary condensation and polymerization reactions, leading to high solid yields and relatively low amounts of condensable vapors and gases.

Overall, slow pyrolysis provides a robust and controllable route for the thermal decomposition of biomass under mild conditions (Pereira et al., 2022). Although the process yields lower amounts of condensable liquids compared to faster modes, its simplicity, scalability, and adaptability to diverse feedstocks makes it a reliable foundation for both energy recovery and the production of carbon-rich solids (Mujtaba et al., 2023; Ronsse et al., 2015).

2.2.2 Fast Pyrolysis

Fast pyrolysis is a thermochemical conversion process designed to maximize the production of condensable vapors, which upon cooling form a liquid known as bio-oil (Jones et al., 2013; Jerzak et al., 2024). It represents a thermal decomposition, which takes place in the absence of oxygen, generally at a temperature range that goes from 450 to 650 ℃, and heating rates exceeding 1000 ℃/s(Pattiya, 2018; Bridgwater, 2012). This combination of conditions leads to the breakdown of the organic structure and results in a high yield of vapors and aerosols and a smaller quantity of non-condensable gases and solid char.

In contrast to slow pyrolysis, fast pyrolysis requires very short vapor residence times, generally below 2 seconds, to prevent secondary cracking reactions that would otherwise increase gas formation at the expense of liquid products (Bridgwater, 2012; Jerzak et al., 2024). Under optimal conditions, around 500 ℃, bio-oil yields of 60–70 wt% can be achieved, while biochar and non-condensable gas account for approximately 15–25 wt% and 10–20 wt%, respectively (Figure 2.5) (Pattiya, 2018; Bridgwater, 2012; Rogers and Brammer, 2012).

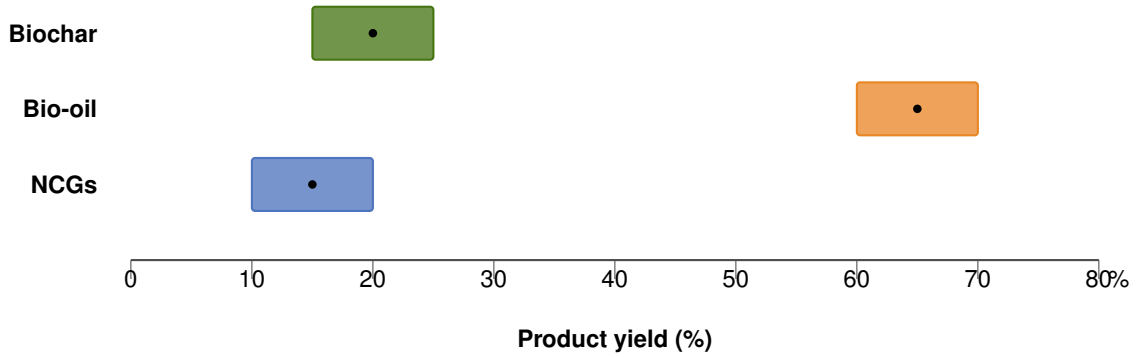

Figure 2.5: Fast pyrolysis — typical yield ranges and operating conditions. Biochar: 15–25%, Bio-oil: 60–70%, Non-condensable gas: 10–20%. The process occurs at moderate temperatures (450–650 ℃), with heating rates typically exceeding 1000 ℃ s^{-1} and vapor residence times below 2 s. These conditions favor rapid thermal decomposition and high production of condensable vapors, which upon cooling form liquid bio-oil. The process is optimized around 500 ℃ to maximize liquid yields while minimizing gas and char formation.

The primary vapors formed are subsequently cooled and condensed into a dark brown liquid with a heating value around 16–19 MJ/kg (Bridgwater, 2012; Rogers and Brammer, 2012). This bio-oil can be upgraded to hydrocarbons suitable for use in engines, turbines, or boilers, offering a promising renewable alternative for energy and chemical production (Lachos-Perez et al., 2023; Jones et al., 2013; Talmadge et al., 2021; Santos et al., 2025). A wide range of reactor configurations has been developed to perform fast pyrolysis efficiently. Among these, fluidized-bed reactors are the most common, due to their excellent temperature control, uniform heat distribution, and scalability (Pattiya, 2018; Bridgwater, 2012). After exiting the reactor, the resulting vapors and aerosols pass through a cyclone to separate char particles before being condensed in a bio-oil recovery system (Papari and Hawboldt, 2018). The advantages of fast pyrolysis are numerous: the process operates at atmospheric pressure, is relatively simple and continuous, and can handle a wide variety of feedstocks, from agricultural and forestry residues to

industrial wastes (Segers et al., 2024; Pereira et al., 2022; Jerzak et al., 2024; Ferrari et al., 2025). It yields a liquid product that is easy to store, transport, and further process.

2.2.3 Flash Pyrolysis

Flash pyrolysis represents the most severe form of thermochemical conversion within the pyrolysis spectrum. It is characterized by very high operating temperatures, typically between 800 and 1000 °C, extremely high heating rates exceeding $700\ ^{\circ}\mathrm{C\,s^{-1}}$, and ultrashort vapor residence times, generally below 0.5 s (Pattiya, 2018; Bridgwater, 2012). Under these extreme conditions, biomass devolatilization occurs almost instantaneously, promoting the secondary cracking and reforming of primary vapors, which leads to the formation of large quantities of non-condensable gases (NCGs) such as CO_2, CO, H_2, CH_4, and light hydrocarbons (Pattiya, 2018; Bridgwater, 2012). The production of condensable vapors and solid char is consequently minimized as shown in Figure 2.6 and typical product distributions reported in the literature indicate that flash pyrolysis yields approximately 5–10 wt% char, 10–20 wt% condensable bio-oil, and 60–80 wt% non-condensable gases (Pattiya, 2018; Bridgwater, 2012).

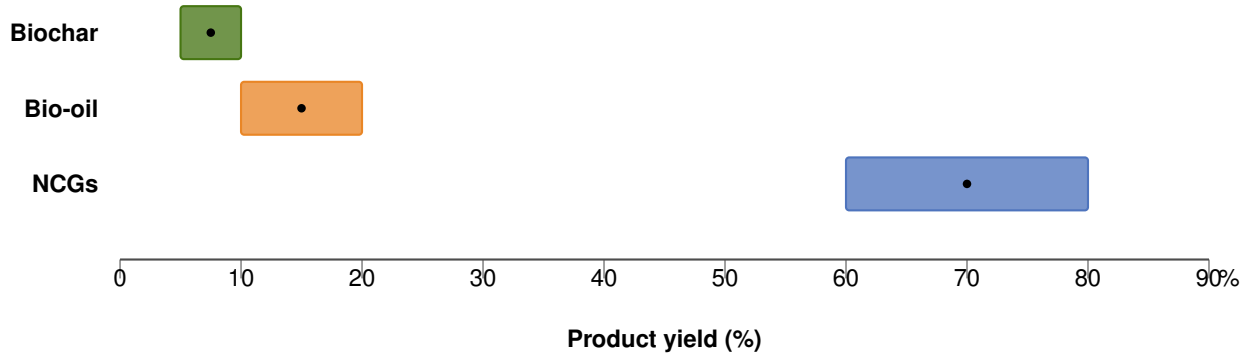

Figure 2.6: Flash pyrolysis — typical yield ranges and operating conditions. Biochar: 5–10%, Bio-oil: 10–20%, Non-condensable gas: 60–80%. The process is carried out at very high temperatures (800–1000 °C), with heating rates exceeding 700 °C s^{-1} and vapor residence times below 0.5 s. These extreme conditions promote secondary cracking and reforming reactions, favoring gas production over condensable liquids or solid char.

In contrast to fast pyrolysis, where the main goal is to maximize liquid bio-oil yields, flash pyrolysis favors gas production due to the dominance of thermal cracking reactions and limited residence time for vapor condensation (Segers et al., 2024; Bridgwater, 2012; Jerzak et al., 2024). The process mechanisms are highly dependent on efficient heat and mass transfer across the feedstock particles, often enhanced by techniques such as ablation heating. Reported gas yields vary widely depending on the feedstock and reactor design but generally increase sharply with temperature and heating rate increase. Typical configurations, such as wire-mesh or entrained-flow reactors, allow direct contact between the biomass and the heat source, enabling near complete vaporization and gas formation (Pattiya, 2018; Jones et al., 2013). The resulting gas mixture possesses a moderate calorific value $5.7\text{–}14.6\ \mathrm{MJ\,m^{-3}}$ (Mujtaba et al., 2023), making it suitable for use as a combustion fuel, a fluidizing or carrier gas within the pyrolysis plant, or as feedstock for hydrogen-rich syngas production through reforming (Jones et al., 2013). The composition of the gas reflects the biomass components: cellulose mainly contributes to CO formation, hemicellulose enhances CO_2 generation, while lignin increases CH_4 and heavier hydrocarbons. Although flash pyrolysis demands precise temperature control and high energy input, it represents an efficient route for on-site fuel gas generation and provides valuable insights into the high-temperature

kinetics of biomass decomposition.

The three main pyrolysis regimes — slow, fast, and flash — differ significantly in operating conditions, product distribution, and dominant reaction mechanisms (Bridgwater, 2012; Pereira et al., 2022; Jerzak et al., 2024). Table 2.3 provides a comparative overview of the key process parameters and typical product yields reported in the literature, summarizing the trends discussed in the previous paragraphs.

Table 2.3: Comparative overview of slow, fast, and flash pyrolysis in terms of operating conditions and typical product yields.

Pyrolysis Type	**Temperature Range (°C)**	**Heating Rate**	**Vapor Residence Time**	**Main Product**	**Typical Product Yield (wt%)**
Slow	300–650	< 1 °C s^{-1} ($\approx$ 5–20 °C min^{-1})	Minutes – hours / days	**Biochar**	Biochar 30–40; Bio-oil 20–35; Syngas 15–25
Fast	450–650	> 1000 °C s^{-1}	≤ 2 s	**Bio-oil**	Bio-oil 60–70; Biochar 15–25; Syngas 10–20
Flash	800–1000	> 700 °C s^{-1}	< 0.5 s	**Syngas**	Syngas 60–80; Bio-oil 10–20; Biochar 5–10

In addition to the specific operating conditions summarized in the table, the overall distribution of products in biomass pyrolysis is strongly influenced by two fundamental parameters: temperature and heating rate (Mujtaba et al., 2023; Jones et al., 2013; Liu et al., 2025). Their combined effect governs the extent of devolatilization, secondary cracking, and condensation phenomena, ultimately determining the relative yields of char, condensable bio-oil, and non-condensable gases, as illustrated in Figure 2.7.

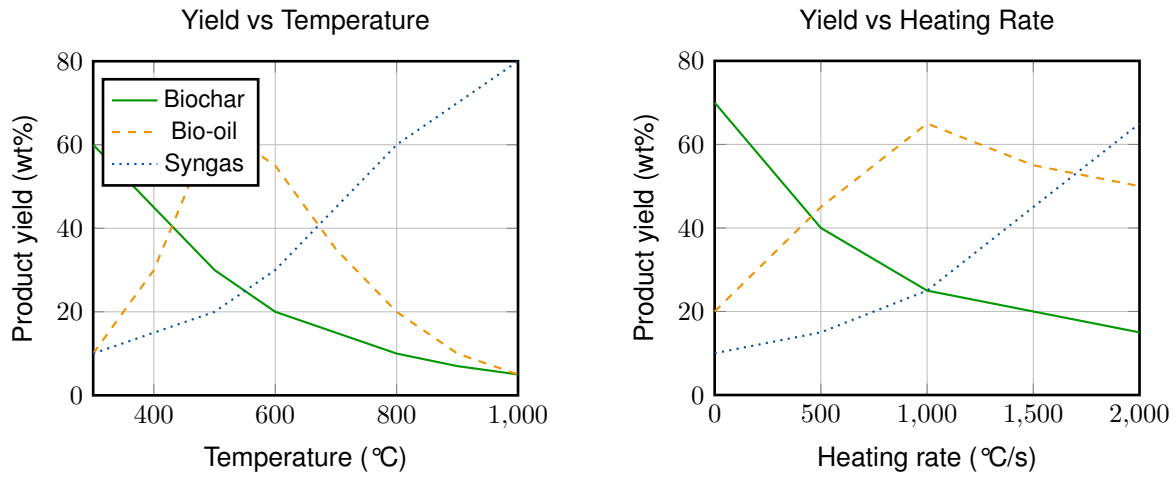

Figure 2.7: Schematic influence of temperature and heating rate on the product yield distribution in biomass pyrolysis. Both increasing temperature and heating rate favor the formation of gaseous products (syngas) at the expense of condensable liquids and solid char.

2.3 Biomass: types and moisture content

According to EIA (U.S. Energy Information Administration, 2023), biomass is a renewable organic material that comes from plants and animals and can be converted into heat, electricity, or liquid and gaseous biofuels.

Biomass comprises a broad spectrum of organic materials of biological origin (Oliveira Farrapeira et al., 2021; Pereira et al., 2022); the following are included:

- **Wood and wood processing waste** — includes firewood, wood pellets, and wood chips, as well as lumber and furniture mill sawdust and waste, and black liquor from pulp and paper mills. These resources are mainly used for heat and power generation through combustion or gasification (Pereira et al., 2022).
- **Agricultural crops and waste materials** — such as corn, soybeans, sugar cane, switchgrass, woody plants, algae, and crop or food processing residues. These biomasses are primarily used for the production of biofuels (bioethanol, biodiesel, and bio-oil) through biochemical or thermochemical conversion (Pereira et al., 2022).
  - **Spent Coffee Grounds (SCGs)** — a specific residue generated from coffee brewing processes, rich in organic compounds (lipids, polysaccharides, and proteins) and minor lignocellulosic fractions. Due to their high volatile content, low ash concentration, and intrinsic oil fraction, SCGs represent a promising feedstock for low-temperature pyrolysis aimed at bio-oil and biochar production (Vardon et al., 2013; Choe, 2025; Bartolucci et al., 2024). Their wide availability from coffee industries also supports circular economy strategies (Thoppil and Zein, 2021; Pongsiriyakul et al., 2024).
- **Biogenic materials in municipal solid waste** — including paper products, cotton and wool textiles, as well as food, yard, and wood wastes. These streams represent an important renewable

resource for waste-to-energy processes and material recovery.

- **Animal manure and human sewage** — organic residues that can be anaerobically digested to produce biogas, which is a renewable natural gas rich in methane, and a digestate rich in nutrients for use in agriculture.

The energy stored in all forms of biomass ultimately originates from the process of photosynthesis, through which plants capture solar radiation and convert it into chemical energy in the form of carbohydrates. During this process, carbon dioxide from the atmosphere and water absorbed from the soil are transformed into glucose and oxygen, according to the following general reaction:

$$6\,H_2O + 6\,CO_2 + \text{radiant energy} \rightarrow C_6H_{12}O_6 + 6\,O_2$$

A schematic overview of the photosynthetic process and the main categories of biomass sources is presented in Figure 2.8.

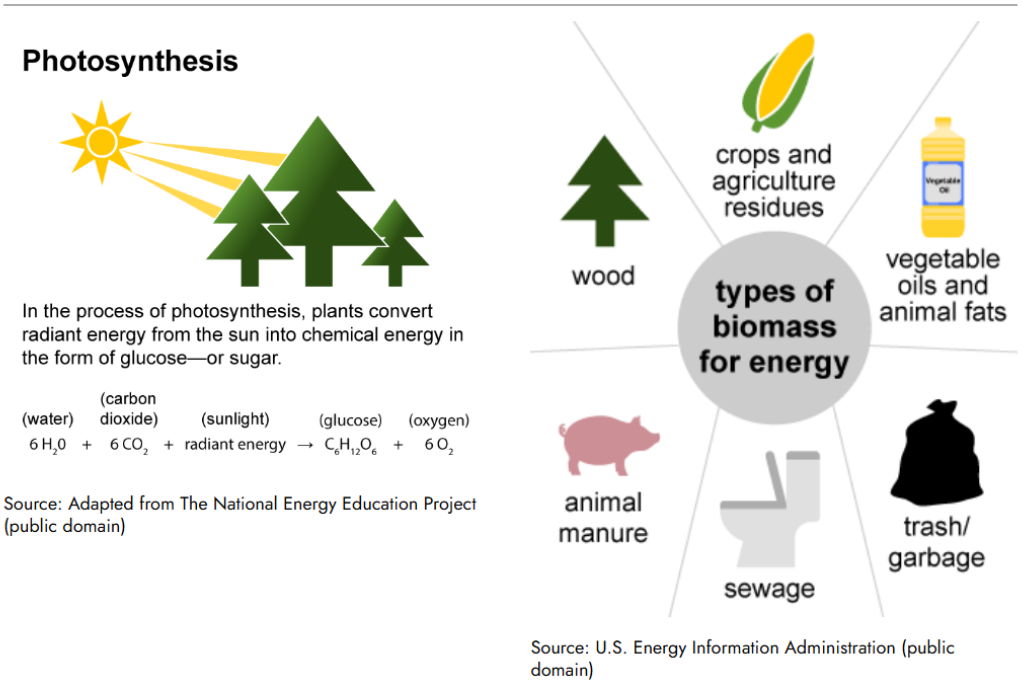

Figure 2.8: Illustration of the photosynthetic process and the main categories of biomass used for energy production.

A part from being a renewable energy source, biomass is recognized also as a fundamental raw mateial for the production of a wide range of bio-based products, chemicals and functional materials. (Segers et al., 2024; Mujtaba et al., 2023; Pereira et al., 2022; Barahmand et al., 2025). For this reason, it's important to invest in its valorization in order to reduce the dependence on fossil carbon, contribute to industrial innovation, promote waste reduction and achieve sustainable resource management.

From a structural and compositional perspective, most solid plant-based biomasses, often referred to as lignocellulosic biomass, consists of cellulose, hemicelluloses, and lignin (Figure 2.9), along with smaller fractions of extractives, proteins, and inorganic components (Segers et al., 2024; Pereira et al.,

2022). The relative proportions of these constituents determine the thermal behavior and conversion efficiency of the feedstock (Pattiya, 2018; Bridgwater, 2012; Jones et al., 2013).

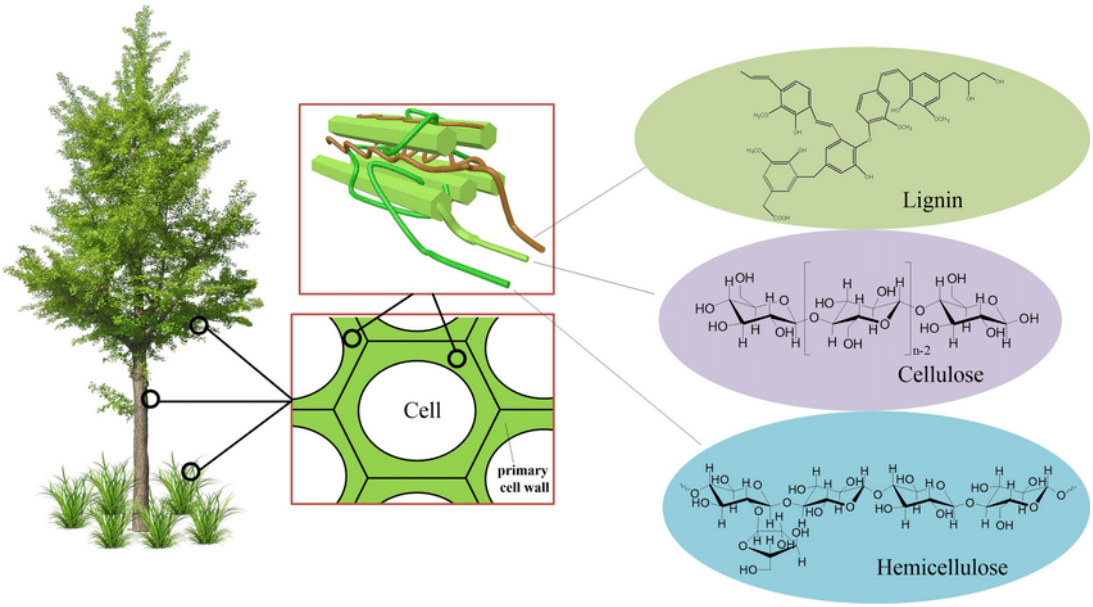

Figure 2.9: Interaction of cellulose, hemicellulose and lignin in the cell wall of lignocellulosic biomass. Credit: Zhengqiu et al.

Cellulose is a linear polysaccharide formed by glucose units. Its extensive intra- and intermolecular hydrogen bonding provides mechanical strength but also results in hygroscopicity and swelling. Cellulose depolymerizes mainly into oxygenated volatiles during heating, contributing significantly to bio-oil formation. Hemicellulose is a heterogeneous, amorphous polysaccharide composed of pentoses and hexoses. Its lower degree of polymerization and thermochemical stability make it the first constituent to degrade (typically 200–300 °C), releasing CO, CO_2 and light organics. Lignin is an aromatic, three-dimensional polymer formed from three principal monolignols (Park et al., 2021). Because its various oxygen-containing functional groups possess different thermal stabilities, lignin decomposes gradually over a broad temperature range (≈100–900 °C). As a result, it is the main precursor of char and largely responsible for the higher heating value of solid products (Bridgwater, 2012; Ronsse et al., 2015; Pandey and Kim, 2011; Lu and Gu, 2022); biomass with higher lignin content typically yields more solid residue after thermal treatment (Segers et al., 2024; Pereira et al., 2022).

The heterogeneity among biomass types results in distinct process performances and product distributions, making the characterization of each feedstock a key element for its efficient conversion (Pereira et al., 2022; Li et al., 2017). Woody biomass, rich in lignin, tends to produce more stable chars and bio-oils, while agricultural residues with higher ash content favor gas production (Puri et al., 2024). Aquatic and algal biomasses, on the other hand, are characterized by high nitrogen and mineral content, influencing both reaction pathways and emission profiles (Table 2.4).

Table 2.4: Main biomass categories and representative examples. Spent Coffee Grounds (SCG) are highlighted as a specific food-processing residue of particular interest for thermochemical conversion.

Category	**Typical sources**	**Main conversion routes**	**Characteristics**
Wood & wood processing waste	Firewood, wood pellets, wood chips; lumber/furniture mill sawdust; black liquor (pulp & paper)	Combustion, gasification, fast pyrolysis	High lignin, low ash; good-quality bio-oils and chars; stable supply from forestry residues.
Agricultural crops & waste materials	Corn, soybeans, sugarcane, switchgrass, woody energy crops; algae; crop & food-processing residues (husks, bagasse)	Fermentation (bioethanol), transesterification (biodiesel), fast pyrolysis, anaerobic digestion	Variable ash/alkali content; widely used for biofuels; pretreatment often required.
Spent Coffee Grounds (SCG)	Residues from coffee brewing (households, cafés, industry)	**Low-temperature pyrolysis** (bio-oil, biochar), extraction of oils, anaerobic digestion	High volatiles, intrinsic oil fraction, low ash; moderate N/proteins; abundant waste stream $\rightarrow$ circular economy valorization.
Biogenic materials in municipal solid waste (MSW)	Paper products; cotton & wool textiles; food, yard & wood wastes (organic fraction of MSW)	Waste-to-energy (combustion), anaerobic digestion, RDF/SRF production	Heterogeneous composition; requires sorting/pretreatment; variable moisture and ash content.
Animal manure & human sewage	Livestock manure; sewage sludge	Anaerobic digestion (biogas/RNG), co-digestion, hydrothermal processes	Nutrient-rich streams; high moisture; suitable for biogas and nutrient recovery.

Another parameter that strongly influences the overall energy balance and products quality is moisture content. (Li et al., 2017). This is caused by the fact that high water content increases the energy demand for drying, lowers the reactor temperature and results in a final bio-oil with higher water and oxygen content. (Liu et al., 2025).

For these reasons, feedstocks intended for fast and flash pyrolysis are typically pre-dried to moisture levels below 10 wt%, (Westerhof et al., 2007), whereas slow pyrolysis processes can work with higher moisture levels without any significant performance loss(Pattiya, 2018).

In addition to organic composition, the inorganic fraction plays a crucial role in biomass conversion (Liu et al., 2025). Alkali and alkaline earth metals (K, Na, Ca, Mg), often present in significant amounts, can catalyze cracking, gasification, and repolymerization reactions, thus altering the product yields and influencing the stability of bio-oil and char (Puri et al., 2024; Pereira et al., 2022). Excessive ash content may also cause fouling and corrosion in thermochemical systems, underscoring the importance of proper feedstock preparation (Puri et al., 2024). All the above mentioned parameters are summerized in Table 2.5

Table 2.5: Influence of feedstock composition on product distribution and properties in fast pyrolysis.

Parameter	**Thermal behaviour**	**Main effect on products**
Moisture content	Evaporation absorbs heat	↓ reactor temperature; ↑ water in oil; ↓ HHV; undesirable >10 wt%
Cellulose	Decomposition 220–350 °C	↑ volatiles; precursors: levoglucosan, acids; ↑ bio-oil yield
Hemicellulose	Decomposition 200–330 °C	↑ CO_2, furans; contributes to liquid; low char
Lignin	Broad decomposition 160–900 °C	↑ char; ↑ aromaticity; ↑ viscosity of oil; ↑ molecular weight
Extractives	Volatile degradation	↓ levoglucosan; ↓ oil yield; removal improves oil stability
Inorganic species (K, Na)	Catalytic cracking activity	↑ char; ↓ liquid yield; ↑ secondary reactions

To mitigate these effects and improve the homogeneity and reactivity of biomass, various pretreatment methods are commonly employed (Pereira et al., 2022; Liu et al., 2025). They partially overcomes these challenges by altering the physical and chemical structure of biomass, making cellulose and hemicellulose more accessible and thus enabling faster and more efficient conversion. Biomass pretreatment methods are generally classified into four categories: mechanical, chemical, thermal and biological (Segers et al., 2024).

- Mechanical pretreatments such as grinding and sieving reduce particle size and improve heat and mass transfer, promoting uniform temperature profiles during conversion.
- Chemical pretreatments target the removal or modification of hemicellulose and lignin to increase cellulose digestibility; common approaches include acid and alkaline treatments, organosolv, steam-explosion, and ionic-liquid pretreatments. These methods often decrease the degree of polymerization, disrupt the lignin matrix, and cleave cell-wall linkages, thereby facilitating downstream hydrolysis and increasing ethanol yields in biochemical routes (Liu et al., 2025).
- Thermal pretreatment involves slow heating, which induces devolatilization and modifications to the physical and chemical integrity of biomass. Torrefaction, the most relevant thermal method, removes moisture and partially decomposes hemicellulose, yielding a hydrophobic, brittle solid

with enhanced grindability, reduced fibrousness, and improved energy density (Mujtaba et al., 2023; Jones et al., 2013). These transformations facilitate co-firing in pulverized coal boilers and increase the fuel flexibility of biomass streams (Jerzak et al., 2024).

- Biological pretreatment employs microorganisms—primarily white-rot fungi, brown-rot fungi, and bacteria—to selectively degrade lignin and hemicellulose, enhancing accessibility of polysaccharides. Although biologically based approaches operate under mild conditions, require little energy input, and avoid chemical reagents, their slow reaction rates and need for controlled environments limit industrial applicability.

Table 2.6 summerizes the above described pretretments and their respective effects.

Table 2.6: Effect of biomass pretreatment on fast pyrolysis performance.

Pretreatment	**Main action**	**Effect on products/performance**
Mechanical (milling, size reduction)	↓ particle size; ↑ surface area; ↑ heat/mass transfer	↑ conversion efficiency; more uniform heating; potential entrainment losses if excessively fine
Chemical (acid/alkali, organosolv, AFEX, ILs)	Partial lignin/hemicellulose removal; ↓ polymerization; cleavage of structural linkages	↑ cellulose accessibility; ↑ bio-oil yield; ↓ char; altered product composition; improved reactivity
Thermal (drying, torrefaction)	Moisture removal; partial devolatilization; hemicellulose degradation; ↑ hydrophobicity; ↑ grindability	↑ HHV; ↑ storage stability; ↓ fibrousness; product more suitable for co-firing; possible ↓ liquid oxygenates
Biological (fungal, microbial)	Selective lignin/hemicellulose degradation under mild conditions	↓ onset temperature; ↑ conversion; ↑ liquid yield; low energy input but slow processing

While these intrinsic biomass properties govern its fundamental decomposition pathways, process parameters, related to reactor operation, influence product formation through different mechanisms. In the following, these parameters are considered.

2.3.1 Temperature

Temperature is one of the most critical parameters in pyrolysis (Jones et al., 2013; Liu et al., 2025). Generally, increasing temperature reduces char yield while increasing gas production due to enhanced devolatilization and secondary cracking reactions (Nascimento et al., 2023; Li et al., 2017). For most lignocellulosic feedstocks, the maximum bio-oil yield occurs around 500 °C, whereas higher temperatures (>600 °C) favor gas formation (Pattiya, 2018; Rogers and Brammer, 2012). The char yield decreases from about 45 wt% at 350 °C to 25 wt% at 550 °C, while surface area, carbon content, and aromaticity increase (Puri et al., 2024; Li et al., 2017). The higher heating value (HHV) of char also increases

with temperature due to carbon enrichment, though excessive heating may reduce HHV by promoting dehydrogenation and mineral concentration (Pereira et al., 2022; Liu et al., 2025) (Figure 2.10). Elevated temperatures also increase the production of polycyclic aromatic hydrocarbons (PAHs), indicating stronger thermal cracking and potential toxicity at >700 ℃ (Pandey and Kim, 2011).

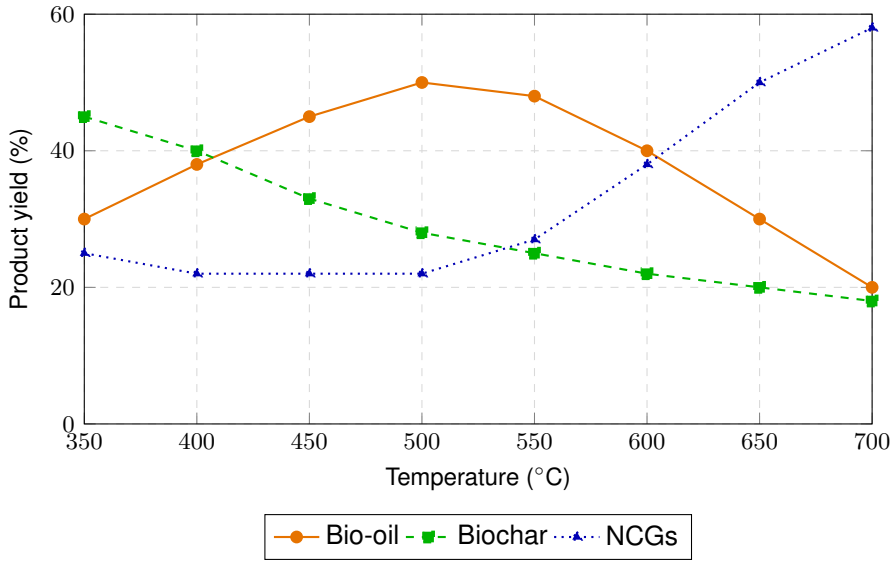

Figure 2.10: Effect of temperature on product yields from lignocellulosic biomass. Maximum liquid yield is obtained around 500–550 °C. Data representative of fast pyrolysis under high heating rate ($>$ 100 °C/s).

2.3.2 Heating Rate

The heating rate (HR) dictates the relative proportions of the three pyrolysis products (Pattiya, 2018; Jones et al., 2013; Liu et al., 2025). Low HRs (0.1–1 ℃/min), typical of slow pyrolysis, favor char formation (up to 70–80 wt%), while for fast pyrolysis, heating rates typically exceed 1000 ℃/s (Segers et al., 2024). Systems operating at heating rates around 10–200 ℃/s are considered “intermediate” because heat transfer is faster than in slow pyrolysis but still insufficient to reach the rapid devolatilization of fast or flash pyrolysis (Pereira et al., 2022). These conditions typically occur in reactors with limited heat-transfer efficiency, such as fixed-bed designs.

Increasing HR enhances fragmentation and depolymerization, reducing the time for secondary char–vapor reactions and leading to higher bio-oil yields (Westerhof et al., 2007; Liu et al., 2025). Conversely, too rapid heating can reduce secondary cracking and increase the formation of light gases (Figure 2.11). Heating rate also affects biochar morphology, indeed greater HRs result in smoother surfaces and lower pore volume because of the rapid release of volatiles. (Puri et al., 2024; Pereira et al., 2022).

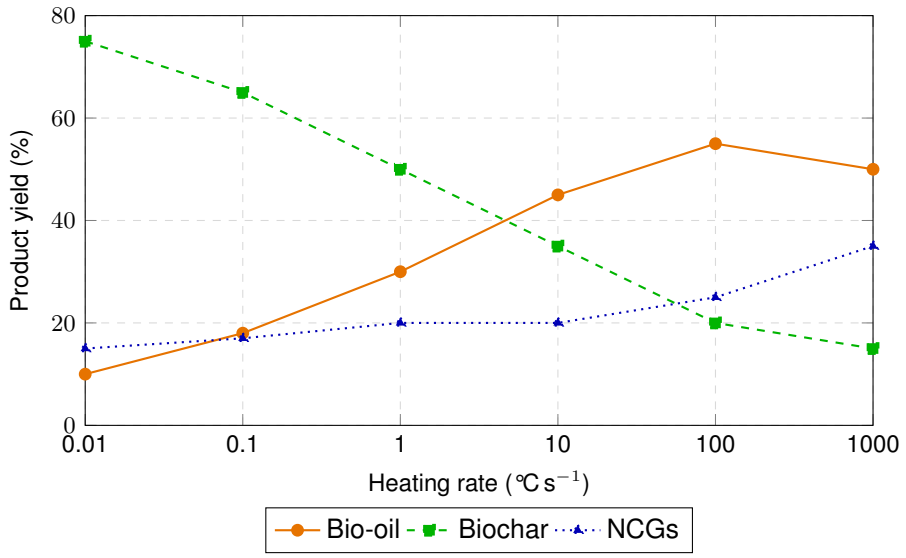

Figure 2.11: Qualitative influence of heating rate on product yields under typical fast-pyrolysis conditions (500–550 °C). Low heating rates (slow pyrolysis) favor char formation; increasing heating rate enhances bio-oil production, while very high heating rates promote light-gas formation.

2.3.3 Pressure

Pyrolysis is commonly performed at atmospheric pressure, but elevated pressures (>1 atm) can enhance biochar yield by increasing vapor residence time and promoting recondensation of volatiles on the char surface (Segers et al., 2024; Jones et al., 2013; Li et al., 2017). Higher pressures also result in chars with greater carbon concentration, stability, and electrical conductivity, beneficial for carbon sequestration or soil amendment (Pereira et al., 2022) (Figure 2.12).

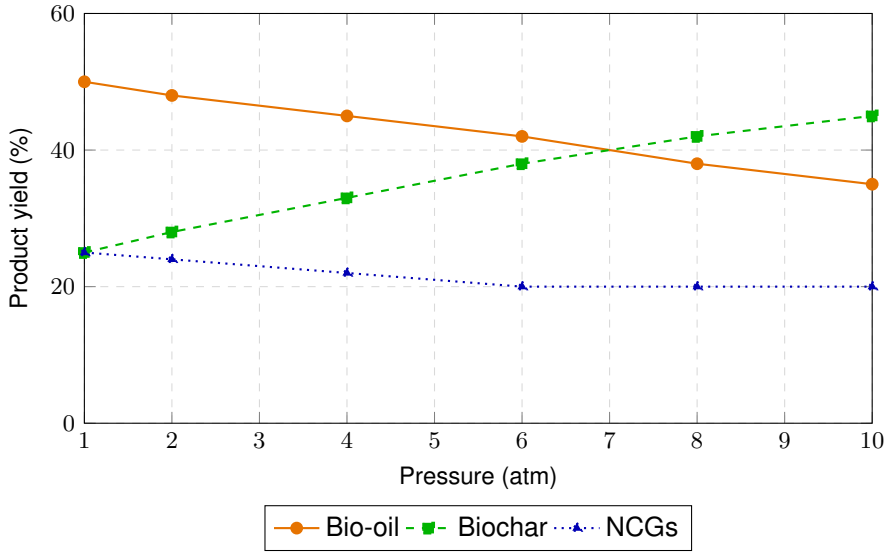

Figure 2.12: Qualitative effect of pressure on product yields under generic fast-pyrolysis conditions (500–550 °C; 30–40 °C min^{-1}). Increasing pressure tends to enhance char yield via vapor recondensation and deeper carbonization, while bio-oil and gas fractions decrease.

However, combining high temperature and high pressure tends to favor gas formation and reduces overall solid yield (Jones et al., 2013; Liu et al., 2025) (Figure 2.13).

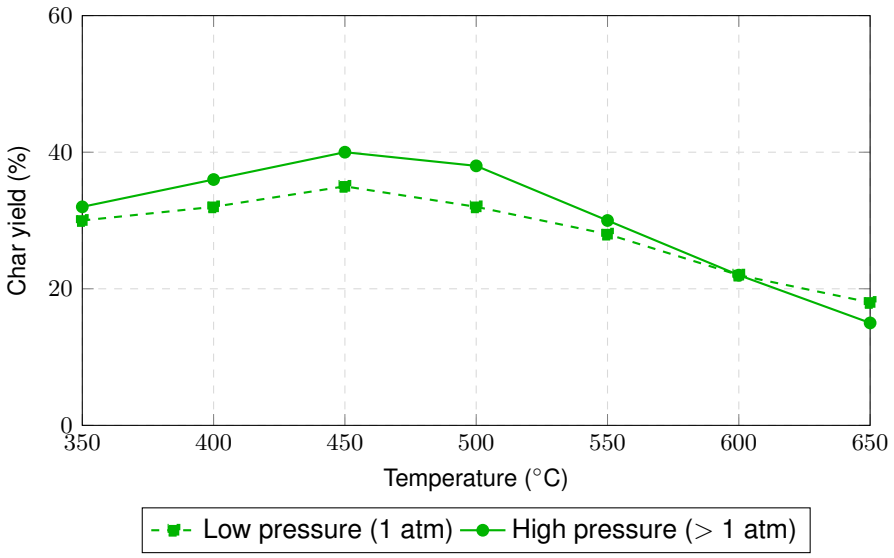

Figure 2.13: Qualitative interaction between temperature and pressure on char yield. Elevated pressure increases char formation at mid temperatures (400–500 °C) but at high temperatures (>550 °C) gasification dominates and solid yield decreases.

2.3.4 Residence Time

Residence time significantly influences product distribution (Jones et al., 2013; Liu et al., 2025). Short vapor residence times (<2 s) are essential for fast pyrolysis, minimizing secondary cracking and maximizing bio-oil yield (Pattiya, 2018; Westerhof et al., 2007). In contrast, longer residence times favor repolymerization and char growth, increasing solid yield but reducing liquid recovery (Pereira et al., 2022; Li et al., 2017) (Figure 2.14).

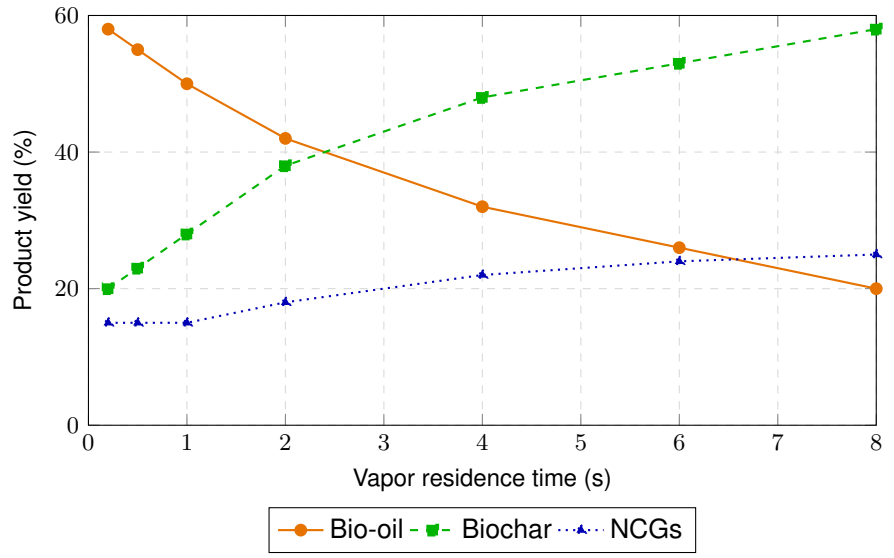

Figure 2.14: Qualitative effect of vapor residence time on product yields (generic fast-pyrolysis conditions). Short residence times favor liquid production; longer residence times increase char formation.

The interaction between residence time and temperature is often non-linear: prolonged residence times at low temperatures (<400 ℃) may lower char yield, while at higher temperatures they enhance carbonization and increase char stability (Jones et al., 2013; Liu et al., 2025) (Figure 2.15).

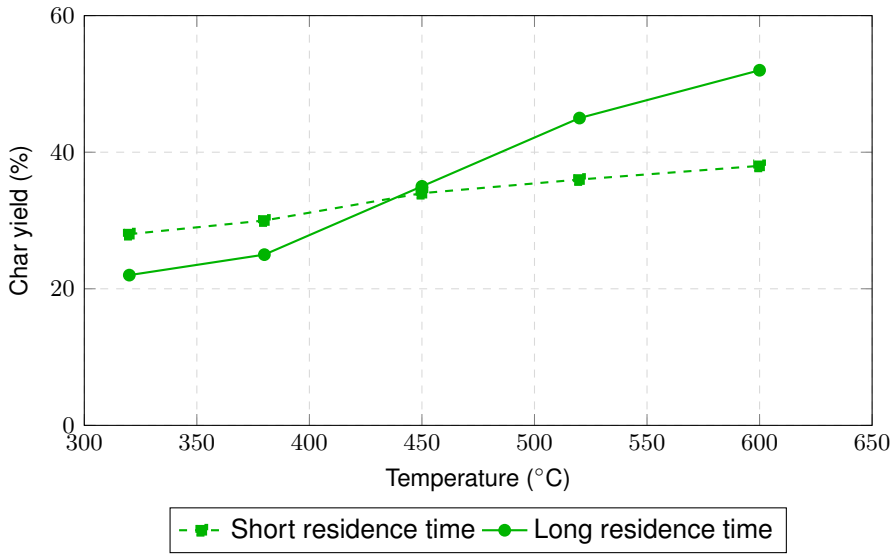

Figure 2.15: Effect of temperature and vapor residence time on char yield. At low temperatures ($< 400°$C), longer residence time may reduce char yield due to incomplete carbonization. At higher temperatures, longer residence enhances carbonization and increases char stability and yield.

2.3.5 Carrier Gas Flow Rate

The carrier gas (usually N_2 or Ar) serves to purge volatile products and control vapor residence time (Pattiya, 2018; Jones et al., 2013). A higher flow rate accelerates vapor removal, reducing secondary reactions and improving bio-oil quality, though it may slightly decrease char yield (Westerhof et al., 2007; Liu et al., 2025). Conversely, lower flow rates allow greater vapor–solid interaction, increasing repolymerization and secondary char formation (Pereira et al., 2022) (Figure 2.16). The choice of gas also influences product chemistry: H_2 and CO_2 can participate in reforming reactions, altering gas composition and enhancing hydrogen yield (Jones et al., 2013).

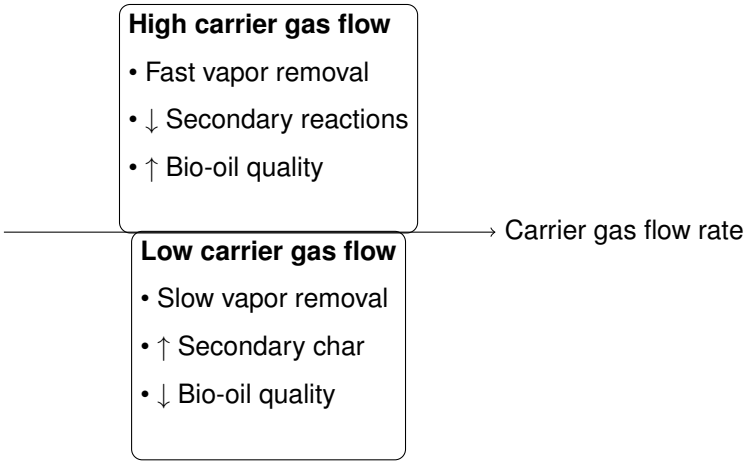

Figure 2.16: Effect of carrier gas flow rate on vapor residence time and product distribution during pyrolysis.

The influence of temperature, heating rate, pressure, residence time, and carrier gas highlights how operating conditions can steer product distribution and quality. However, these effects remain strongly

dependent on the intrinsic nature of the feedstock (Jones et al., 2013; Jerzak et al., 2024). Overall, biomass represents a complex yet versatile renewable resource whose properties must be carefully characterized and, when necessary, conditioned before processing (Pereira et al., 2022). Its composition, ash content, and moisture level govern both the technical feasibility and the environmental sustainability of downstream conversion routes. Understanding these intrinsic characteristics is essential for selecting appropriate thermochemical or biochemical technologies and optimizing product yield and quality (Pereira et al., 2022).

2.4 Spent Coffee Grounds as a Biomass Feedstock

Coffee is the second most consumed beverage in the world, and its global production results in an enormous generation of waste (Nascimento et al., 2023; Thoppil and Zein, 2021; Al Balushi et al., 2025). During coffee processing and consumption, a variety of residues are produced, including husk, pulp, mucilage, parchment, defective beans, silverskin, and spent coffee grounds (SCGs), (Tamilselvan et al., 2024) as shown in Figure 2.17.

Figure 2.17: Coffee residues

Among these, SCGs are the most abundant waste, generated after coffee brewing in households, cafés, and industrial facilities (Dari et al., 2025; Bartolucci et al., 2024; Stylianou et al., 2018). It is estimated that approximately 15 million tons of SCGs are produced annually worldwide, with 0.91 kg of waste generated per kilogram of ground coffee, and up to 2 kg of wet sludge per kilogram of instant coffee manufactured (Vardon et al., 2013). If disposed improperly, these residues can become environmental pollutants due to the presence of toxic compounds such as polyphenols, tannins, and caffeine.

Spent Coffee Grounds are a promising renewable feedstock within the context of a circular bioeconomy, as they contain significant amounts of polysaccharides (cellulose and hemicellulose, ≈50 wt%), lignin (≈20 wt%), proteins (10–20 wt%), and lipids (≈15 wt%) (Krause et al., 2019; Bartolucci et al., 2024; Solomakou et al., 2022). The main fatty acids are linoleic (≈45 wt%) and palmitic (≈38 wt%). They also contain valuable bioactive compounds such as antioxidants, polyphenols, and alkaloids, making them attractive for biochemical valorization (Pereira et al., 2022; Solomakou et al., 2022). The main compounds are resumed in Table 2.7.

Table 2.7: Chemical composition of spent coffee grounds (SCGs) reported in literature.

Component	**Content (% wt, wet basis)**
Moisture	1.20–74.70
Cellulose	12.40 ± 0.80
Hemicellulose	39.10 ± 1.90
Arabinose	3.60–6.00
Mannose	19.10–47.00
Galactose	16.40–30.00
Lignin (total)	23.90 ± 1.70
Insoluble	17.60 ± 1.60
Soluble	6.30 ± 0.40
Fat (lipids)	2.30–19.00
Ash	0.40–2.20
Protein	4.30–17.40
Total dietary fibers	36.90–60.50
Insoluble	50.80 ± 1.60
Soluble	9.70 ± 2.70

From an energy perspective and due to their composition, SCGs are highly suitable for thermochemical conversion processes such as pyrolysis. The high heating value (HHV) of SCGs, reported between 18 and 20 MJ/kg, is comparable to other lignocellulosic residues, confirming their potential as a feedstock for energy and chemical recovery (Krause et al., 2019; Thoppil and Zein, 2021; Matrapazi and Zabaniotou, 2020).

Among different thermochemical conversion processes, fast pyrolysis has attracted particular interest due to its ability to maximize the liquid bio-oil yield under moderate residence times and heating rates (Pattiya, 2018; Bartolucci et al., 2024; Jerzak et al., 2024). According to several and as shown in Figure 2.18, the optimum temperature range for bio-oil production lies between 500 and 550 ℃, where the highest bio-oil yields (40–58 wt%) are typically observed (Primaz et al., 2018; Bartolucci et al., 2024). Beyond 550 ℃, secondary cracking reactions take place and promote the formation of gaseous products, reducing the liquid yield as a consequence (Jones et al., 2013). In contrast, lower temperatures (<400 ℃) favor solid biochar production, limiting the liquid product (AlMallahi et al., 2023).

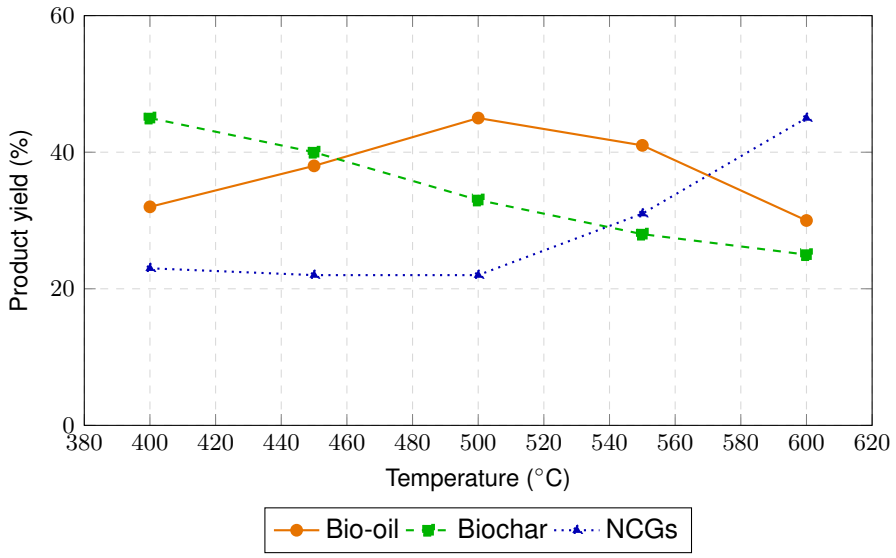

Figure 2.18: Effect of pyrolysis temperature on product yields from spent coffee grounds (SCGs) at a heating rate of 30–40 °C min^{-1}. Bio-oil yield peaks at 500–550 °C, beyond which secondary cracking reactions increase gas production and reduce the liquid fraction.

In addition to temperature, also the heating rate plays a crucial role in determining product distribution and bio-oil characteristics (Eke et al., 2020; Bartolucci et al., 2024; Li et al., 2017). At low heating rates (typically below $10°\mathrm{C} \cdot \mathrm{min}^{-1}$), heat transfer to the particle core is slower, leading to prolonged devolatilization and promoting secondary char formation. As a result, bio-oil yields are lower, and the liquid fraction often contains a higher proportion of oxygenated and heavy compounds. In contrast, higher heating rates ($20 - 100\ °\mathrm{C} \cdot \mathrm{min}^{-1}$) favor rapid depolymerization and volatilization, reducing the residence time of primary vapors within the hot zone. This minimizes secondary cracking and condensation reactions, thereby increasing the yield of lighter and less oxygenated compounds. However, higher heating rates can lead to the complete breakdown of lignin-derived compounds, producing a bio-oil with a wider range of molecular weights and more unstable components (Figure 2.19).

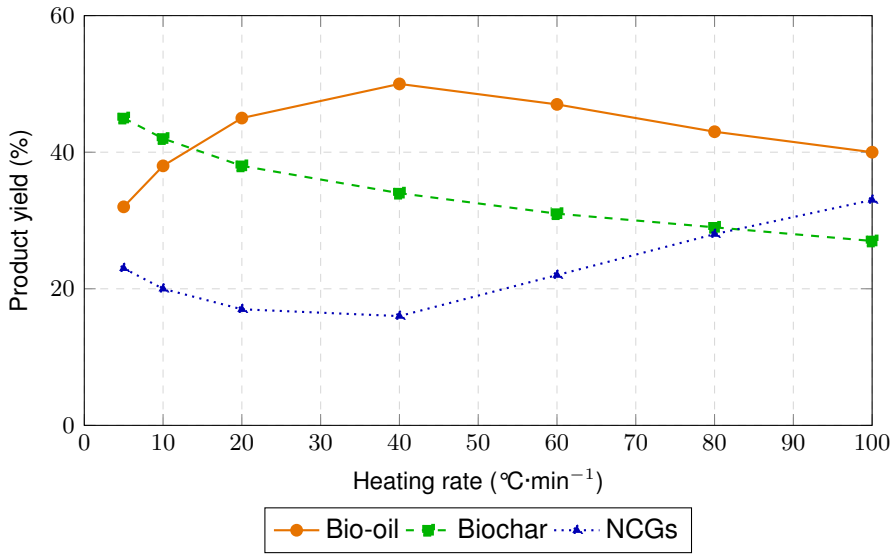

Figure 2.19: Effect of heating rate on product yields from SCGs under fast-pyrolysis conditions. The heating rate was varied between 30–40 °C min^{-1}, while the pyrolysis temperature was maintained within the range 500–550 °C. Higher heating rate values generally promote bio-oil formation by limiting secondary cracking, whereas lower values favor char production.

Overall, an intermediate heating rate (around $20 - 40\ ^\circ\mathrm{C} \cdot \mathrm{min}^{-1}$) is often considered optimal for maximizing both the quantity and quality of bio-oil derived from spent coffee grounds, ensuring a balance between devolatilization efficiency and vapor residence time (Bartolucci et al., 2024).

Besides temperature and heating rate, product distribution is also influenced by residence time, particle size, and carrier gas flow rate (Jones et al., 2013; Liu et al., 2025). On the one hand short vapor residence time and small particle sizes promote heat transfer and reduce secondary cracking, thus improving bio-oil yield (Westerhof et al., 2007). On the other hand, high moisture contents or long residence times enhance char and gas formation (Pereira et al., 2022). Even though their influence is lower compared to that of temperature and heating rate, it's important to optimize them for ensuring the best possible final quality.(Bartolucci et al., 2024).

During pyrolysis, the main macromolecular constituents of spent coffee grounds —cellulose, hemicellulose, lignin, proteins, and lipids—undergo complex decomposition reactions that determine the yield and composition of the resulting products (Vardon et al., 2013; Bartolucci et al., 2024; Liu et al., 2025). Understanding the thermal behaviour of SCGs is therefore essential for defining suitable operating conditions for bio-oil production (Bartolucci et al., 2024).

Thermogravimetric analyses (TGA/DTG) of SCGs reported in literature show three main stages of mass loss (Figure 2.20)(Krause et al., 2019; Bartolucci et al., 2024):

1. **Moisture release** (below $150\ ^\circ\mathrm{C}$): evaporation of physically bound water.

2. **Active pyrolysis zone** $(200 - 400\ ^\circ\mathrm{C})$: decomposition of cellulose and hemicellulose, generating volatile oxygenated compounds such as acetic acid and furfural.

3. **Lignin degradation and char formation** $(400 - 600\ ^\circ\mathrm{C})$: slow breakdown of aromatic structures leading to phenolic vapors and residual char.

The presence of lipids and proteins in SCGs slightly changes the degradation profile to higher temperatures (300-550 ℃) and leads to the formation of additional long-chain hydrocarbons and nitrogen-containing species in the volatile phase (Bartolucci et al., 2024). These effects explain the unique composition of the SCGs bio-oil compared to conventional lignocellulosic feedstocks.

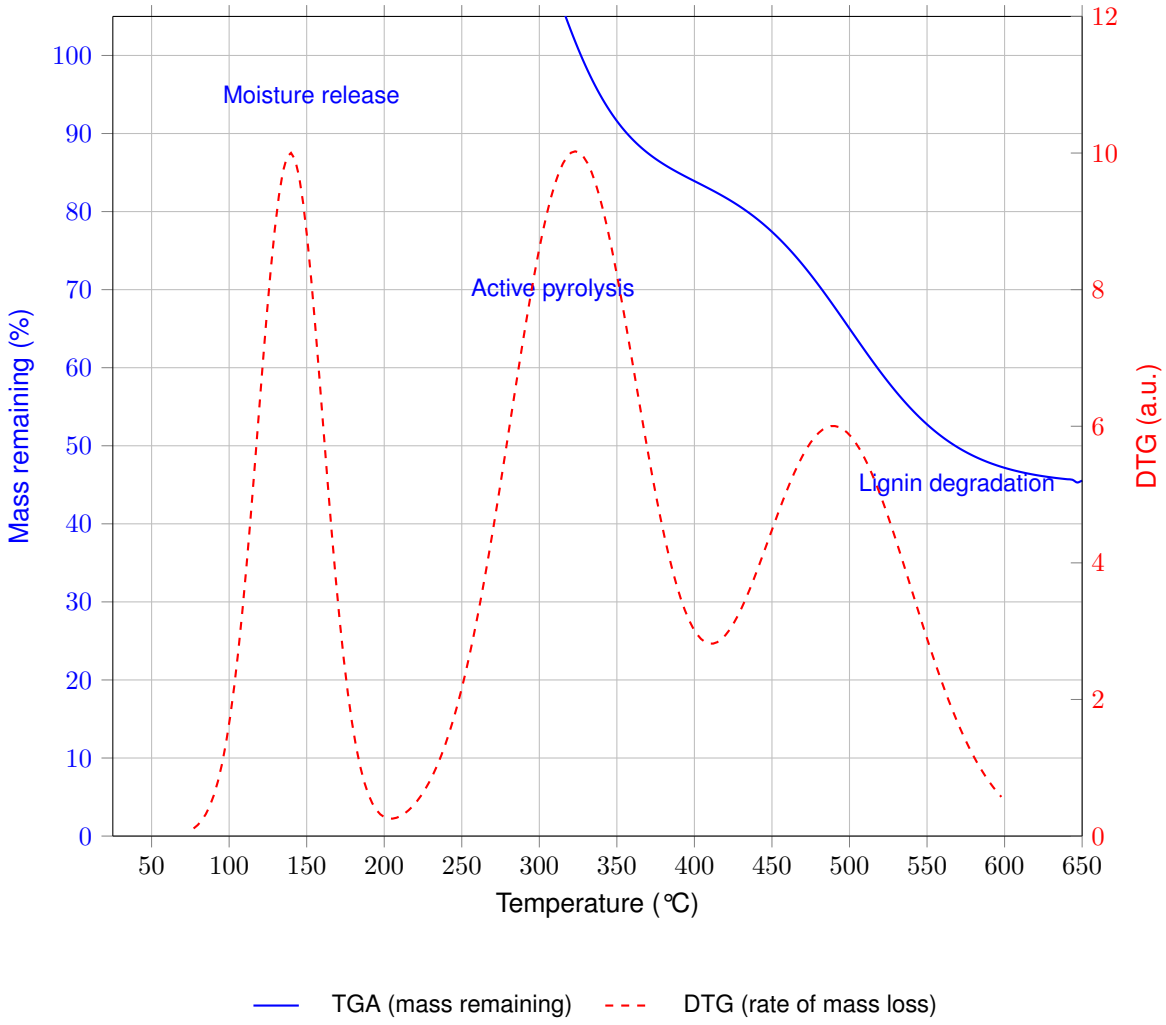

Figure 2.20: Schematic thermogravimetric (TGA) and derivative thermogravimetric (DTG) profile of spent coffee grounds (SCGs). The blue solid line is the TGA curve (mass remaining), the red dashed line is the DTG curve (rate of mass loss).

The bio-oil composition derived from SCGs differs significantly from that of conventional lignocellulosic feedstocks (Pereira et al., 2022). Analysis has shown that SCG bio-oil is rich in fatty acids (palmitic, oleic, stearic acids), phenolics, furans, and nitrogenated compounds (Krause et al., 2019; Malagón-Romero et al., 2023; Vilas-Boas et al., 2025). The oxygen content decreases from approximately 35–40% in the feedstock to 13–16% in the bio-oil, while carbon density increases, yielding a higher heating value (HHV) between 28.00 and 41.00 MJ/kg, notably higher than that of ethanol (28.90 MJ/kg) (Bartolucci et al., 2024). However, SCGs bio-oils also exhibit higher nitrogen content (2.60–4.30 wt%), derived from the protein fraction of the feedstock, which can pose challenges for direct fuel applications but offers potential for specialty chemical production (Pereira et al., 2022). The main compositional and energetic differences between raw spent coffee grounds and the corresponding bio-oil obtained via

fast pyrolysis are summarized in Table 2.8. The data highlight the strong deoxygenation and carbon enrichment of the product, which lead to a significant increase in energy density.

Table 2.8: Comparison between raw spent coffee grounds (SCGs) and the corresponding bio-oil produced by fast pyrolysis.

Property	**Raw SCGs (feedstock)**	**Bio-oil (after pyrolysis)**
Oxygen content (wt%)	35.00–40.00	13.00–16.00
Carbon content (wt%)	45.00–50.00	70.00–75.00
Hydrogen content (wt%)	6.00–8.00	8.00–10.00
Nitrogen content (wt%)	1.00–2.00 (proteins)	2.60–4.30
Higher heating value (MJ/kg)	18.00–22.00	28.00–41.00
Major chemical families	Polysaccharides, lipids, proteins, lignin	Fatty acids, phenolics, furans, N-compounds
Dominant fatty acids	Linoleic (≈45.00 wt%), Palmitic (≈38.00 wt%)	Palmitic, Oleic, Stearic acids
Physical appearance	Solid, granular biomass	Dark brown viscous liquid
Main transformation	Thermal degradation of biopolymers	Deoxygenation and condensation reactions
Potential applications	Waste biomass, compost, extraction of bioactives	Biofuel precursor, chemical feedstock

In summary, pyrolysis of spent coffee grounds stands out as a sustainable pathway for upcycling coffee waste into high-value bioproducts, aligning with the principles of the circular economy (Dari et al., 2025; Pereira et al., 2022; Pongsiriyakul et al., 2024). While spent coffee grounds represent the most extensively studied coffee-derived residue, several other products generated along the coffee value chain, such as green coffee and coffee cherry husk, have been investigated for their potential valorization.

2.4.1 Green Coffee

Green Coffee refers to unroasted coffee beans, collected before undergoing any thermal treatment (Figure 3.13) (Dari et al., 2025; Al Balushi et al., 2025). In this state, the biomass retains its native chemical structure, with higher moisture content and a greater proportion of organic acids, lipids and thermally labile compounds compared with roasted coffee residues (Pongsiriyakul et al., 2024).

Figure 2.21: Green Coffee

From a chemical perspective, green coffee is particularly rich in phenolic compounds, mainly chlorogenic acids (Choe, 2025), which represent one of the most abundant classes of bioactive molecules in coffee beans. These compounds are widely recognized for their antioxidant properties and play a key role in determining the overall chemical quality of coffee-derived materials.

Several studies have shown that the phenolic content and antioxidant capacity of green coffee are significantly higher than those of roasted coffee (Choe, 2025; Romani et al., 2016), as thermal processing leads to partial degradation or transformation of phenolic compounds. As a result, green coffee is often adopted as a reference material in studies aimed at evaluating the impact of processing steps on the chemical composition and antioxidant potential of coffee.

2.4.2 Coffee Cherry Husk

Coffee cherry husk refers to the solid by-product obtained during the dry processing of coffee cherries and mainly consists of the outer layers of the fruit, including the pulp, skin, mucilage residues and parchment, while the coffee bean itself is removed (Figure 2.22)(Dari et al., 2025; Al Balushi et al., 2025). Compared to green coffee beans, coffee cherry husk contains a higher fraction of non-structural components, such as sugars, organic acids and fibrous materials, resulting in a distinct chemical composition

(Stylianou et al., 2018; Barahmand et al., 2025).

Figure 2.22: Enter Caption

From a chemical standpoint, coffee cherry husk is known to retain phenolic compounds and other bioactive molecules, which are primarily associated with the pulp and skin of the coffee fruit (Dari et al., 2025; Solomakou et al., 2022). These compounds have been widely reported for their antioxidant properties and have attracted increasing interest in the context of coffee by-product valorization.

2.5 Products and Yields

The thermal decomposition of biomass through pyrolysis leads to the formation of three main products: a solid carbonaceous residue (biochar), a liquid condensate (bio-oil), and a mixture of permanent gases, commonly referred to as non-condensable gases (NCGs) or syngas (Setter et al., 2020; Pereira et al., 2022; Jerzak et al., 2024). These products are generated simultaneously through complex devolatilization, condensation, and carbonization reactions that occur during the heating of biomass in the absence of oxygen (Jones et al., 2013). Although they originate from the same process, each fraction has distinct physical, chemical, and energetic properties, which define its potential applications in energy production, materials synthesis, and environmental technologies (Jerzak et al., 2024; Ferrari et al., 2025).

The biochar fraction is a solid material rich in fixed carbon and inorganic minerals. It can serve as a solid fuel, a carbon sequestration medium, or an adsorbent in soil and water treatment. The bio-oil fraction is a dark, viscous liquid composed of hundreds of oxygenated organic compounds. It represents the main energy carrier in fast pyrolysis and can be used directly as a heating fuel or upgraded into hydrocarbons similar to conventional fossil fuels (Pattiya, 2018). The gaseous fraction, consisting primarily of CO_2, CO, H_2, and CH_4, possesses a moderate heating value and can be recycled within the process to provide the heat required for pyrolysis reactions or used externally for combustion and co-firing. Together, these three products define the overall energy balance and technological viability of the pyrolysis process (Rogers and Brammer, 2012; Jones et al., 2013). Their relative yields depend on the pyrolysis regime (slow, intermediate, or fast) and on the reaction pathways involved (Segers et al., 2024; Pereira et al., 2022; Li et al., 2017), but in all cases, understanding their composition, properties, and potential uses is essential for optimizing biomass conversion systems.

The following subsections describe each product in detail, highlighting their characteristics, formation mechanisms, and main applications.

2.5.1 Biochar

Biochar is the solid carbonaceous residue produced during the pyrolysis of biomass in the absence of oxygen (Pereira et al., 2022; Nematian et al., 2021). It typically contains a high proportion of carbon and small amounts of oxygen, hydrogen, and inorganic minerals originally present in the feedstock (Cai et al., 2020). With a heating value of about 20–30 MJ/kg, biochar can serve as a solid fuel for boilers or be co-fired with fossil fuels (Segers et al., 2024; Pereira et al., 2022). Alternatively, it can be steam-reformed or thermally cracked to generate syngas or hydrogen, making it a valuable by-product of the pyrolysis process (Sikarwar et al., 2016; Ronsse et al., 2015; Jones et al., 2013).

Typical ranges reported in the literature for biochars obtained from lignocellulosic biomass are summarized in Table 2.9.

Table 2.9: Typical properties of biochar from biomass pyrolysis.

Property	**Description / Typical values**
Physical state	Solid, black, carbonaceous material with porous structure and high stability.
Typical yield (wt%)	15.00–35.00, depending on feedstock composition, temperature, and heating rate.
Composition / constituents	Mainly fixed carbon (60–90 wt%), small amounts of hydrogen and oxygen, and inorganic minerals (ash).
Elemental features	C: 60–90 wt%; H: 1–4 wt%; O: 5–20 wt%; N: 0.5–2 wt%. Low H/C ratio (<0.4) for chars produced above 500°C, indicating high aromaticity and stability.
Heating value	20–30 MJ/kg, depending on carbon content and feedstock type.
pH / Reactivity	Typically alkaline (pH 6–10); chemically stable and resistant to degradation.
Dependence on temperature	Higher pyrolysis temperature and heating rate reduce yield but increase fixed carbon content, aromaticity, and stability.

In recent years, the importance of biochar has increased substantially due to its wide range of environmental and industrial applications. In agriculture, it acts as an efficient soil conditioner that improves organic carbon content, cation exchange capacity, aeration, water retention, and microbial activity, while mitigating soil acidification (Nematian et al., 2021; Ferrari et al., 2025). Studies have shown that biochar addition can reduce CH_4 and N_2O emissions by altering abiotic and biotic soil processes, with emission reductions of up to 50% for N_2O and complete suppression of CH_4 in some trials. These effects contribute to carbon sequestration, since biochar can retain up to 50% of the original biomass carbon, thus playing a significant role in climate change mitigation (Segers et al., 2024; Pereira et al., 2022).

Beyond soil amendment, biochar can be physically or chemically activated to enhance its surface area and porosity, making it suitable for adsorption of pollutants, removal of heavy metals and organic contaminants, and as a support or catalyst in chemical and electrochemical processes (Cai et al., 2020; Pereira et al., 2022; Zakzeski et al., 2010), including supercapacitors and fuel cells. Its adsorptive ca-

pacity depends strongly on the feedstock and pyrolysis temperature, which also influence its stability and aromaticity (Jones et al., 2013). Chars with a low H/C ratio (< 0.4), typically obtained at temperatures above 500 ℃, are highly stable and suitable for long-term carbon storage or even safe use in animal applications (Ronsse et al., 2015; Pereira et al., 2022). The main applications for biochar are summerized in Figure 2.23.

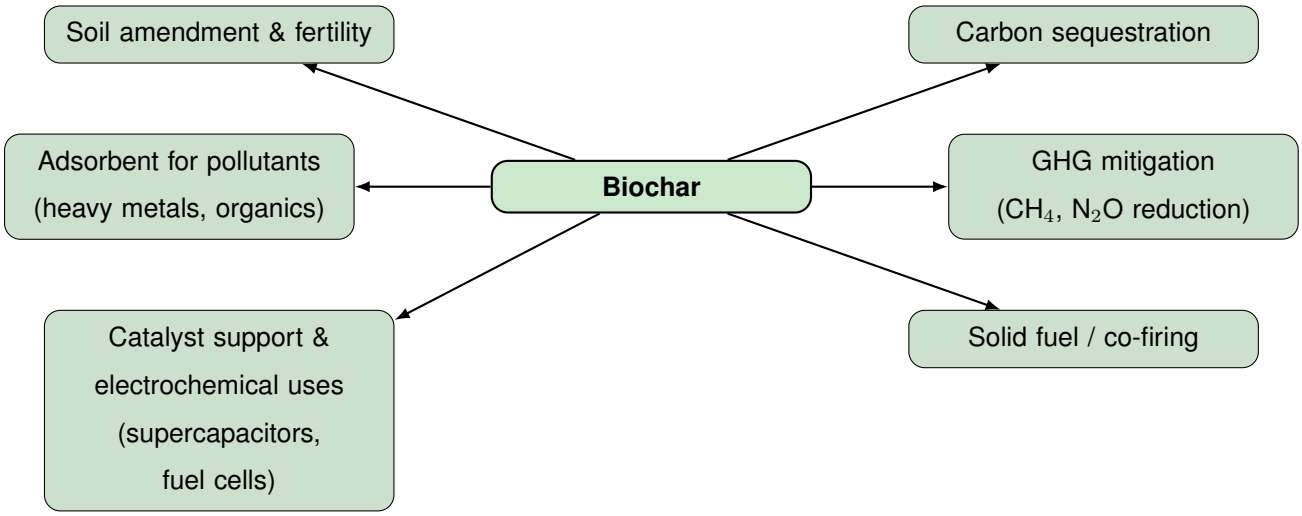

Figure 2.23: Applications of biochar from biomass pyrolysis.

Biochar yield and quality are strongly affected by process parameters such as temperature, heating rate, residence time, and feedstock composition (Jones et al., 2013; Liu et al., 2025; Ferrari et al., 2025). Generally, higher temperatures and faster heating rates decrease the char yield but increase its fixed carbon content and stability (Puri et al., 2024). Moreover, the introduction of steam during pyrolysis can enhance char yield due to secondary reactions involving gas–solid interactions (Jones et al., 2013).

Current studies focus on the co-pyrolysis of biomass and plastics, in order to obtain high-quality char with desirable characteristics. (Cai et al., 2020; Duongbia et al., 2025; Pereira et al., 2022; Barahmand et al., 2025).

2.5.2 Bio-Oil

Bio-oil is a liquid product obtained from the thermal decomposition of biomass during pyrolysis (Lachos-Perez et al., 2023; Jerzak et al., 2024; Barahmand et al., 2025). However, the terminology used in the literature varies depending on the feedstock, process conditions, and intended applications. In studies focused on energy production and thermochemical conversion, the term bio-oil or pyrolytic liquid is generally adopted. Conversely, when the condensate is derived from lignocellulosic materials at lower heating rates or is used for agricultural and food applications, it is often referred to as wood vinegar or liquid smoke (Mattos et al., 2019; Ouattara et al., 2023). These products share a similar origin but differ significantly in their chemical composition, water content, and functional properties, reflecting the diversity of production pathways and end-uses reported in the literature. Table 2.10 resumes the main termrs used.

Table 2.10: Main terminology used in the literature to refer to pyrolysis-derived liquid products.

Term used	**Typical context**	**Notes**
Bio-oil	Energy production, fast pyrolysis	General and most common technical term; obtained from rapid heating of lignocellulosic biomass under oxygen-free conditions.
Wood vinegar	Slow pyrolysis, carbonization, agriculture	Rich in acetic acid and phenolics; used as biostimulant, natural pesticide, or soil conditioner.
Liquid smoke	Food industry, aroma production	Used as flavoring agent or preservative; derived from condensable vapors of biomass pyrolysis.
Pyrolytic liquid / *Pyrolysis condensate*	Generic research context	Neutral terminology for the liquid fraction collected from pyrolysis condensers.
Aqueous phase / *Organic phase*	Product separation and upgrading studies	Describe the two immiscible fractions of bio-oil after condensation.
Phenolic-rich fraction, *acetic acid-rich liquid*	Analytical chemistry, product valorization	Denomination based on dominant chemical constituents identified through GC–MS or HPLC.

In this work, the term bio-oil is used to refer to the liquid fraction obtained from the fast pyrolysis of spent coffee grounds (Bartolucci et al., 2024). Bio-oil is a complex, dark-brown mixture composed of water, fine char particles, and a wide range of organic compounds derived from the decomposition of cellulose, hemicellulose, and lignin (Oliveira Farrapeira et al., 2021; Lachos-Perez et al., 2023; Pereira et al., 2022; Gracia-Vitoria et al., 2023; Machado et al., 2022). These include acids, alcohols, aldehydes, ketones, furans, esters, phenols, and lignin-derived oligomers (Vilas-Boas et al., 2025). Because bio-oil retains nearly the same elemental composition as the original biomass, it typically contains high oxygen content (35–50%), low pH (2–4), and 15–30 wt% water (Rogers and Brammer, 2012). Moreover, the high heating value of bio-oil strongly depends on the feedstock: values can reach 40 MJ/kg for oil from lipid-rich seeds, but are generally 20–25 MJ/kg for lignocellulosic biomass (Table 2.11).

Table 2.11: Typical properties of bio-oil from biomass fast pyrolysis.

Property	**Description / Typical values**
Physical state	Dark brown viscous liquid containing fine char particles and water.
Typical yield (wt%)	40–60, depending on feedstock and process temperature.
Composition / constituents	Water (15–30 wt%), oxygenated organics such as acids, aldehydes, ketones, alcohols, phenols, furans, and lignin-derived oligomers.
Elemental features	C: 45–60 wt%; H: 6–8 wt%; O: 35–50 wt%; N: 0.1–0.5 wt%. High oxygen content and low H/C ratio compared to fossil fuels.
Heating value	20–25 MJ/kg for lignocellulosic feedstocks; up to 40 MJ/kg for lipid-rich biomass.
pH / Reactivity	Acidic (pH 2–4) and chemically unstable; prone to polymerization and phase separation during storage.
Dependence on temperature	Maximum liquid yield at 500–550°C; higher temperatures promote secondary cracking and gas formation.

Bio-oil can be separated into water-soluble and water-insoluble fractions (Westerhof et al., 2007; Schulzke et al., 2016; Figueiredo et al., 2017). The former contains light oxygenated compounds such as alcohol and acids, while the latter, known as pyrolytic lignin, consists of larger aromatic molecules derived from lignin and represents up to 40 w$\widehat{\%}$ of the oil (Zhang et al., 2007). These lignin-derived compounds tend to polymerize and condense during storage, leading to an increase in molecular weight, viscosity, and eventual phase separation into a heavy tar-like fraction and a lighter aqueous phase (Lachos-Perez et al., 2023; Pereira et al., 2022). The high oxygen and water contents also make bio-oil chemically unstable, corrosive, and immiscible with hydrocarbon fuels, which limits its direct use as a transportation fuel (Lachos-Perez et al., 2023; Jones et al., 2013; Gracia-Vitoria et al., 2023; Santos et al., 2025).

Despite these challenges, bio-oil remains an attractive renewable energy carrier (Shah et al., 2016; Rogers and Brammer, 2012). It can be directly used as a substitute for fuel oil or diesel in stationary applications such as boilers, furnaces, engines, and turbines, provided that certain system modifications are made (Pattiya, 2018). Combustion tests have shown lower NO_x emissions compared to conventional fuels, although CO and particulate emissions may increase due to incomplete combustion and the presence of non-volatile compounds. In addition to its energy use, bio-oil is a valuable chemical feedstock (Lachos-Perez et al., 2023; Pereira et al., 2022; Machado et al., 2022; El-Sayed, 2025). It contains hundreds of identifiable compounds that can be recovered or converted into phenols and aromatics which are precursors for resins, solvents, and specialty (Hu et al., 2022). Figure 2.24 summerizes bio-oil's main applications.

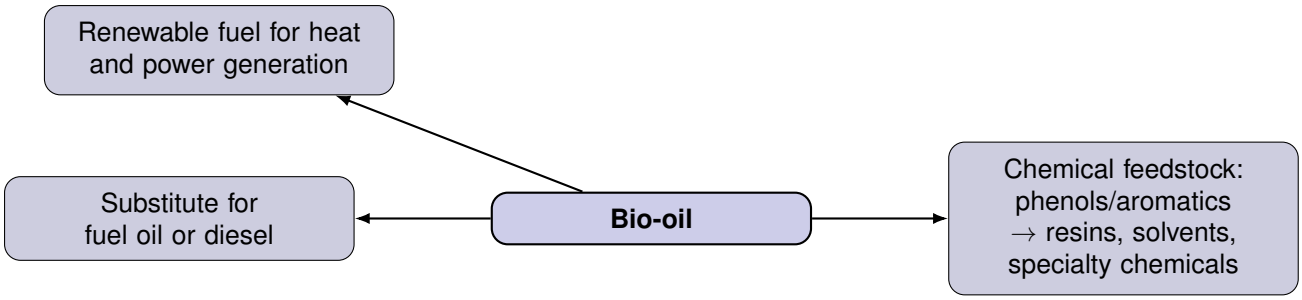

Figure 2.24: Applications of bio-oil from biomass pyrolysis.

2.5.3 Syngas

The gaseous fraction, commonly referred to as non-condensable gases (NCGs) or syngas, represents the third major product of biomass pyrolysis (Jones et al., 2013). It consists primarily of carbon dioxide (CO_2), carbon monoxide (CO), hydrogen (H_2), and methane (CH_4), with smaller quantities of light hydrocarbons such as ethane (C_2H_6), ethylene (C_2H_4), propane (C_3H_8), and propylene (C_3H_6) (Pattiya, 2018). The composition and yield of non-condensable gases are strongly dependent on the biomass composition, heating rate, temperature, and residence time. The three main components of biomass—cellulose, hemicellulose, and lignin—contribute differently to gas formation (Pereira et al., 2022): cellulose decomposition tends to produce CO, hemicellulose releases CO_2, while lignin generates CH_4 and heavier hydrocarbons (Segers et al., 2024). Gas yields generally increase with temperature (Jones et al., 2013), as secondary cracking and reforming reactions convert condensable vapors and char into gaseous species (Pattiya, 2018). No clear linear relationship with the heating rate has been identified (Pereira et al., 2022), indicating that factors such as reactor configuration, particle size, feedstock moisture content, and carrier gas flow exert significant influence (Westerhof et al., 2007; Pattiya, 2018). The heating value of the non-condensable gases varies from 5.7 to 14.6 MJ/m³, depending on the relative proportions of CO, CH_4, and H_2 (Pattiya, 2018; Sikarwar et al., 2016; Jones et al., 2013). Typical syngas compositions from fast pyrolysis contain 20–45% CO_2, 15–35% CO, 10–20% H_2, and 2–10% CH_4. The calorific value can be improved by optimizing process parameters or by introducing catalysts and steam reforming to promote hydrogen production (Sikarwar et al., 2016).

Typical compositions and properties reported in the literature for syngas produced during biomass fast pyrolysis are summarized in Table 2.12.

Table 2.12: Typical properties of syngas (non-condensable gases) from biomass pyrolysis.

Property	**Description / Typical values**
Physical state	Gas mixture produced as the non-condensable fraction during pyrolysis; colorless and combustible.
Typical yield (wt%)	10–25, increasing with temperature and secondary cracking of condensable vapors.
Composition / constituents	Mainly CO_2, CO, H_2, CH_4; also C_2–C_3 hydrocarbons such as ethane, ethylene, propane, and propylene.
Elemental features	Carbon-rich and hydrogen-containing gases; H_2/CO ratio typically between 0.3 and 1.0.
Heating value	5.7–14.6 MJ/m^3, depending on the proportion of CO, CH_4, and H_2.
pH / Reactivity	Neutral gas mixture; highly reactive and combustible.
Dependence on temperature	Gas yield increases with temperature due to secondary cracking and reforming reactions; higher temperatures enhance H_2 and CO formation.

From an energy standpoint, the gaseous product is combustible and can be recycled within the pyrolysis unit to provide heat or serve as a fluidizing and carrier gas in fluidized-bed systems (Segers et al., 2024; Jones et al., 2013; Jerzak et al., 2024). The simultaneous presence of CO, CH_4, and H_2 makes the gas suitable for industrial combustion, co-firing, or synthetic fuel production after reforming (Talmadge et al., 2021). Moreover, the use of syngas for combined heat and power (CHP) generation has been explored as a route to enhance the overall energy efficiency of pyrolysis-based systems (Sikarwar et al., 2016). Beyond its energetic applications, the gaseous fraction offers valuable insight into the reaction mechanisms governing pyrolysis and the thermal degradation pathways of biomass. The analysis of gas evolution provides crucial information on reaction kinetics and the contribution of different biomass components to gas formation.

Ultimately, optimizing the yield and composition of non-condensable gases, particularly by increasing the H_2/CO ratio, is a key step toward the integration of biomass pyrolysis with renewable hydrogen and syngas-based fuel production, reinforcing its role in sustainable energy systems (Figure 2.25) (Sikarwar et al., 2016; Jones et al., 2013; Barahmand et al., 2025).

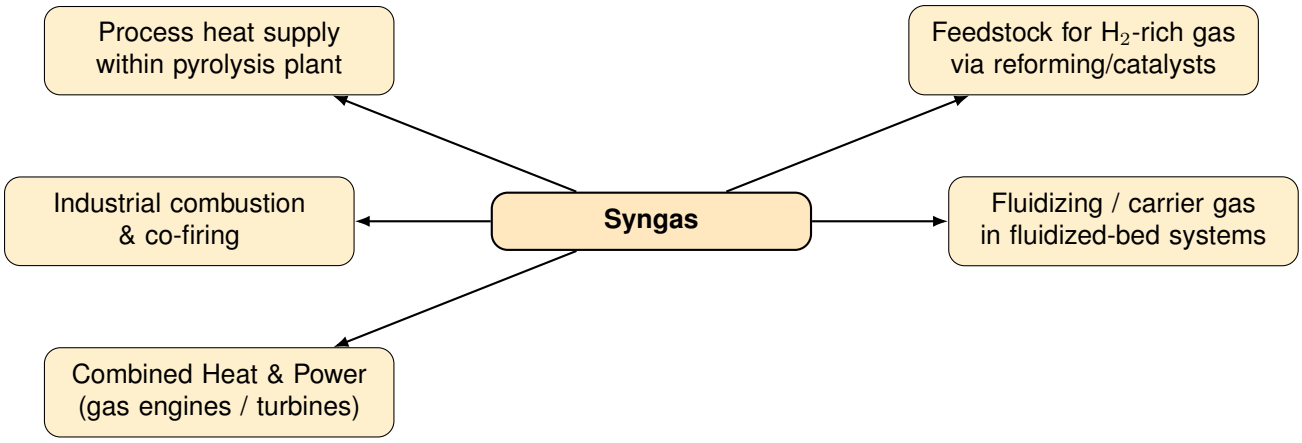

Figure 2.25: Applications of syngas from biomass pyrolysis.

2.6 Influence of Process Parameters

The distribution and properties of pyrolysis products are strongly influenced by several operating and material parameters, summerized in Table 2.13 (Jones et al., 2013; Jerzak et al., 2024). These include the feedstock composition, reaction temperature, heating rate, residence time, pressure, and carrier gas flow rate (Pattiya, 2018). Understanding their individual and combined effects is essential to optimize product yields and tailor biochar, bio-oil, or gas compositions for specific applications (Westerhof et al., 2007; Pereira et al., 2022).

Biomass is composed primarily of cellulose, hemicellulose, lignin, extractives, water, and inorganic minerals (ash) (Pereira et al., 2022). Each component decomposes differently, producing distinct fractions of solid, liquid, and gaseous products (Jones et al., 2013).

• Moisture content plays a critical role in fast pyrolysis efficiency (Eke et al., 2020; Jones et al., 2013). Excessive moisture content (>10 wt%) reduces the reactor temperature due to the latent heat of vaporization. Moreover, it increases the water content of bio-oil, leading to lower heating value, higher acidity, and lower density. Therefore, for optimal performance, the moisture content should remain below 10 wt%.

• Cellulose and hemicellulose decompose rapidly between 220–400 ℃, generating mainly volatile compounds and bio-oil precursors such as levoglucosan, furfural, and organic acids (Segers et al., 2024). Lignin, in contrast, decomposes over a wider range (160–900 ℃) and contributes more significantly to char formation and aromatic compounds. Higher lignin content generally results in bio-oils with higher viscosity and molecular weight (Segers et al., 2024; Pereira et al., 2022).

• Extractives, including fats, resins, and terpenes, can decrease the bio-oil production and prevent the creation of levoglucosan.(Westerhof et al., 2007). Char reactivity and bio-oil stability are improved by their removal (Jones et al., 2013).

• Inorganic species, particularly alkali metals (K, Na), act as catalysts that promote char formation and secondary reactions, thus reducing liquid yields (Puri et al., 2024).

Table 2.13: Influence of feedstock composition on product distribution and properties in fast pyrolysis.

Parameter	**Thermal behaviour**	**Main effect on products**
Moisture content	Evaporation absorbs heat	↓ reactor temperature; ↑ water in oil; ↓ HHV; undesirable >10 wt%
Cellulose	Decomposition 220–350 ℃	↑ volatiles; precursors: levoglucosan, acids; ↑ bio-oil yield
Hemicellulose	Decomposition 200–330 ℃	↑ CO_2, furans; contributes to liquid; low char
Lignin	Broad decomposition 160–900 ℃	↑ char; ↑ aromaticity; ↑ viscosity of oil; ↑ molecular weight
Extractives	Volatile degradation	↓ levoglucosan; ↓ oil yield; removal improves oil stability
Inorganic species (K, Na)	Catalytic cracking activity	↑ char; ↓ liquid yield; ↑ secondary reactions

Feedstock pretreatment aims to improve biomass reactivity and product quality (Segers et al., 2024; Pereira et al., 2022; Liu et al., 2025).

• Physical pretreatments, such as grinding or milling, reduce particle size and optimize heat transfer. For most fast pyrolysis reactors, particle diameters below 5 mm are preferred. In fact, while too-small particles run the risk of becoming trapped in the gas stream, larger particles may result in incomplete conversion.(Jones et al., 2013).

• Chemical pretreatments remove catalytic minerals, thereby increasing organic liquid yields (Jones et al., 2013).

• Thermal pretreatment such as drying and torrefaction (200–300 ℃) decreases moisture and volatile content, enhances grindability, and improves bio-oil quality by reducing acidity and increasing heating value (Mujtaba et al., 2023; Jones et al., 2013).

• Biological pretreatments, such as fungal degradation using Pleurotus ostreatus or Irpex lacteus, selectively reduce lignin and lower pyrolysis onset temperature, facilitating decomposition at milder conditions (Segers et al., 2024). The above described are summerized in Tabale 2.14

Table 2.14: Effect of biomass pretreatment on fast pyrolysis performance.

Pretreatment	**Main action**	**Effect on products**
Physical (milling)	↓ particle size; ↑ heat transfer	↑ conversion; ↓ char; risk entrainment if too small
Chemical (washing)	Removal of alkali metals	↑ liquid yield; ↓ catalytic cracking
Thermal (drying, torrefaction)	↓ moisture, ↓ volatiles; ↑ grindability	↓ acidity of oil; ↑ HHV; ↑ stability
Biological (fungal)	Partial lignin removal; selective degradation	↓ onset temperature; ↑ oil yield; milder pyrolysis

2.7 Alternative thermochemical pathways

Besides pyrolysis, several thermochemical processes can be used to convert biomass (Pereira et al., 2022; Jerzak et al., 2024). Among the most relevant are torrefaction, carbonization, and gasification, which differ significantly in operating temperature, reaction environment, and final product distribution (Segers et al., 2024). In the following paragraphs, these processes are briefly introduced to highlight their main characteristics and how they compare to pyrolysis.

2.7.1 Torrefaction

Torrefaction is a thermochemical pretreatment of lignocellulosic biomass that improves its physicochemical properties and enhances its suitability for energy conversion (Pereira et al., 2022; Jerzak et al., 2024). It is conducted at 200–300 °C under inert or low-oxygen conditions (typically N_2 or Ar) and atmospheric pressure, generally employing low heating rates and residence times sufficient to trigger partial decomposition while avoiding complete pyrolysis (Mujtaba et al., 2023). Although sometimes described as a form of mild pyrolysis, torrefaction differs from conventional pyrolysis in both aims and outcomes: rather than maximizing condensable volatiles or gas production, torrefaction primarily focuses on upgrading the properties of the solid product, reducing moisture affinity, increasing energy density, and improving grindability.

The process can be described through a sequence of steps. First, the biomass is heated to remove free moisture, without significant chemical change. Second, as temperature increases, bound water is released and the first light volatiles are generated. Once the material reaches the torrefaction window, the third step begins: hemicellulose undergoes partial decomposition and devolatilization, while cellulose is only slightly depolymerized and lignin largely preserved (Mujtaba et al., 2023; Pandey and Kim, 2011). This step leads to the release of gases such as CO_2, CO, and light oxygenated compounds, causing a mass loss of typically 20–30%. As a consequence of the removal of oxygen-rich functional groups, the O/C ratio decreases and the solid becomes progressively more hydrophobic and carbon-rich. Meanwhile, the fibrous structure of the biomass breaks down, making the material more malleable and easier to grind. Finally, the torrefied biomass is cooled under inert conditions to prevent oxidation (Mujtaba et al., 2023; Pereira et al., 2022). The process is summerized in the following Figure 2.26:

These structural and chemical transformations result in a solid product with higher heating value, lower hygroscopicity, greater biological stability, and improved grindability and bulk density, which facilitate storage and transportation (Jones et al., 2013). Thanks to these upgraded fuel properties, torrefied biomass is particularly suitable for co-firing in coal power plants, as well as for pelletization, gasification, and metallurgical use, where it can partially substitute coal or charcoal. Overall, torrefaction functions as a pre-pyrolysis upgrading step, improving biomass quality to enhance its performance in subsequent thermochemical conversion (Nhuchhen et al., 2014; Pereira et al., 2022; Jerzak et al., 2024).

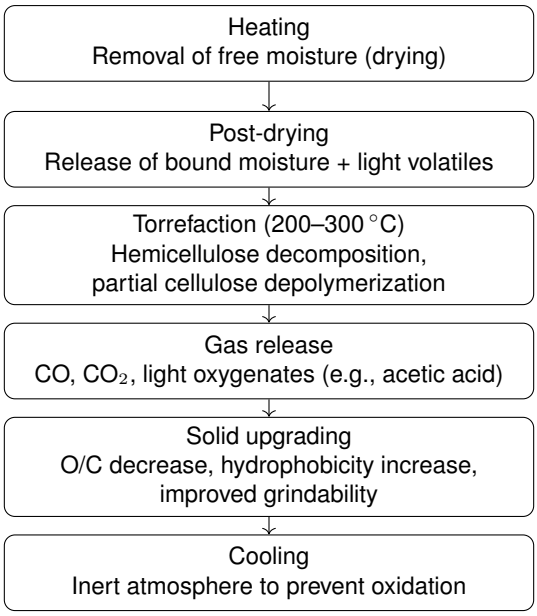

Figure 2.26: Schematic process flow of biomass torrefaction.

2.7.2 Carbonization

Carbonization is a thermochemical process in which biomass is heated for long times at temperatures typically above 400 °C, in an oxygen-limited environment (Pereira et al., 2022; Pandey and Kim, 2011). Unlike fast pyrolysis, which aims at maximizing liquid production, carbonization focuses on maximizing fixed carbon yield and producing a solid carbon-rich product such as charcoal, biochar, biocoke, or activated carbon (Segers et al., 2024; Pereira et al., 2022; Jerzak et al., 2024). This procedure is generally slower than pyrolysis, since the residence time of heating and devolatilization is extended. This to allow deeper transformation of the solid base. During carbonization, biomass undergoes several sequential stages. First, predrying removes free moisture until 100 °C. Drying follows and bound water is evaporated at nearly constant temperature, representing one of the most energy-demanding steps. As a consequence of temperature increases, light volatile compounds are released, and the decomposition of hemicellulose begins around 200–300 °C (Pandey and Kim, 2011). The heating step continues to 300–400 °C, leading to complete decomposition of hemicellulose and cellulose. At this stage, lignin begins to break down, producing a solid enriched in fixed carbon. At temperatures above 400 °C, deep carbonization occurs, yielding a highly carbonaceous char.

Depending on final temperature and residence time, the process can evolve toward coking (>1000 °C), producing biocoke suitable for metallurgical applications (Zakzeski et al., 2010). Alternatively, charcoal may undergo activation, in which treatment with superheated steam at 800 °C removes residual tars and opens micropores, creating activated carbon with high surface area for adsorption and purification (Puri et al., 2024). Although usually carried out under oxygen-limited conditions, small oxygen traces can partially combust part of the biomass, supplying the heat required for the process and improving temperature distribution within the reactor. Carbonization substantially reduces volatile matter, while increasing carbon concentration, structural stability, and hydrophobicity of the solid product (Pereira et

al., 2022). A schematic overview of the process is presneted in Figure 2.27

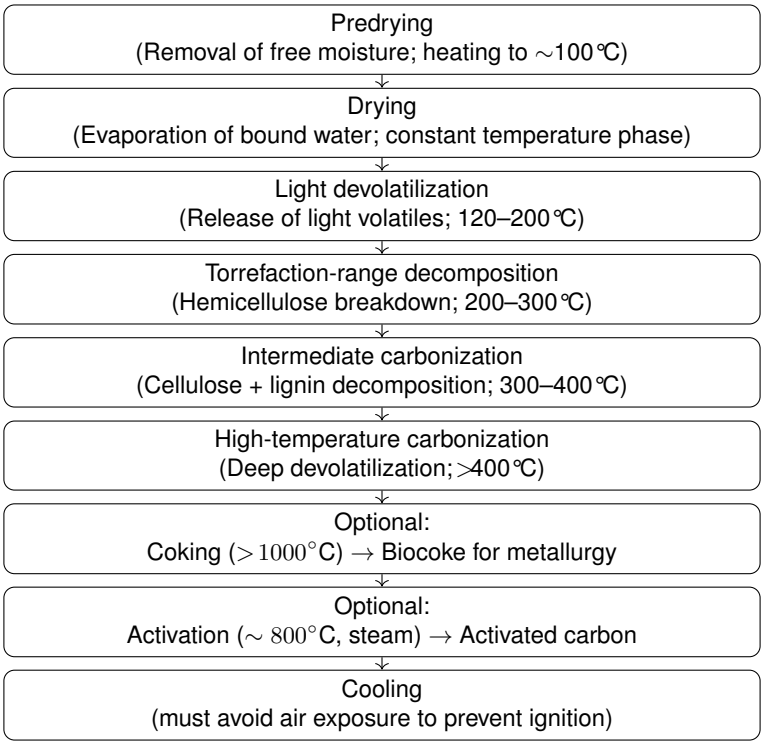

Figure 2.27: Main stages of the biomass carbonization process.

Since more mass is lost as volatiles during carbonization than during torrefaction, the result is a solid with a higher carbon content but a lower energy yield (Segers et al., 2024; Pereira et al., 2022; Jerzak et al., 2024). Nevertheless, the final product offers favorable qualities for utilization in the metallurgical sectors as a reducing agent, fuel, soil amendment or adsorbent. (Ronsse et al., 2015).

2.7.3 Gasification

Gasification is a thermochemical conversion process in which biomass is transformed into a combustible gaseous through partial oxidation at elevated temperatures (Pattiya, 2018; Jones et al., 2013). Unlike direct combustion or pyrolysis aimed at solid or liquid products, gasification operates under sub-stoichiometric oxygen (or steam), promoting partial oxidation rather than complete burning. The process involves several overlapping steps: drying, pyrolysis, oxidation and reduction, together producing syngas primarily composed of H_2, CO, CO_2, CH_4 and light hydrocarbons (Pereira et al., 2022). Modern gasification systems are valued for their ability to handle diverse biomass feedstocks and to generate synthesis gas suitable for power production, chemical synthesis, and hydrogen generation.

Biomass gasification proceeds through four main, partly overlapping, stages: first, drying around 100 ℃ removes free and bound moisture without chemical conversion; second, pyrolysis (≈200–600 ℃) thermally decomposes the feed into char (Pattiya, 2018), volatile gases and tars; third, oxidation / partial combustion (≈800–1400 ℃) introduces a limited amount of O_2 (or air) so that a fraction of volatiles/char combusts, supplying heat for promoting primary tar cracking; finally, in the reduction zone (≈700–1000 ℃) hot gases pass over the remaining char, driving key gas–solid reactions that convert CO_2, H_2O and hydrocarbons into CO and H_2 while further cracking residual tars, thus delivering a cleaned syngas suitable for power generation or chemical upgrading (Sikarwar et al., 2016). A schematic overview of the process is presneted in Figure 2.28

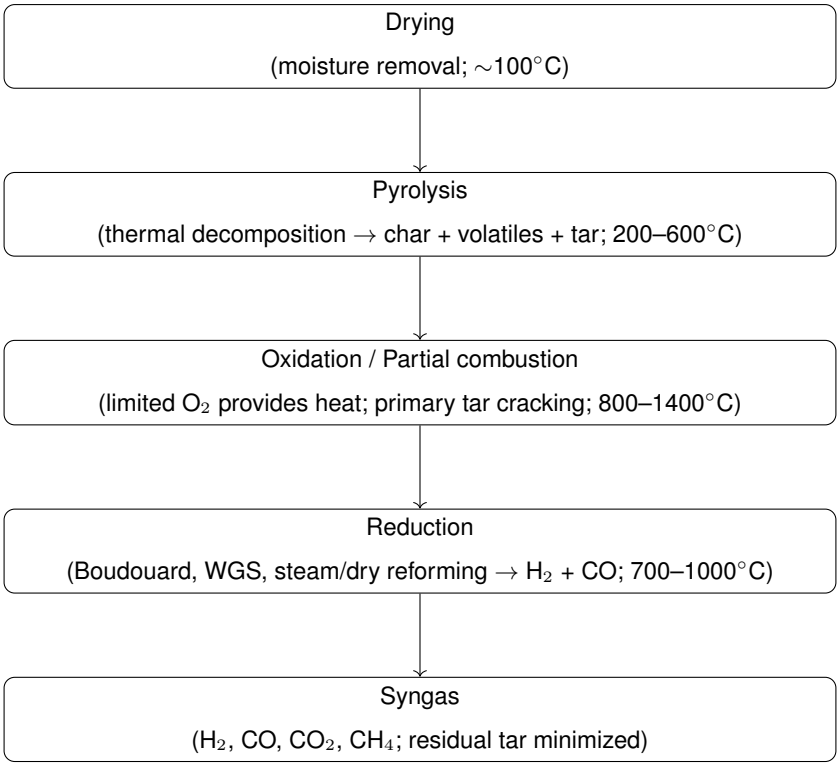

Figure 2.28: Main stages of biomass gasification: drying, pyrolysis, oxidation/partial combustion, and reduction leading to syngas.

Overall, biomass gasification represents a flexible and efficient route for valorizing lignocellulosic

waste into energy-rich gases and chemical feedstocks (Segers et al., 2024; Pereira et al., 2022; Jerzak et al., 2024). Its development is driven by improvements in reactor design, tar mitigation, integrated pollutant removal, and syngas conditioning, which together can reduce environmental impact and enhance economic feasibility (Sikarwar et al., 2016).

To conclude, fast pyrolysis, carbonization, gasification, and torrefaction represent distinct thermochemical routes for converting lignocellulosic biomass, each optimized toward different products and operational conditions (Pereira et al., 2022; Jones et al., 2013; Jerzak et al., 2024). Fast pyrolysis relies on high heating rates and moderate temperatures to maximize liquid bio-oil production, whereas carbonization operates at lower heating rates and longer residence times to increase fixed-carbon content in the solid product. Gasification involves partial oxidation at elevated temperatures to convert biomass into a combustible gas mixture (syngas), mainly composed of CO, H_2, CH_4, and CO_2, suitable for energy generation and chemical synthesis. Torrefaction, instead, is a mild pretreatment at sub-pyrolytic temperatures intended to enhance the fuel properties of biomass, producing a hydrophobic, energy-dense solid with high char yield. A comparative summary of the key operational parameters and product distributions is provided in Tables 2.15 and 2.16.

Table 2.15: Comparison of thermochemical conversion processes (Part 1). Credits: Ronsse et al.

	Fast pyrolysis	**Carbonization**
Temperature	$\sim$500°C	$>$400°C
Heating rate	Fast, up to 1000°C/min	$<$80°C/min
Reaction time	Few seconds	Hours–days
Pressure	Atmospheric (and vacuum)	Atmospheric (or elevated up to 1 MPa)
Medium	Oxygen-free	Oxygen-free or oxygen-limited
Liquids (bio-oil)	75%	30%
Noncondensable gases	13%	35%
Char/solids	12%	35%

Table 2.16: Comparison of thermochemical conversion processes (Part 2). Credits: Ronsse et al.

	Gasification	**Torrefaction**
Temperature	600–1800°C	$<$300°C
Heating rate	–	–
Reaction time	–	$<$2 h
Pressure	Atmospheric, pressurized up to 8 MPa	Atmospheric
Medium	Oxygen-limited (air or steam/oxygen)	Oxygen-free
Liquids (bio-oil)	5%	5%
Noncondensable gases	85%	15%
Char/solids	10%	80%

2.8 Separation and Purification Techniques

Bio-oil is characterized by significant concentrations of oxygen, water, and organic acid, which results in thermal instability, high viscosity, high acidity, corrosiveness and low heating value (Lachos-Perez et al., 2023; Gracia-Vitoria et al., 2023; Santos et al., 2025). For instance, the acidity of pyrolysis liquids is mainly derived from volatile acids, such as acetic acid, contributing to chemical instability and corrosion. Therefore, bio-oil requires further processing to enhance its applications and economic value (Pereira et al., 2022). In this context, it's important to distinguish between upgrading, separation and purification (Lachos-Perez et al., 2023; Papari and Hawboldt, 2018). Upgrading refers to chemical or physical treatments aimed at improving the bulk properties of the whole oil, such as reducing viscosity, improving stability, or increasing energy density. Separation involves fractioning the complex bio-oil mixture into groups of compounds or fractions based on their physical or chemical properties. The goal is obtaining streams enriched in valuable groups of molecules such as phenols, organic acids and aldehydes. Purification is the subsequent step, aimed at removing impurities or contaminants from a given fraction to increase the concentration and quality of a specific compound, thereby making it suitable for industrial or food-grade applications. In this section, several methods and technologies have been presented for oil separation and purification. Each technique is suited to specific types of compounds and brings its own advantages and limitations. By applying such methods, it is possible to transform raw pyrolysis oil into a refined product with higher industrial and economic value (Lachos-Perez et al., 2023; Papari and Hawboldt, 2018; Pereira et al., 2022).

2.8.1 Distillation

Distillation is one of the most established separation techniques, based on differences in boiling point and volatility (Pereira et al., 2022). However, when applied to bio-oil under atmospheric conditions, it often leads to undesirable side reactions such as coke formation and oil aging, leaving up to 40–50% of solid residue when heated above 100 ℃ (Lachos-Perez et al., 2023; Abdullah et al., 2017; Sui et al., 2025; Fonseca and Funke, 2024). Important chemicals, like acetic acid, can be recovered only when combined with reactive esterification, but with a miximum yield of about 30% . As a result, traditional distillation is seen as being both economically inefficient and energy-intensive. To overcome these limitations molecular distillation comes into play. It minimizes heat degradation while separating light, intermediate, and heavy fractions. It operates at low pressure and short residence times. (Lachos-Perez et al., 2023; Papari and Hawboldt, 2018). It can effectively remove acidic components, reducing the pH of bio-oil and eliminating water even at 50 ℃, without coke formation. However, it still struggles to isolate single pure compounds (Gracia-Vitoria et al., 2023). Atmospheric distillation, applied between 80 and 250 ℃, remains attractive for its simplicity and ability to produce useful fractions without waste streams (Papari and Hawboldt, 2018). During this process, volatile compounds such as acids, alcohols, and aldehydes are recovered, while phenolics tend to degrade at high temperatures. Typically, 40% non-distillable residue is left, representing the heavy fraction. Although operationally simple, secondary reactions lead to water formation and product instability, requiring post-treatment for stabilization. Alter-

native methods, such as steam and hydro distillation, enhance volatile compound recovery using water or steam as carriers (Lachos-Perez et al., 2023; Abdullah et al., 2017). Steam distillation injects steam directly into the bio-oil stream, reducing viscosity and improving mass transfer. When combined with ohmic heating, it achieves more uniform heating and higher energy efficiency, yielding improved volatile fractions. In hydro distillation, the oil is immersed in water and heated, and vapors carrying bioactive molecules and essential oils are condensed and collected. Ohmic-assisted configurations further enhance uniformity and speed. Pessure-swing distillation (PSD), one of the more sophisticated solutions, overcomes azeotropic constraints, by switching between low (1–2 atm) and high (10–15 atm) pressure columns, (Lachos-Perez et al., 2023; Papari and Hawboldt, 2018). This reduces the impact on the environment by enabling separation beyond azeotropes and achieving purities of up to 99.5 mol% without the need for additional solvents. Thus, PSD is a valid and effective technique, especially when combined with energy recovery system (Barahmand et al., 2025). Lastly, chemicals with close boiling points or high thermal sensitivity can be separated with better results using spinning band distillation (SBD). (Lachos-Perez et al., 2023; Papari and Hawboldt, 2018). It uses a rotating band inside the column and so improves vapor-liquid interaction and increases separation efficiency. SBD has been used to purify phenolic fractions in pyrolysis applications, producing high-purity phenol with little degradation and little pressure decrease. Because of its accuracy, scalability, and energy economy, SBD is a viable choice for recovering high-value bio-oil fractions and fine compounds.

All the techniques are summerized in table 2.17

Table 2.17: Comparison of the main distillation techniques applied to bio-oil.

Technique	**Operating principle**	**Advantages**	**Limitations**
Atmospheric distillation	Separation based on boiling points at ambient pressure (80–250 °C).	Simple operation; useful volatile fraction recovery.	Coke formation; bio-oil aging; heavy residue (40%).
Molecular / short-path distillation	Separation under very low pressure and short residence time.	Minimal thermal degradation; removes acids; no coke; low T (50–150 °C).	Cannot isolate pure single compounds; vacuum system required.
Steam distillation	Injection of steam enhances volatility and mass transfer.	Improved recovery of volatiles; reduced viscosity.	Still induces thermal stress; limited to volatile species.
Hydro-distillation	Bio-oil heated while immersed in water; vapors carry volatiles.	Mild conditions; suited for bioactive/thermo-sensitive compounds.	Not effective for heavy phenolics; high water load.
Pressure-swing distillation (PSD)	Alternates low- and high-pressure columns to break azeotropes.	High purity (up to 99.5%); solvent-free; energy recovery possible.	Complex equipment; energy-intensive without heat integration.
Spinning band distillation (SBD)	Rotating band increases vapor–liquid contact efficiency.	High separation efficiency; ideal for close b.p. compounds.	Limited throughput; suited for fine-chemical recovery.

2.8.2 Condensation

Condensation is the process by which a substance transitions from the gaseous to the liquid phase. In bio-oil recovery, it is employed to fractionate compounds with different boiling points, offering a simple and effective separation technique easily integrated into pyrolysis setups (Westerhof et al., 2007; Papari and Hawboldt, 2018; Vilas-Boas et al., 2025; Barahmand et al., 2025). Fractional condensation involves cooling vapors to condense them into liquid fractions with distinct properties (Westerhof et al., 2007; Schulzke et al., 2016; Fonseca and Funke, 2024): a light fraction rich in water, C1–C4 compounds, monophanols, and sugars, and a heavy fraction composed of oligomeric aerosols. The efficiency of this process depends on temperature and pressure control, reactor composition, and condenser design, including the number and temperature of stages. Multi-stage systems operating between 0 and 150 °C enable recovery of low-water (< 5 wt%) and high-calorific fractions (30 MJ/kg) (Westerhof et al., 2007; Schulzke et al., 2016). Chai et al., 2014 obtained a 9.7 % energy-enriched fraction at 23.7 °C, and

Raimundo et al., 2018 using a packed condenser at 157 ℃, produced a 7.4 wt% water-free oil. Westerhof et al., 2007 showed that tuning condenser temperature (25–70 ℃) allows selective recovery of acetic acid, hydroxyacetaldehyde, acetol, and heavier oligomers (Schulzke et al., 2016; Sui et al., 2025). Water removal enhances oil stability, while sugar-rich fractions can serve in biochemical processes. Condensation systems are generally divided into surface condensers and liquid condensation systems (LCS) (Westerhof et al., 2007; Abdullah et al., 2017). Indirect vapor–surface contact is the basis of surface condensers (single, multi-stage, or fractional), where temperature control allows the separation of streams that are rich in phenolics and water. In contrast, LCS systems use direct vapor-liquid contact and often use spray towers, which offer superior heat transmission and aerosol capture. The most basic configurations are single condenser systems, which collect all vapors in a single step. (Papari and Hawboldt, 2018). The resulting liquid typically contains 20–30 wt% water, with HHV of 16–19 MJ/kg, pH 2.5–3, and 0.2–1 wt% solids. Chai et al., 2014 showed that lowering the condenser temperature from 40 ℃ to 10 ℃ increased oil yield up to 55.7 %. Although simple and low-cost, single condensers produce heterogeneous oils with high water content and limited selectivity. Multi-stage condensers employ two or more cooling stages, often below 15 ℃, extending vapor residence time and increasing recovery efficiency (Westerhof et al., 2007; Schulzke et al., 2016). Chai et al., 2014 obtained 60 % bio-oil yield from eucalyptus, containing 26 wt% water and 18.4 MJ/kg HHV. Although they demand more complicated setups and cooling power, multi-stage systems improve yield and stability. The most selective separation is achieved using fractional condensation, also known as staged condensation (Westerhof et al., 2007; Schulzke et al., 2016). It is possible to isolate oils with low water (2–3 weight percent) and acid content by consecutively running condensers above 80 ℃. Liquid collection systems (LCS), shown in Figure 2.29, are equally critical, determining how condensates are captured and stabilized (Westerhof et al., 2007; Abdullah et al., 2017).

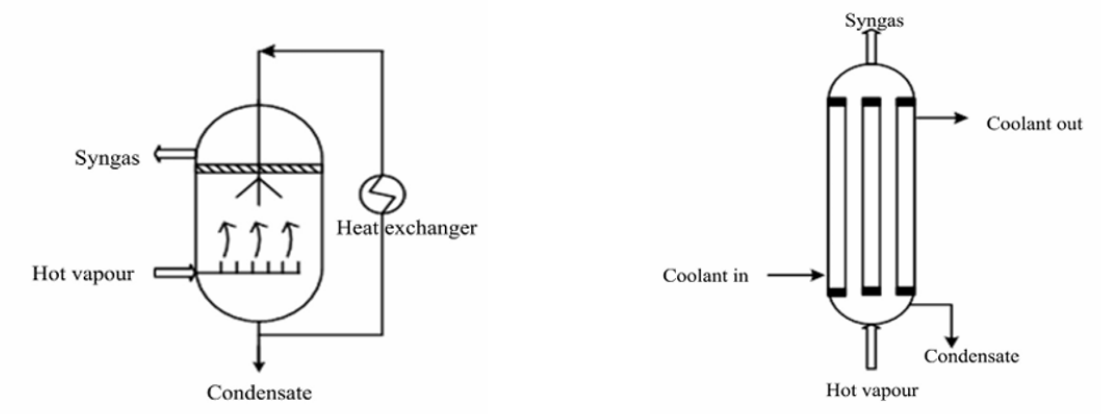

Figure 2.29: Comparison between direct and indirect condensation systems for bio-oil recovery. Left: spray column system. Right: heat exchanger condenser .

Direct condensation, typically using spray towers, ensures high aerosol capture but may induce

cracking reactions. Indirect systems, such as shell-and-tube, coil, or Allihn condensers, avoid direct vapor–liquid contact, minimizing fouling and polymerization (Papari and Hawboldt, 2018). Graham condensers provide large surface areas but are prone to coke deposition, while spiral and coil designs improve heat exchange and scalability. Although indirect systems offer better control and oil quality, they require higher maintenance and investment.

2.8.3 Extraction

Extraction is a promising method for upgrading pyrolysis oil, allowing the separation of its complex mixture into valuable fractions through an energy-efficient and cost-effective process (Lachos-Perez et al., 2023; Pereira et al., 2022; Sui et al., 2025). This section focuses on liquid–liquid extraction (LLE), a versatile approach adaptable to different solvents and separation goals (Figure 2.30) (Jones et al., 2013).

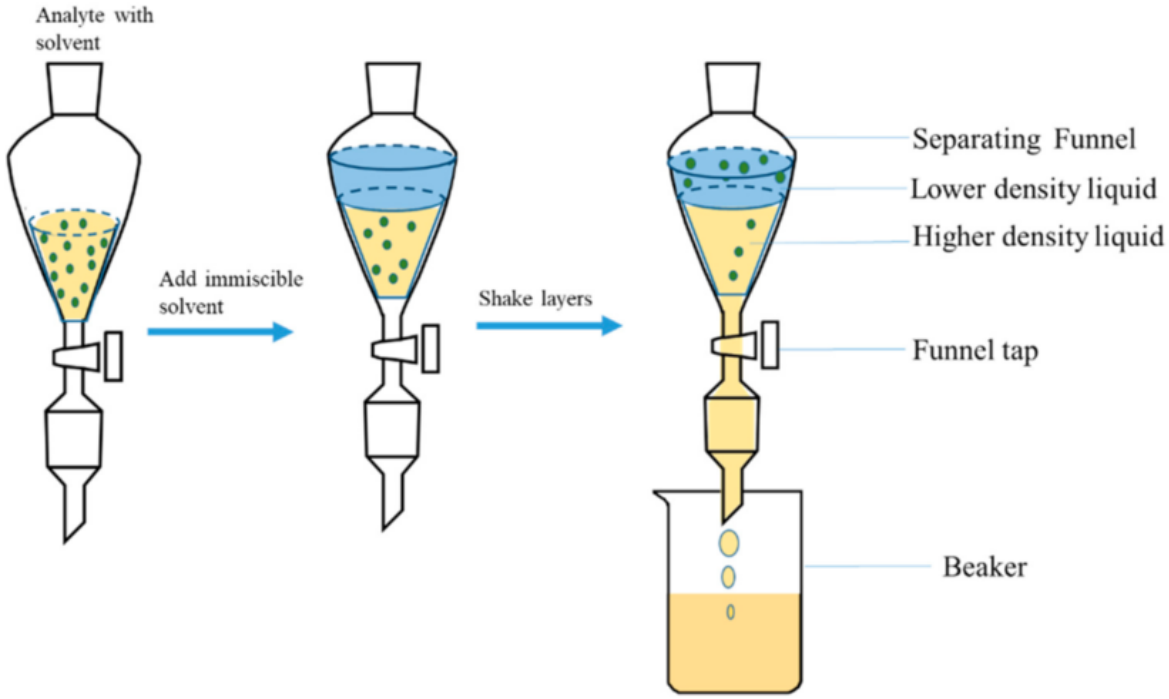

Figure 2.30: Schematic representation of liquid–liquid extraction (LLE) applied to bio-oil. The process separates the feed into two immiscible phases—an organic phase enriched in hydrophobic compounds and an aqueous or solvent-rich phase containing polar oxygenates—based on differences in solubility and chemical affinity.

Depending on the solvent, three main strategies are distinguished: water extraction, organic solvent extraction, and advanced selective methods. Water extraction induces phase separation when 50–70% water is added to bio-oil, producing a heavy, tar-like phase rich in lignin derivatives and a watery phase containing cellulose and hemicellulose derived compounds (Lachos-Perez et al., 2023; Westerhof et al., 2007; Gracia-Vitoria et al., 2023). It was found that a water to oil ratio of 0.65–0.7 (forest residues) and 0.5 (pine-derived oil) maximized separation, with 80–90% of oxygenates transferred to the aqueous phase and it was observed that the stability of the bio-oil and the degree of phase split depend on

the relative content of lignin oligomers, sugars, and light C_1–C_4 molecules acting as solvents. The process effectively removes polar oxygenates, improving oil stability and lowering acidity, but generates an aqueous effluent rich in organics that requires treatment or valorization (Pereira et al., 2022). Solvent extraction selectively transfers compounds into a suitable solvent based on polarity and chemical affinity (Lachos-Perez et al., 2023; Pereira et al., 2022; Zakzeski et al., 2010). The process produces a solvent-soluble fraction enriched in target compounds and a non-soluble residue. Solvents investigated include alcohols, ethyl acetate, diethyl ether, n-hexane, octane, chloroform, dichloromethane, and petroleum ether. There are two popular approaches: acid-base extraction, which uses pH control to separate acids and phenolics in a sequential manner, and polarity-based extraction, which divides compounds according to polarity. Hydrophobic phenolics are separated by non-polar solvents such as hexane and chloroform, while acids are recovered by ethyl acetate. Even with excellent selectivity, problems like cost, environmental effect, and solvent recovery still need to be optimized for each feedstock. For this reason, better techniques have been created to increase sustainability and efficiency (Lachos-Perez et al., 2023; Jerzak et al., 2024; Santos et al., 2025).

2.8.4 Membrane separation

Membrane technologies such as microfiltration ($0.05 - -10\ \mu\mathrm{m}$), ultrafiltration (1–100 nm), and nanofiltration (<2nm) have been investigated for upgrading and fractionating bio-oil (Lachos-Perez et al., 2023; Susanto et al., 2024; Barahmand et al., 2025). They are considered more energy-efficient and selective than conventional processes like distillation, thanks to their higher surface area-to-volume ratio and the ability to finely tune separation (Lachos-Perez et al., 2023; Susanto et al., 2024). Among the methods explored, nanofiltration has been applied to recover acetic acid from aqueous pyrolysis condensates, often in combination with reverse osmosis (Lachos-Perez et al., 2023; Susanto et al., 2024). A schematic representation of the MF–UF–NF separation principles is shown in Figure 2.31.

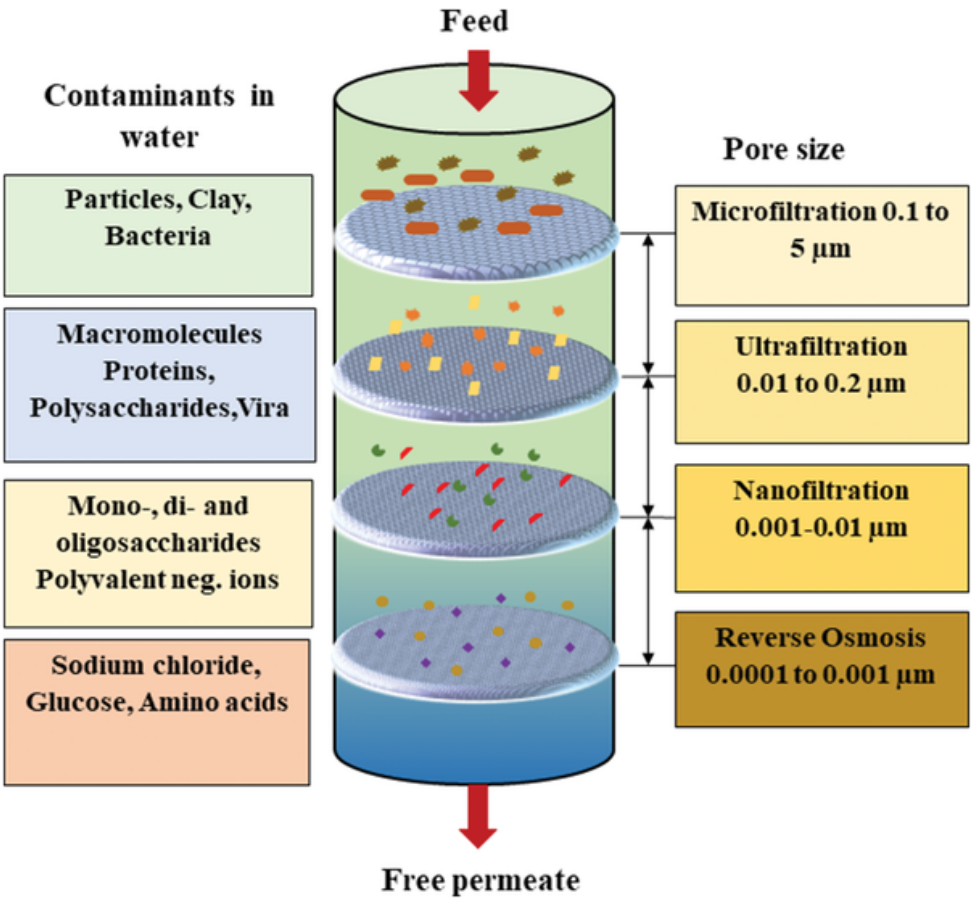

Figure 2.31: Schematic representation of pressure-driven membrane processes used for bio-oil upgrading, including microfiltration (MF), ultrafiltration (UF), and nanofiltration (NF). The three techniques separate compounds according to pore size and molecular weight cut-off (MWCO), enabling selective removal of oligomers, phenolics and oxygenated species.

Even though commercial cellulose acetate and polyamide membranes achieves good separation, the high phenolic content of condensates caused severe corrosion and fouling highlights the need for pretreatment (Lachos-Perez et al., 2023; Susanto et al., 2024).

However, repeated regeneration significantly reduces performance, and the recovered fractions are often contaminated by high ash contents, limiting direct applicability (Lachos-Perez et al., 2023). To address the thermal sensitivity of bio-oil, pervaporation has been tested as an alternative (Lachos-Perez et al., 2023). In this process, selected compounds permeate as vapor under reduced pressure, allowing fractionation without relying on boiling points. Polyvinyl alcohol membranes, sometimes cross-linked with acids, have shown promising separation of acetic acid from model solutions, while the addition of fillers such as zeolites increased selectivity (Lachos-Perez et al., 2023). However, the complexity of real aqueous pyrolysis condensates—with their high concentrations of aromatics and phenolics—makes pervaporation less efficient, since coupling effects reduce membrane selectivity (Lachos-Perez et al., 2023). Fouling is also a persistent problem, leading researchers to suggest multi-stage membrane integration systems, though these remain at the research stage (Lachos-Perez et al., 2023).

2.8.5 Chromatography

Chromatography is traditionally regarded as an analytical tool for identifying components in complex organic mixtures, but it can also serve as a powerful purification technique for isolating valuable fractions from pyrolysis oil (Lachos-Perez et al., 2023; Vilas-Boas et al., 2025; Machado et al., 2022). Unlike separation methods such as distillation or condensation, chromatography enables fine purification by exploiting the differential affinity of compounds between a stationary phase (solid or liquid supported on a solid surface) and a mobile phase (liquid or gas). This allows the selective recovery of high-value chemicals, even when present in complex mixtures at low concentrations. For this reason, chromatography is best classified as a purification technology rather than a separation method. Several chromatographic techniques have been investigated for pyrolysis oil upgrading:

• Liquid Chromatography (LC): Thanks to its versatility in combining different stationery and mobile phases, LC can separate a broad range of polar and non-polar compounds. High-performance liquid chromatography (HPLC) and its variants are especially relevant, enabling the fractionation of phenolics, carboxylic acids, and sugars. Gel permeation chromatography (GPC), also known as size-exclusion chromatography, is useful for removing high-molecular-weight lignin-derived oligomers. Ion-exchange chromatography (IEC) can recover carboxylic acids and amino acids and has been applied for eliminating inhibitors from biomass hydrolysates.

• Gas Chromatography (GC): it has limited preparative use in bio-oil upgrading because many bio-oil compounds are thermally unstable. Still, it works effectivelly for separating volatile fractions and is also frequently used in conjunction with mass spectrometry for in-depth characterization.

• Column Chromatography: This is one of the most used preparative methods applied to bio-oil. Column chromatography separates fractions according to polarity. It uses stationary phases such as silica gel, alumina, or macroporous resin. However, its poor throughput restricts its application to high-value chemicals.

Studies applying chromatography to pyrolysis oils report that column chromatography can selectively isolate phenols and hydrocarbons with very high purity (Lachos-Perez et al., 2023), while size-exclusion chromatography is effective for separating heavy lignin-derived oligomers. Ion-exchange chromatography has demonstrated up to 80% recovery of acetic acid under optimized conditions, and reversed-phase LC has shown strong reproducibility in recovering phenolic and aromatic fractions. These examples confirm that chromatography is particularly effective for the purification of fine chemicals. A simplified visual representation of chromatographic purification is shown in Figure 2.32.

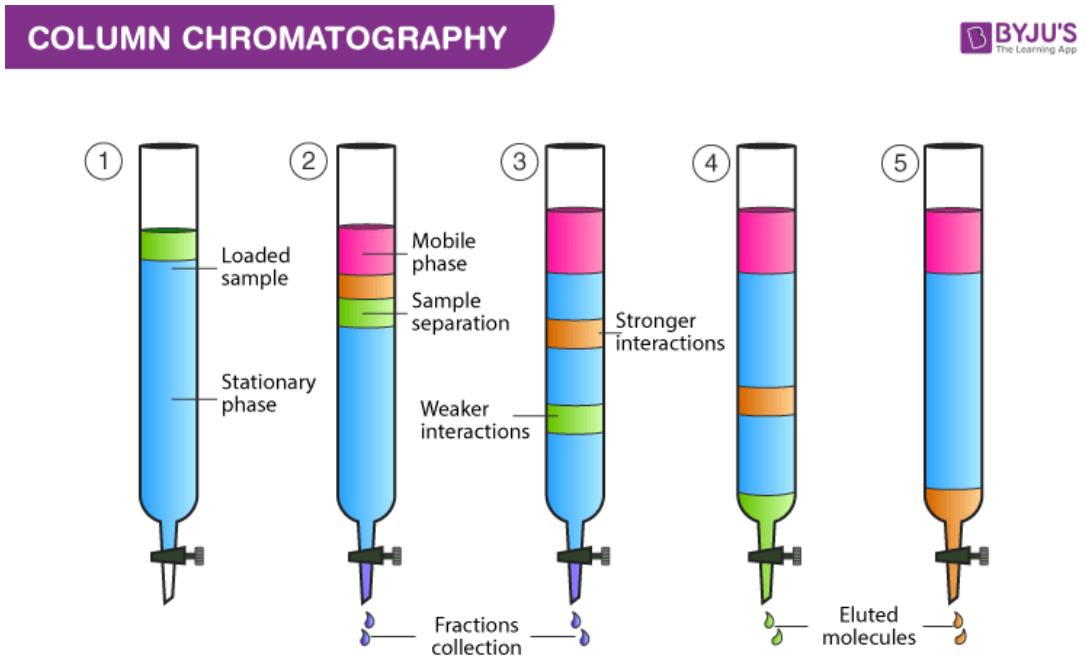

Figure 2.32: Schematic representation of chromatographic purification, illustrating the separation of a complex bio-oil mixture into individual fractions as compounds elute with different affinities toward the stationary and mobile phases. Credit: Byjus.

To conclude, distillation remains indispensable for producing bulk fractions and removing water or acids, but it suffers from side reactions and thermal instability of the oil. Condensation systems, whether single-stage, multi-stage, or fractional, are relatively simple and cost-effective, but they produce broad fractions with limited chemical refinement. Extraction methods, particularly liquid–liquid extraction and water addition, are versatile in selectively transferring oxygenated or acidic compounds to different phases, yet they demand careful optimization of solvents, recovery strategies, and environmental compatibility. Membrane technologies offer the promise of energy efficiency and high selectivity but are still hindered by fouling, instability, and scale-up limitations. Finally, chromatography, although excellent in precision, is better suited for niche, high-value applications rather than large-scale upgrading (Santos et al., 2025). The common denominator across all these technologies is the trade-off between selectivity, scalability, and cost (Papari and Hawboldt, 2018). Bulk separation methods (distillation, condensation) achieve large yields but limited refinement. More sophisticated processes (extraction, membranes, chromatography) provide sharper selectivity and higher purity, but at the expense of complexity, cost, or throughput. For this reason, many experimental studies point toward integrated approaches, where sequential application of different technologies compensates for the limitations of each (Lachos-Perez et al., 2023; Jones et al., 2013). For example, distillation may be employed to remove water-rich fractions, followed by extraction or chromatography to recover fine chemicals from the remaining oil. Similarly, combining membranes with extraction or chromatography could improve energy efficiency and product recovery. A summary of the main advantages and limitations of the separation techniques discussed above is reported in Table 2.18.

Table 2.18: Summary and comparison of main separation and purification techniques for bio-oil upgrading.

Technique	**Strengths**	**Limitations**
Distillation	- Produces bulk light/middle/heavy fractions - Removes water and acids - Simple and scalable (atmospheric)	- Thermal degradation, coking, oil aging - Low selectivity - High residue (up to 40%)
Condensation (single- or multi-stage)	- Very simple and low-cost - Effective for broad fraction recovery - No solvents required	- Limited chemical refinement - Broad cuts; poor selectivity
Extraction (LLE, water addition, solvent-based)	- High selectivity based on polarity or pH - Effective for recovering acids, phenolics, sugars - Water addition forms two stable phases	- Solvent recovery and environmental impact - Aqueous effluents requiring treatment - Process optimisation required for each feedstock
Membrane technologies (MF/UF/NF, pervaporation)	- Energy efficient - Tunable cut-off and moderate selectivity - Mild operating conditions (no thermal cracking)	- Severe fouling in real bio-oils - Instability and performance loss - Scale-up challenges
Chromatography	- Excellent selectivity and purity - Suitable for fine-chemical recovery	- High cost - Limited scalability - Used mainly for niche applications

In conclusion, the upgrading of pyrolysis oil through separation and purification should not be regarded as the search for a single, optimal technology, but rather as the design of tailored process chains that adapt to the variability of biomass feedstocks and the intended applications of the products. Future research must therefore focus on integrated, flexible systems that balance efficiency, cost, and sustainability, ensuring that pyrolysis oil upgrading can play a viable role in circular economy.

Chapter 3

Materials and Methods

The following chapter presents the materials and methods adopted in this study for the investigation of the pyrolysis of spent coffee grounds (SCGs). The experimental activity is designed to support the chemical characterization of the products obtained from the thermochemical conversion process and to provide the necessary data for the subsequent techno-economic assessment.

This chapter describes the characteristics of the feedstock, the experimental setup used for the pyrolysis test and the operating conditions selected for the process. In addition, the analytical techniques employed for the characterization of bio-oil and biochar are presented, including the methods used to evaluate antioxidant activity, total phenolic content, pH and thermal behavior.

Finally, the methodological approach adopted for the economic evaluation is outlined, defining the main assumptions and indicators used in the analysis.

The chapter is organized as follows:

- Section 3.1 describes the biomass feedstock, including collection and pretreatment procedures;
- Section 3.2 outlines the experimental setup and operating conditions of the pyrolysis process, as well as the experimental procedure and product collection;
- Section 3.3 presents the mass balance and yield determination methodology;
- Section 3.4 describes the chemical characterization methods applied to bio-oil;
- Section 3.5 discusses the characterization of biochar as a co-product of the pyrolysis process;
- Section 3.6 describes the cost assessment methodology;
- Section 3.7 summarizes the main assumptions adopted in the study.

3.1 Biomass Feedstock and Preparation

3.1.1 Biomass Collection

The feedstock used in the experiment consists of spent coffee grounds (SCGs) collected on-site at the UNAERP university, in Ribeirão Preto, São Paulo, Brazil. According to the cafeteria staff, the facility produces approximately 16 kg of SCGs per day. The collection takes place directly after the coffee preparation (Figure 3.1).

Figure 3.1: Filtration unit and collection containers where spent coffee grounds are accumulated. Credit: Author

The ratio between the mass of roasted coffee used and the mass of waste generated is approximately 1:1, meaning that for every kilogram of ground coffee consumed in beverage preparation, around 1 kg of solid residue is produced. To quantify the availability of feedstock, the SCGs daily production is set at 16kg/day, considering 5 working days per week over 52 weeks per year. Table 3.1 summarises the corresponding weekly, monthly and annual generation rates.

Table 3.1: Estimated Production of Spent Coffee Grounds at UNAERP

Time scale	SCG production	Calculation
Daily	16 kg/day	Given
Weekly	80 kg/week	16×5
Monthly	320 kg/month	80×4
Annual	4160 kg/year	80×52

3.1.2 Biomass Pretreatment

Since the SCGs are collected right after the coffee production, they naturally exhibit a high initial moisture content and therefore, before each experiment, a pretretment step is necessary.

The wet SCGs are dried in a laboratory oven (Figure 3.2a). The material is spread in a thin, uniform layer over a perforated tray to promote even evaporation. Drying is carried out at 100 ℃ for 24 h, a duration sufficient to achieve complete removal of free moisture and obtain a stable dry mass. At the end of the process, the SCGs appeared completely dry and ready to be introduced into the reactor (Figure 3.2b).

(a) Oven used for drying the SCG prior to pyrolysis. Credit: Author

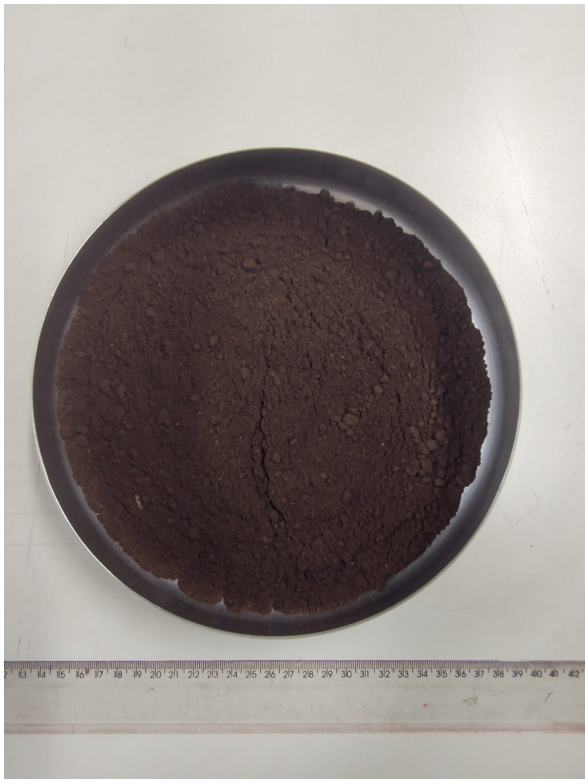

(b) Dried SCG after 24 h of oven drying at 100 ℃. Credit: Author

Figure 3.2

3.2 Experimental Setup and Procedure

3.2.1 Pyrolysis Experimental Setup

After the pretreatment step, the dried SCGs are introduced into a pyrolysis system.

Figure 3.3 represents a schematic flowsheet of the process, showing the main process units and the overall material flow.

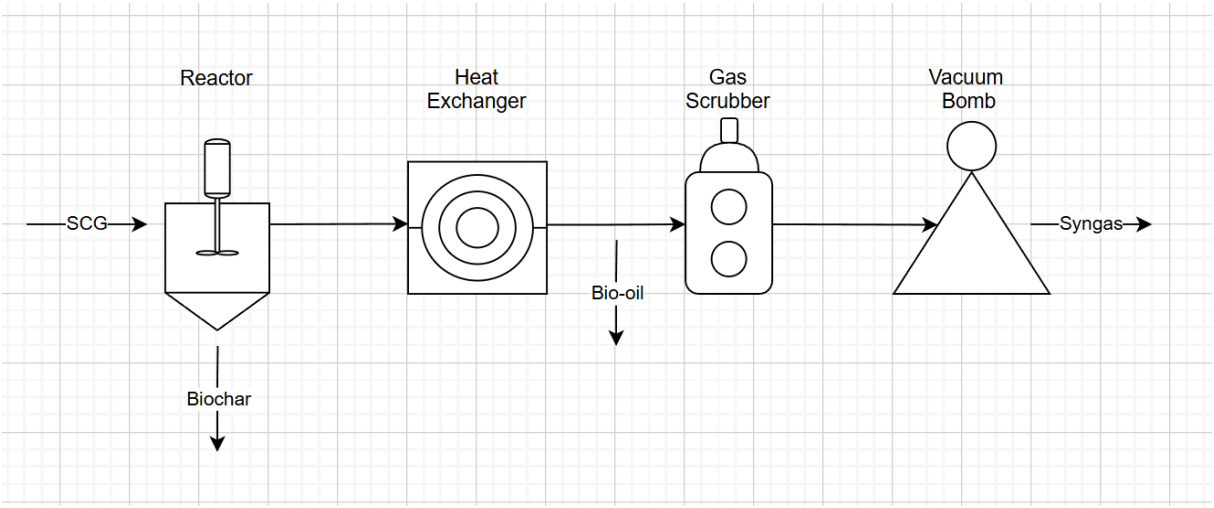

Figure 3.3: Schematic flowsheet of the laboratory-scale pyrolysis system.

It is made up of a pyrolysis reactor (1), a coil-type heat exchanger (2), a drain system for collecting bio-oil samples (3), a packed-bed gas scrubber (4) and a vacuum pump (5). The system is also equipped with three temperature sensors, two of which are located inside the reactor. They are responsible for measuring the internal and external temperature of the equipment, while a third sensor is positioned at the entrance of the packed-bed gas scrubber. A gas sensor was also used, located at the outlet of the coil, which is responsible for measuring the concentration of various combustible gases generated during the process.

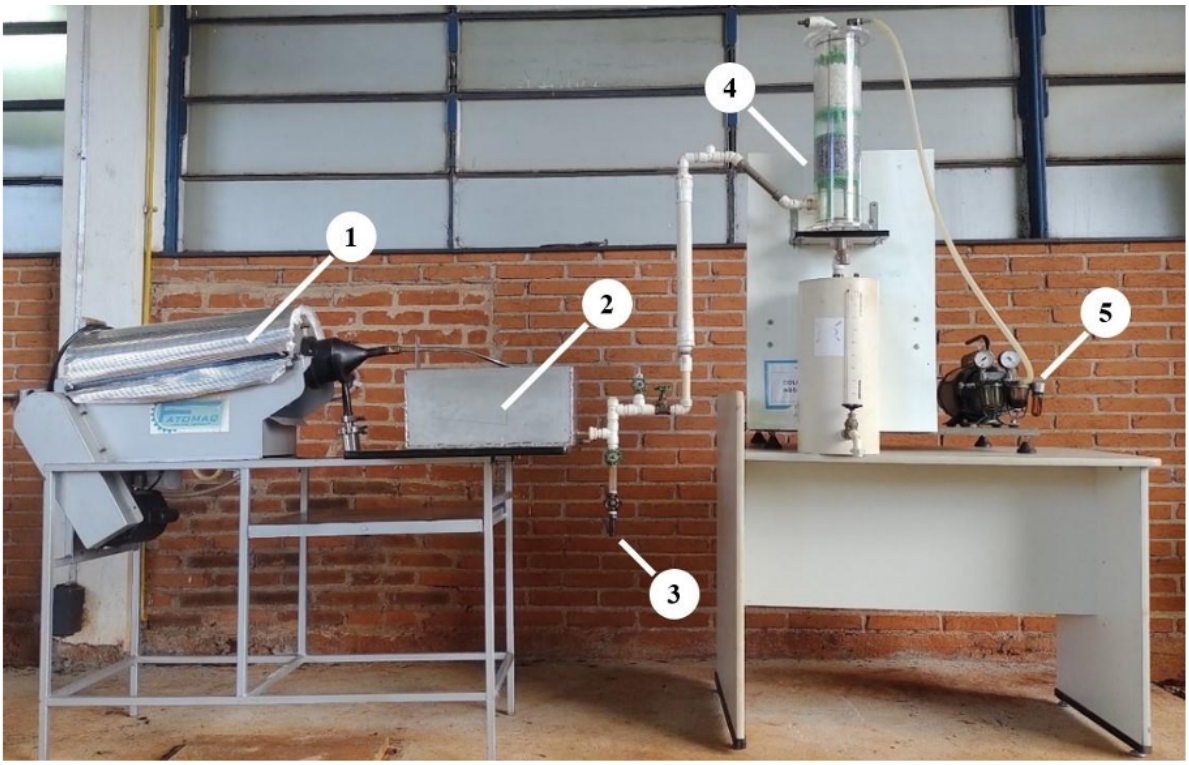

Figure 3.4: Experimental unit setup to carry out pyrolysis tests.

The process begins in the pyrolysis reactor, built from a Fatomaq coffee-bean roaster. The equipment consists of a cylindrical drum with a capacity of 20 L that rotates at 30 rpm. The material to be pyrolyzed is placed inside this drum. At the reactor outlet, a funnel was built and installed, as shown in Figure 3.5, with the purpose of collecting the first amounts of condensed oil, as well as allowing the connection of the reactor to the heat exchanger.

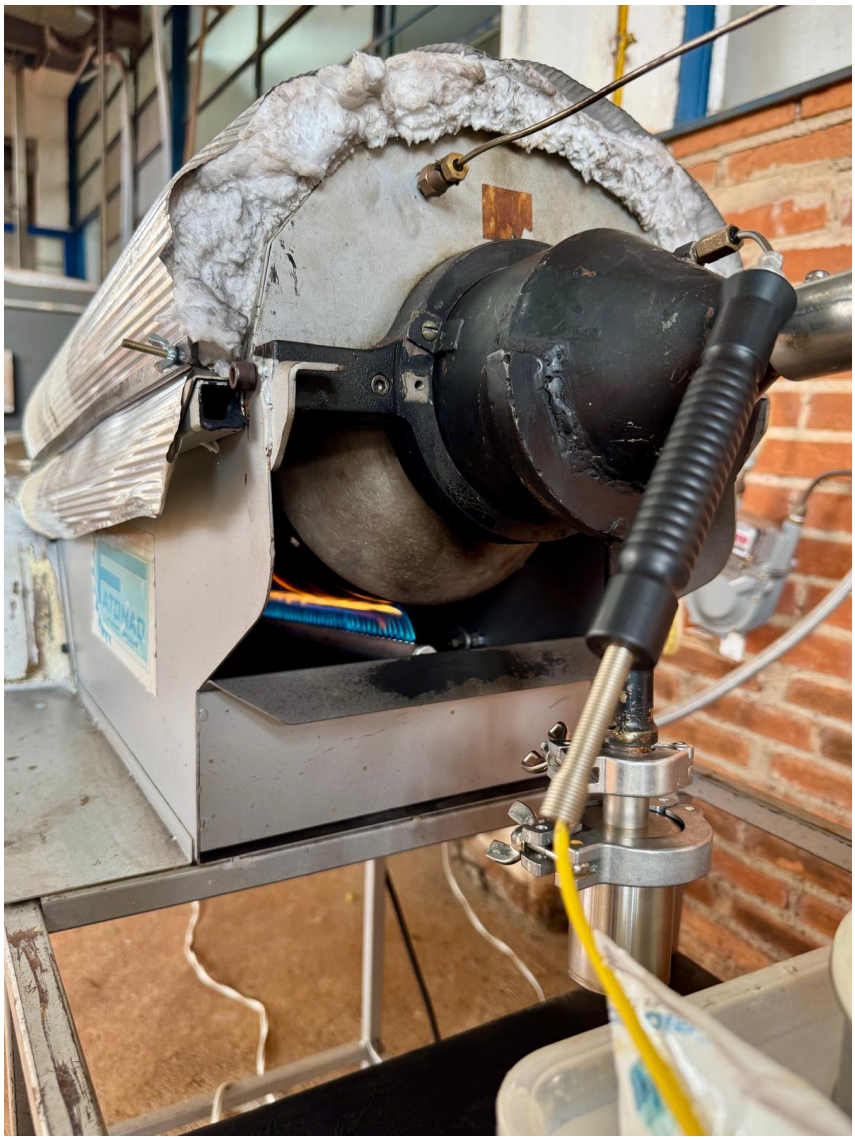

Figure 3.5: Funnel at the reactor outlet with a compartment for bio-oil collection. Credit: Author

During the first 30 minutes of the reaction, the reactor is heated up to a maximum temperature of 400 ℃. During this period, the material inside the reactor undergoes thermal decomposition, releasing gases and vapors that are directed to the heat exchanger. The heat exchanger consists of a stainless-steel coil installed inside a box. During the experiment, the coil is immersed in an ice–water mixture, allowing the vapors to be condensed and thus forming the liquid fraction (bio-oil) of the process. The heat exchanger is shown in Figure 3.6.

Figure 3.6: Heat Exchanger. Credit: Author

At the outlet of the coil, a drain system was installed, consisting of a transparent plastic tube where the generated oil samples can be deposited and collected. Since the system operates under vacuum, the tube has a gate valve at each end, allowing bio-oil samples to be collected without oxygen entering the system. The drain system is shown in Figure 3.7.

Figure 3.7: Drain system with deposited bio-oil sample. Credit: Author

The drain system tube has a storage capacity of 20 mL of oil.

A tower gas scrubber treats the gaseous fraction (pyrolysis gas) that leaves the heat exchanger before it is released into the atmosphere. A circulating aqueous solution made up of 8 L of water, 10 mL of 40% NaCl, and 5 mL of a 1% phenolphthalein solution is present in the scrubber reservoir. The gas neutralization process may be seen in real time due to phenolphthalein's function as an acid-base indicator. Under basic circumstances, the solution looks highly pink, as it approaches neutrality, it turns pale pink and when acidic species are present it becomes colorless.

The gas scrubber and the color change of the medium are shown in Figure 3.8.

Figure 3.8: Gas-scrubbing column showing the three color states observable during the experiment: basic (pink), neutral (light pink), and acidic(colorless).Credit: Author

Finally, the outlet of the gas scrubber is connected to a vacuum pump as shown in Figure 3.9, which exhausts the treated gases. After 30 minutes of heating, the reactor burner is turned off and the system is allowed to cool for 30 minutes.

Figure 3.9: Vacuum Pump. Credit: Author

After this period, the reactor is opened to remove the solid fraction, known as biochar.

3.2.2 Operating Conditions

The operating parameters adopted during the test are summarized in Table 3.2

Table 3.2: Operating conditions adopted during the pyrolysis experiment.

Parameter	**Value**
Biomass mass	100 g
Reactor operation	Single-run experiment (one feed load)
Drum rotation speed	30 rpm
Heating duration	30 min
Cooling duration	30 min
Maximum temperature	400°C
Heating system	Built-in electric heater
Condensation system	Stainless-steel coil + ice–water bath
Gas handling	Scrubber unit + vacuum pump

3.2.3 Experimental Procedure and Product Collection

The pyrolysis experiment was conducted using 100 g of dried spent coffee grounds. After pretreatment, the biomass was loaded into the rotating drum of the reactor, which was then sealed to avoid air ingress. Throughout the run, the drum rotated at approximately 30 rpm to promote homogeneous mixing and heat distribution. The built-in electric heating system was activated and maintained for 30 minutes, during which the internal temperature gradually increased to approximately 400 ℃. After the heating period, the system was switched off and allowed to cool naturally for an additional 30 minutes while remaining closed.

During both the heating and cooling phases, the condensable vapors produced inside the reactor were routed through a stainless-steel coil immersed in an ice–water bath, where they condensed and accumulated in a transparent drain tube positioned at the coil outlet (Figure 3.10).

(a) Reactor and condensation coil used during the pyrolysis experiment. Credit: Author

(b) Transparent drain tube equipped with two valves for bio-oil collection.Credit: Author

Figure 3.10

The tube is equipped with two gate valves, enabling the isolation and extraction of liquid fractions without exposing the system to ambient air.

After the cooling phase, the reactor chamber was opened and the solid residue (biochar) was manually removed from the rotating drum (Figure 3.11). The recovered char was stored in airtight containers to prevent moisture uptake prior to weighing and further analysis.

Figure 3.11: Manual collection of the biochar after the cooling phase of the reactor. Credit: Author

The non-condensable gases exiting the condensation system passed through the scrubber column, where the circulating indicator solution progressively changed color in response to the varying acidity of the gas stream. After scrubbing, the treated gas was exhausted by the vacuum pump and released into the ambient environment throughout a tube (Figure 3.12).

Figure 3.12: Outlet line through which the purified gases are released after passing through the scrubber. Credit: Author

3.3 Mass Balance and Yield Determination

At the end of the pyrolysis experiment, the mass balance was evaluated in order to quantify the distribution of products and to determine how much of the initial material remained as solid or liquid products, and how much was converted into non-condensable gases. Since the SCGs were oven-dried before the experiment, the residual moisture content is negligible and was therefore not included in the mass balance. The symbols used are summarized in Table 3.3.

Table 3.3: Definition of mass symbols used in the mass balance.

Symbol	Description
m_B	Initial mass of dried biomass introduced into the reactor.
m_C	Mass of biochar collected at the end of the experiment.
m_O	Mass of bio-oil obtained after condensation.
m_G	Mass of non-condensable gases, calculated by difference from the mass balance.
m_F	Generic mass of a product fraction used for yield calculations.

The overall mass balance of the system is expressed as:

$$m_B = m_C + m_O + m_G \tag{3.1}$$

Rearranging Equation 3.1, the mass of gases produced is calculated as:

$$m_G = m_B - m_C - m_O \tag{3.2}$$

To compare the performance of different feedstocks under identical operating conditions, the percentage yield of each fraction was also determined (Hasan et al., 2022). For a generic fraction of dry mass m_F (biochar, bio-oil or non-condensable gases), the yield η is defined as:

$$\eta = \frac{m_F}{m_B} \times 100 \tag{3.3}$$

All masses (m_B, m_C, m_O) were measured experimentally using a laboratory balance immediately after product collection.

3.4 Chemical characterization of bio-oil

3.4.1 Bio-oil sample preparation

Prior to chemical characterization, the bio-oil sample was subjected to a preliminary filtration step. Filtration was carried out using a filter, shown in Figure 3.13.

Figure 3.13: Filter used for bio-oil sample filtration. Credit: Author

After filtration, the bio-oil samples were diluted with distilled water to avoid instrument saturation and ensure reliable absorbance measurements.

3.4.2 DPPH Antioxidant Activity Analysis

The antioxidant activity of the produced bio-oil was evaluated using the 2,2-diphenyl-1-picrylhydrazyl (DPPH) radical scavenging assay. The procedure was carried out under light-protected conditions due to the photosensitive nature of the DPPH radical.

- A stock DPPH solution was prepared by dissolving DPPH in absolute methanol or ethanol to obtain a final concentration of 0.078 g/L, as shown in Figure 3.14. The solution was stirred until complete dissolution and protected from light by wrapping the container with aluminium foil.

Figure 3.14: Beaker containing the freshly prepared DPPH solution prior to light protection with aluminium foil. Credit: Author

- The absorbance of the DPPH stock solution was measured using a UV–Vis spectrophotometer and adjusted with absolute methanol or ethanol to obtain an initial absorbance value in the range of 0.500–0.600. Absorbance measurements were performed at a wavelength of 517 nm for methanolic solutions and 515 nm for ethanolic solutions.
- Trolox was used as a reference antioxidant standard. A Trolox stock solution was prepared by dissolving the compound in absolute ethanol and subsequently diluted to obtain standard solutions for calibration. All Trolox solutions were homogenized and protected from light prior to analysis.
- Bio-oil samples were appropriately diluted prior to analysis. An aliquot of 0.1 mL of the prepared sample was mixed with 2.9 mL of the adjusted DPPH solution.
- The reaction mixture was shaken for a few seconds and kept in the dark at room temperature for 30 min.
- After the reaction time, the absorbance was measured using a UV–Vis spectrophotometer. The antioxidant activity was determined by comparing the absorbance decrease of the samples with

that of the Trolox standard. A representative image of the reaction mixtures obtained during the DPPH assay is reported in Figure 3.15

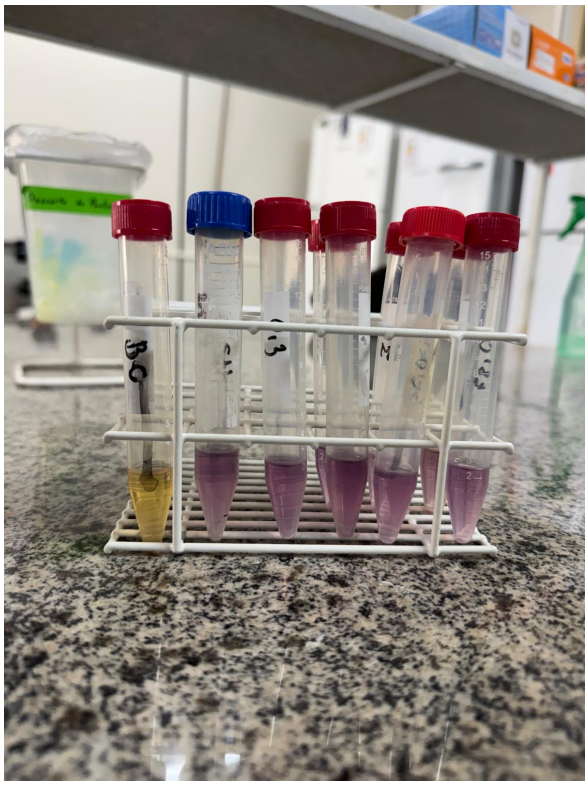

(a) The pink colour corresponds to the DPPH radical solution.

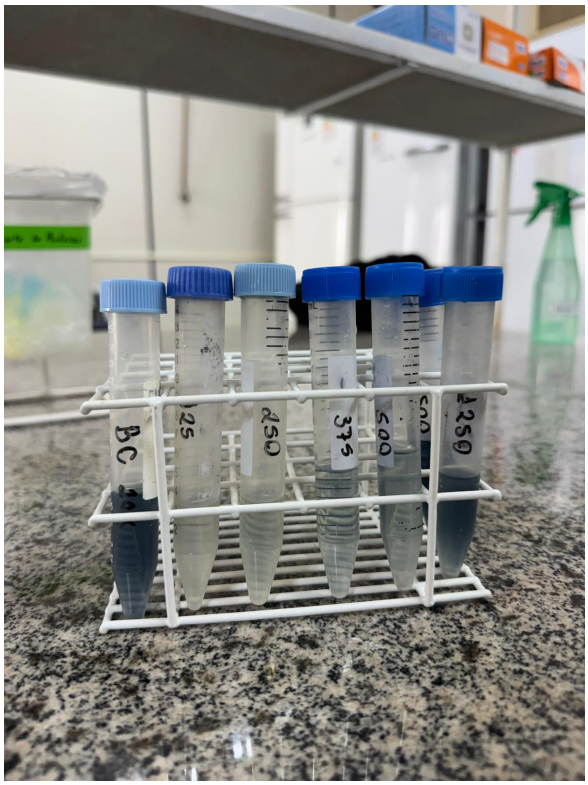

(b) The blue color corresponds to the presence of flavonid compounds.

Figure 3.15

3.4.3 Determination of Total Phenolic Content

The total phenolic content of the produced bio-oil was determined using the Folin–Ciocalteu colorimetric method. The analysis was performed under light-protected conditions due to the photosensitive nature of the reaction.

- A sodium carbonate solution was prepared by dissolving sodium carbonate in distilled water to obtain a 25% (w/v) solution. The solution was stored at room temperature until use.
- Gallic acid was used as the reference standard for the calibration curve. A stock solution was prepared by dissolving gallic acid in absolute ethanol to obtain a concentration of 3000 mg/L. From this stock solution, a series of standard solutions with different concentrations were prepared by appropriate dilution.
- Bio-oil samples were suitably diluted prior to analysis. For the assay, an aliquot of 0.1 mL of the prepared sample or standard solution was transferred into a test tube. Representative images of the sample preparation step are reported in Figure 3.16.

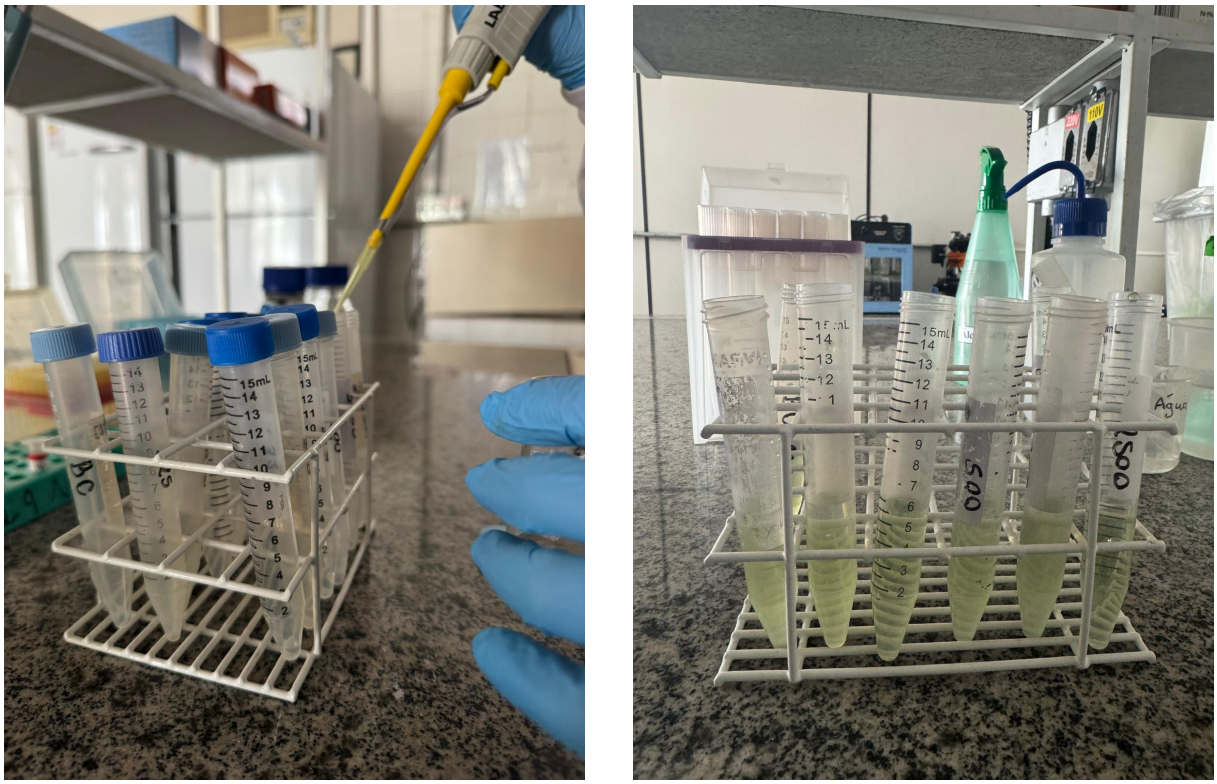

(a) (b)

Figure 3.16: Test tubes containing the prepared liquid samples after the transfer step, prior to reagent addition. Credit: Author

- Subsequently, 5 mL of distilled water were added, followed by the addition of 0.15 mL of the Folin–Ciocalteu reagent. The mixture was homogenized and allowed to react for 3 min at room temperature.
- After this initial reaction time, 1.4 mL of the 25% sodium carbonate solution and 3 mL of distilled water were added (Figure 3.17). The reaction mixture was thoroughly mixed and incubated in the dark at room temperature for 1 hour to allow colour development.

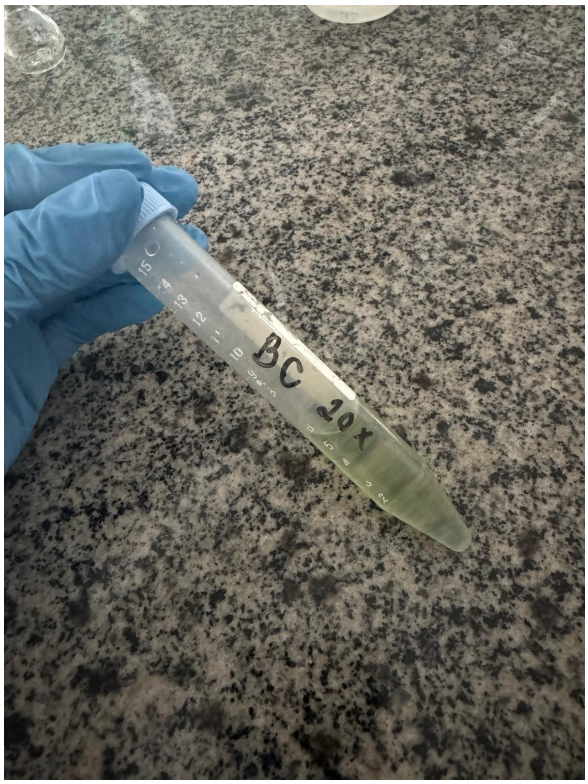

(a) Prepared liquid sample prior to the addition of the sodium carbonate solution. Credit: Author

(b) Prepared liquid sample after the addition of the sodium carbonate solution. Credit: Author

Figure 3.17: Credit: Author

- A blank sample was prepared following the same procedure, replacing the bio-oil sample with distilled water.
- After incubation, the absorbance of samples, standards and blank was measured at a wavelength of 765 nm using a UV–Vis spectrophotometer.
- The total phenolic content was quantified using the calibration curve obtained from gallic acid standard solutions and expressed as gallic acid equivalents (GAE).

3.4.4 pH Measurement

The pH of the liquid samples was measured using a calibrated digital pH meter at room temperature.

3.4.5 Chromatographic Analysis

Gas chromatography–mass spectrometry (GC–MS) was used to characterize the volatile and semi-volatile compounds present in the sample. Analyses were performed on a PerkinElmer Clarus 680 GC–MS system equipped with a PerkinElmer Elite-5 capillary column (length 60 m, internal diameter 0.25 mm, film thickness 0.25 m).

3.4.6 Thermogravimetric Analysis (TGA/DTG)

Thermogravimetric analysis (TGA) was performed to investigate the thermal stability and mass loss behaviour of the bio-oil. The analysis was carried out using a thermogravimetric analyzer, which continuously measures the variation in sample mass as a function of temperature under controlled heating conditions.

For the analysis, a small amount of bio-oil sample was placed in the analyzer and subjected to a programmed temperature increase over a defined temperature range. The mass variation of the sample was automatically recorded during the heating program and collected through dedicated computer software. The resulting thermogravimetric (TGA) curve represents the evolution of sample mass with temperature, while the derivative thermogravimetric (DTG) curve was obtained from the recorded data and used to identify the temperatures corresponding to the maximum mass loss rates. The TGA/DTG data were subsequently used to analyse the volatility profile and thermal degradation behaviour of the bio-oil sample.

3.5 Biochar as co-product of the pyrolysis process

Besides the liquid component, the process of pyrolysis of SCGs also produces a solid carbon-rich byproduct known as biochar. Although this study primarily emphasizes the analysis and enhancement of bio-oil, the biochar produced during the pyrolysis experiments serves as a significant co-product that could enhance the overall financial feasibility of the system. Biochar derived from different types of coffee-based biomass was analyzed by other researchers in the group. The analyses included biochar yield, measurement of moisture content, assessment of ash content and evaluation of fixed carbon. In this thesis, biochar information is used only for yield calculation and for conducting economic assessments.

This approach aims to furnish a more complete evaluation of the potential benefits of pyrolyzing coffee waste.

3.6 Cost Assessment

The economic analysis conducted in this work follows the general framework of Techno-Economic Analysis (TEA), widely adopted in studies on biomass pyrolysis and bio-oil upgrading (Hasan et al., 2022; Jones et al., 2013; Jerzak et al., 2024). The methodological structure is consistent with cost-engineering guidelines reported in technical documents, while market price variability and commercial reference values were taken from dedicated compilations (Rogers and Brammer, 2012; Ferrari et al., 2025). This approach provides a structured methodology which consists of:

- **Cost Classification**: all costs are categorized according to a Cost Breakdown Structure (CBS), distinguishing between direct/indirect, fixed/variable, and recurring/non-recurring costs.
- **Cost Estimation**: for each scenario, the cost was divided into Capital Expanditure (CAPEX) and Operating Expanditure (OPEX) (Jones et al., 2013; Rogers and Brammer, 2012; Nematian et al., 2021).
- **Revenue Estimation**: revenues are derived from the annual production of bio-oil or chemical fractions and the corresponding market prices (Talmadge et al., 2021; Tian et al., 2021; Santos et al., 2025).
- **Economic Indicators**: the profitability of each scenario is evaluated using indicators, such as Annual Profit, Payback Period, Operating Margin (Amjed et al., 2024).
- **Sensitivity Analysis**: key techno-economic parameters (e.g., prices, yields, energy cost, labour cost and CAPEX factors) are varied to assess their effect on the economic indicators and to evaluate the robustness of the results (Amjed et al., 2024; Makepa et al., 2023; Li et al., 2017).

The objective is to evaluate and compare two valorization pathways for the valorization of the bio-oil derived from spent coffee grounds.

3.6.1 Economic Scenarios

Two alternative routes have been considered for the valorization of products obtained from pyrolysis of spent coffee grounds. Both scenarios focus on the commercialization of the liquid fraction, which represents the most valuable output of the process, but they differ in terms of product processing, market target and required technological readiness.

Scenario A This scenario considers the direct commercialization of the crude bio-oil, without any upgrading or purification step. It requires minimal processing and investment and it reflects the simplest valorization strategy.

Scenario B In the second scenario, the raw bio-oil is separated into distinct fractions or compounds.

3.6.2 System Boundaries

The system boundaries define what process stages are included in the techno-economic assessment. Table 3.4 specifies which elements are included and which ones are excluded.

Table 3.4: System boundaries for the techno-economic assessment.

Included in the analysis	**Not included in the analysis**
• Feedstock collection and drying • Pyrolysis operation • Condensation and crude bio-oil recovery • Biochar collection • Energy consumption (reactor and condenser) • Scenario B additional steps	• Transportation of feedstock and final products • Administrative and taxation costs • Marketing and distribution activities • End-use of products • Environmental impact assessment (LCA) • Research and development costs

3.6.3 Cost Classification

A Cost Breakdown Structure (CBS) was developed to classify and organize all cost elements associated with the production and valorization of bio-oil. Figure 3.18 summarizes the type of costs.

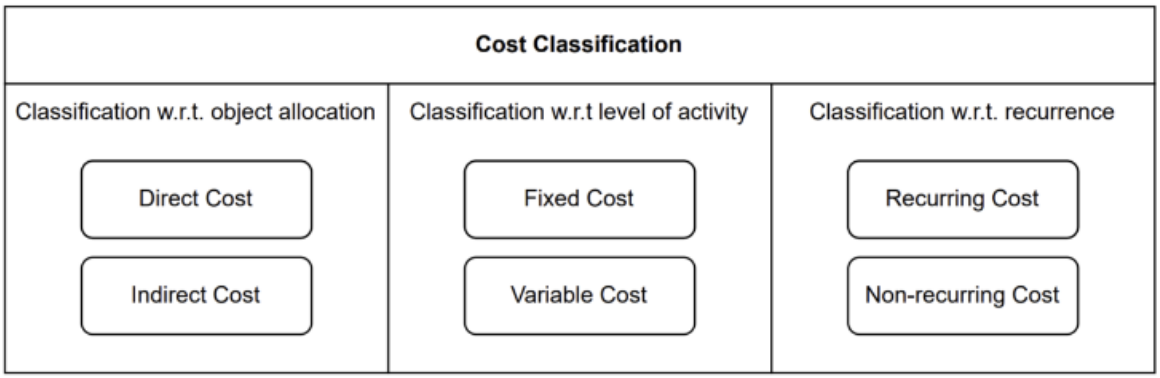

Figure 3.18: Cost Classification

1. **Direct Costs**: Expenses that can be directly linked to a specific cost object, such as the pyrolysis reactor operation, feedstock supply, energy consumption or separation equipment.
2. **Indirect Costs**: Costs that cannot be attributed to a single process step, but support the operations in general. Administrative labour, utilities for auxiliary systems, general overhead or shared services are included.
3. **Fixed Costs**: Costs that remain unchanged regardless of changes in the level of activities. These can include depreciation, insurance and facility leasing.
4. **Variable Costs**: Costs that vary in proportion to changes in the level of activity, such as electricity used, cooling water.

5. **Recurring Costs**: Costs incurred repeatedly throughout the system's lifecycle. These are labour, maintenance, utilities and routine material supply.

6. **Non-recurring Costs**: One-time costs associated with system design, installation, commissioning and prototype development.

This classification is particularly important in the context of the two valorization scenarios, as they rely on different cost drivers.

The next section introduces the cost estimation approach and the assumptions adopted for both scenarios.

3.6.4 CAPEX Estimation Method

CAPEX, which stands for Capital Expanditure, represents the investment made to buy, maintein or upgrade a long term asset.

In this study, the following were considered:

- **equipment cost**: pyrolysis reactor, heating exchanger, galvanized steel funnel, gas scrubber, vacuum pump;
- **installation costs**: piping, valves, instrumentation, mechanical supports;
- **indirect costs**: contingency, engineering and documentation;

Equipment Cost The equipment cost was estimated using a mixed approach. The pyrolysis reactor cost was obtained from the supplier price list, while for costume-made components a cost based on material weight and unit material cost was assigned. Components fully available from previous laboratory projects were not associated with an additional purchase cost.

Installation and Indirect Costs They were estimated by applying standard literature factors commonly used in TEA studies.

CAPEX The total capital investment was calculated as:

$$C_{\text{equipment}} = \sum_i C_{\text{equipment},i} \tag{3.4}$$

$$C_{\text{inst}} = (1 + f_{\text{installation}})\, C_{\text{equipment}} \tag{3.5}$$

$$C_{\text{indirect}} = f_{\text{ind,cap}}\, C_{\text{inst}} \tag{3.6}$$

$$\text{CAPEX} = C_{\text{inst}} + C_{\text{indirect}} \tag{3.7}$$

where $C_{\text{equipment},i}$ represents the purchase cost of the i-th process unit and $C_{\text{equipment}} = \sum_i C_{\text{equipment},i}$ is the total equipment cost. The installation factor $f_{\text{installation}}$ accounts for additional costs associated with mechanical installation, piping, instrumentation, electrical connections and assembly activities. Finally, C_{indirect} represents the indirect capital cost component, including engineering, project management and commissioning activities, and is estimated as a fixed percentage of the installed cost.

3.6.5 OPEX Estimation Method

OPEX, which stands for Operating Expenses, refers to the day-to-day costs that are need to keep the operations and the system running. In this study, the following were considered:

- **feedstock cost**: accounting for the cost of the raw material required for the process;
- **energy consumption**: accounting for the electricity consumption required to heat the reactor and operate auxiliary equipment, such as the condenser, vacuum pump and water pump;
- **labour cost**: required to operate the system and manage tasks;
- **maintenance cost**: including routine maintenance and minor repairs;
- **consumables cost**: accounting for auxiliary materials and minor utilities required for plant operation, such as cooling water.

Feedstock Cost It was set neglected, since SCG represent a waste material.

Energy Consumption It was estimated by considering the rated power of the auxiliary equipment and their operating time per batch. Power ratings expressed in chemical vaporizer (CV) units were converted to kilowatts using the conversion factor:

$$1 \text{ CV} = 0.7355 \text{ kW}.$$

The electricity consumption per batch was calculated as:

$$E_{\text{batch}} = (P_{\text{reactor}} + P_{\text{vacuum}} + P_{\text{pump}})\, t,$$

where P_{reactor}, P_{vacuum} and P_{pump} are the electrical power ratings of the reactor motor, the vacuum pump and the water pump, and t is the operating time per batch.

Annual electricity consumption was calculated by multiplying the batch consumption by the number of batches per year, based on assumed daily operating schedule and annual operating days.

Electricity costs were obtained by multiplying the annual electricity consumption by the electricity price. Local electricity tariffs were obtained for the Brazilian context and converted to euros using the reference exchange rate for the analysis year; this ensures consistency with the overall economic analysis conducted in euros.

Labour Cost It was set to zero, as the system operates at laboratory scale and does not require dedicated operating personnel.

Maintenance Cost It is estimated as a fixed percentage of the CAPEX.

Conumables Cost They were were neglected in Scenario A, as the process does not require additional reagents or auxiliary materials. In Scenario B, consumables related to the upgrading process were instead considered.

OPEX The total annual operating cost was expressed as:

$$OPEX = C_{\text{feed}} + C_{\text{energy}} + C_{\text{labour}} + C_{\text{maintenance}} + C_{\text{consumables}}$$

where $C_{\text{feedstock}}$ represents the cost of the raw material required for the process, C_{energy} accounts for the energy consumption associated with the operations, C_{labour} represents labour costs required to operate the system, $C_{\text{maintenance}}$ includes routine maintenance and minor repair costs, and $C_{\text{consumables}}$ accounts for the consumption of auxiliary materials and minor utilities during operation.

3.6.6 Revenue Estimation

Revenues represent the income generated from the sale of the products obtained from the process. Revenues were estimated from the annual production of bio-oil, biochar and upgraded chemical fractions, depending on the scenario considered.

For each scenario, the annual revenue (R) was calculated as:

$$R = \sum_{j} m_{j,\text{annual}} \cdot P_j$$

where $m_{j,\text{annual}}$ is the annual mass of product j and P_j is the corresponding market reference price.

Scenario A In Scenario A, revenues originate from the sale of crude bio-oil and biochar.

Scenario B In Scenario B revenues include the combined contribution of the separated chemical fractions, each valued according to its specific market price, and the biochar. The market prices of the chemical compounds were derived from international bulk market references, expressed in €/ton and converted to €/kg. Only large-scale industrial prices were considered, in order to ensure a conservative and verifiable economic assessment.

Biochar was considered as a co-product of the pyrolysis process and its contribution to revenues was estimated based on its annual production derived from the experimental mass balance. Since biochar is obtained without additional processing steps, no additional CAPEX or OPEX were attributed to its production. Market prices were obtained from publicly available commercial references.

3.6.7 Economic Indicators

The economic performance of the two scenarios was evaluated using five standard profitability indicators: Annual Profit, Operating Margin, Payback Period, Unit Production Cost and Profit per Unit of Product. These metrics allow comparing the economic feasibility of the two valorisation routes under consistent cost and revenue assumptions.

Annual Profit (Π) represents the yearly economic return of the process and was calculated as:

$$\Pi = R - OPEX$$

where R is the annual revenue and $OPEX$ the annual operating cost, including depreciation.

Operating Margin (OM) expresses the profitability relative to revenues:

$$OM = \frac{\Pi}{R} \times 100$$

Payback Period (PBP) quantifies the time required to recover the initial investment:

$$PBP = \frac{CAPEX}{\Pi}$$

Unit Production Cost (UPC) represents the cost required to produce one unit of product and was computed as:

$$UPC = \frac{OPEX}{m_{annual}}$$

where m_{annual} is the annual mass of product. For Scenario A, m_{annual} corresponds to crude bio-oil production, whereas in Scenario B it represents the total mass of upgraded chemical fractions. UPC provides a direct measure of cost efficiency and enables comparison between the two scenarios independently of scale.

Profit per Unit of Product (Π_{unit}) represents the net economic gain associated with the production and sale of one unit of product and was calculated as:

$$\Pi_{unit} = \frac{\Pi}{m_{annual}}$$

where Π is the annual profit and m_{annual} is the annual mass of product. For Scenario A, m_{annual} corresponds to the annual production of crude bio-oil, whereas in Scenario B it represents the total annual mass of the chemical fractions. This indicator provides an intuitive, unit-based measure of profitability and allows a direct comparison between scenarios on a per-unit basis.

3.6.8 Sensitivity Analysis

A sensitivity analysis was performed to evaluate how uncertainties in key techno–economic parameters affect the profitability of the two scenarios. The analysis aims at identifying which variables have the largest impact on the economic indicators.

The following parameters were selected, based on their relevance in recent TEA studies on biomass pyrolysis:

- product selling prices (crude bio-oil in Scenario A; individual chemical fractions in Scenario B);
- bio-oil and product yields, derived from the experimental mass balances;
- energy cost;
- maintenance cost factor;
- installation and indirect cost factors applied in the CAPEX estimation.

Each parameter was varied individually by ±10% with respect to the base-case value, as shown in Table 3.5, while all other parameters were kept constant. For every variation, the annual profit was recalculated for both scenarios.

Table 3.5: Sensitivity analysis input parameters for Scenario A

Parameter	**Symbol**	**Unit**	**-10%**	**Base case**	**+10%**
Bio-oil selling price	$P_{oil,A}$	€/kg	0.495	0.55	0.605
Biochar selling price	$P_{char,A}$	€/kg	0.45	0.50	0.55
Bio-oil yield	Y_{oil}	%	32.96	36.62	40.28
Biochar yield	Y_{char}	%	27.11	30.12	33.13
Energy cost	P_{el}	€/kWh	0.153	0.17	0.187
Maintenance cost factor	C_{maint}	% of CAPEX	2.7	3.0	3.3
Installation factor	f_{inst}	% of C_{equip}	36	40	44
Indirect cost factor	f_{ind}	% of $C_{installed}$	54	60	66

3.7 Assumptions

This section summarizes the main technical, process and economic assumptions adopted in the techno-economic analysis. The assumptions reported in Table 3.6 are consistently applied throughout the analysis.

Table 3.6: Summary of technical, process and economic assumptions adopted in the techno-economic analysis

Category	Parameter	Symbol	Value	Unit	Source
Feedstock	Annual SCG processed	$M_{\text{SCG,annual}}$	4160	kg/year	This work (derived)
	Residence time	t_{res}	30	min	Experimental setup
Process	Pyrolysis temperature	T_{pyr}	400	°C	Experimental setup
	Bio-oil yield (dry basis)	Y_{oil}	36.62	wt%	Experimental results
	Biochar yield (dry basis)	Y_{char}	30.12	wt%	Experimental results
	Non-condensable gas yield (dry basis)	Y_{gas}	30.79	wt%	Experimental results
Energy	Operating time per batch	t_{batch}	1	h/batch	Experimental setup
	Electricity price range	P_{el}	0.11–0.23	€/kWh	Local utility tariff (Brazil)
	Electricity price (base case)	P_{el}	0.17	€/kWh	Converted from local tariff (Brazil, 2025)
	Currency exchange rate (BRL/EUR)	r_{FX}	6.40	BRL/EUR	Exchange rate (2025)
Economic	Plant lifetime	N	10	years	Assumed
	Pyrolysis reactor purchase cost	C_{reactor}	1383	€	Vendor price
	Stainless steel unit cost	P_{SS}	4.06	€/kg	Local market price
	Galvanized steel unit cost	P_{GS}	2.34–4.06	€/kg	Local market price
	Installation cost factor	f_{inst}	40	% of equipment cost	Literature
	Indirect capital cost factor	f_{ind}	60	% of installed cost	Literature
	Feedstock cost (SCG)	C_{feed}	0	€/kg	Waste material
	Labour cost	C_{labour}	0	€/year	Assumed (laboratory-scale operation)
	Maintenance cost	C_{maint}	3	% of CAPEX	Literature
	Consumables cost – Scenario A	$C_{\text{cons,A}}$	0	€/year	Assumed
	Consumables cost – Scenario B	$C_{\text{cons,B}}$	0	€/year	Assumed / Literature
Product price	Crude bio-oil selling price	P_{oil}	0.55	€/kg	IMARC Group
	Biochar selling price	P_{char}	0.50	€/kg	IBI
	Acetic acid selling price	P_{acetic}	0.60	€/kg	Business Analytiq; IMARC Group
	Phenol selling price	P_{phenol}	0.95	€/kg	Phenol International Price
	Furfural selling price	P_{furfural}	0.90	€/kg	Business Analytiq; IMARC Group
	Formic Acid selling price	P_{formic}	0.70	€/kg	Business Analytiq; IMARC Group
	Acetone selling price	P_{acetone}	1.10	€/kg	Business Analytiq; IMARC Group
	Ethil Acetate selling price	$P_{\text{ethilacetate}}$	0.94	€/kg	Business Analytiq; IMARC Group
	Diacetyl selling price	P_{diacetyl}	3.50	€/kg	Business Analytiq; IMARC Group
	Butyric Acid price	P_{butyric}	2.05	€/kg	Business Analytiq; IMARC Group
	Guaiacol price	P_{guaiacol}	5.90	€/kg	Business Analytiq; IMARC Group
	Ethylphenol price	$P_{\text{ethylphenol}}$	4.20	€/kg	Business Analytiq; IMARC Group
	Catechol price	P_{catechol}	6.30	€/kg	Business Analytiq; IMARC Group
	Ethyl guaiacol price	$P_{\text{ethilguaiacol}}$	6.90	€/kg	Business Analytiq; IMARC Group
	Syringol price	P_{Syringol}	7.60	€/kg	Business Analytiq; IMARC Group
	Isovanillin	$P_{\text{isovanillin}}$	17.20	€/kg	Business Analytiq; IMARC Group
	Levoglucosan	$P_{\text{levoglucosan}}$	5.60	€/kg	Business Analytiq; IMARC Group
	Caffeine	P_{caffeine}	13.50	€/kg	Business Analytiq; IMARC Group

Chapter 4

Experimental Results and Chemical Characterization

This chapter presents the experimental results obtained from the pyrolysis of spent coffee grounds and their subsequent interpretation. Particular attention is given to mass balance and product yields, as they constitute the quantitative base for the techno-economic assessment. The chemical characterization of the bio-oil and biochar fractions is presented according to the analytical techniques described in Chapter 3.

The chapter is organized as follows:

- Section 4.1 presents the mass balance and product yields obtained from the pyrolysis experiments;
- Section 4.2 reports the chemical characterization results of bio-oil;
- Section 4.3 presents the chemical characterization results of biochar;
- Section 4.4 discusses the main chemical results obtained.

4.1 Mass Balance and Product Yields

The mass balance was carried out to quantify the distribution of products obtained from the pyrolysis of spent coffee grounds under the investigated operating conditions. The results refer to a single batch experiment performed using 100 g of oven-dried biomass over a total process time of 30 minutes, reaching a maximum temperature of approximately 400 °C . Product yields were determined following the procedures described in Section 3.3. The overall mass balance and product yields obtained from the pyrolysis experiment are reported in Table 4.1.

Table 4.1: Overall mass balance and product yields obtained from the pyrolysis of spent coffee grounds.

Product	**Mass (g)**	**Yield (wt%)**
Biochar	30.12	30.12
Bio-oil	36.62	36.62
Non-condensable gases	30.79	30.79
Total	**97.53**	**97.53**

The results show that the bio-oil represents the main product fraction, followed by biochar and non-condensable gases. The mass balance closure does not reach 100%, which can be attributed to minor experimental losses and residual moisture in the biomass, considered negligible and therefore not included in the mass balance calculation. The overall product yield distribution is shown in Figure 4.1.

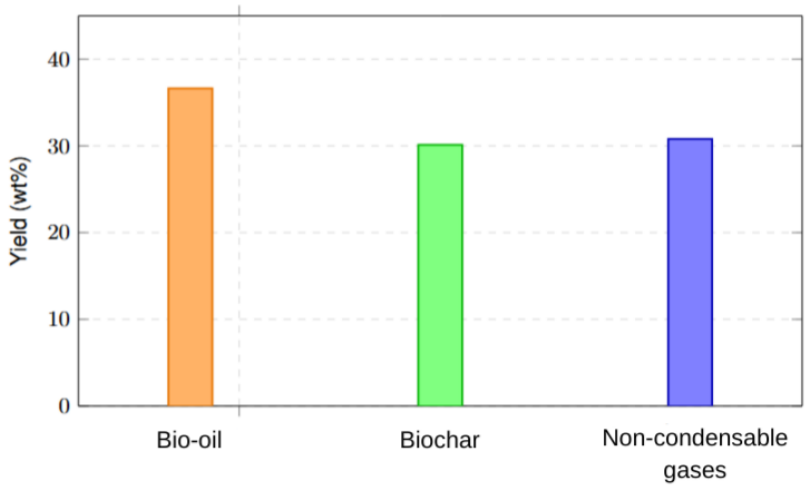

Figure 4.1: Distribution of product yields obtained from the pyrolysis of spent coffee grounds, expressed as weight percentages of the initial dry biomass.

The product yield distribution highlights the relevance of the liquid fraction within the overall mass balance. Given that bio-oil represents the largest product fraction, further insight into its formation dynamics is explored. The bio-oil yield was monitored as a function of process time and temperature, allowing the identification of the main stages of liquid production during the heating phase (Figure 4.2).

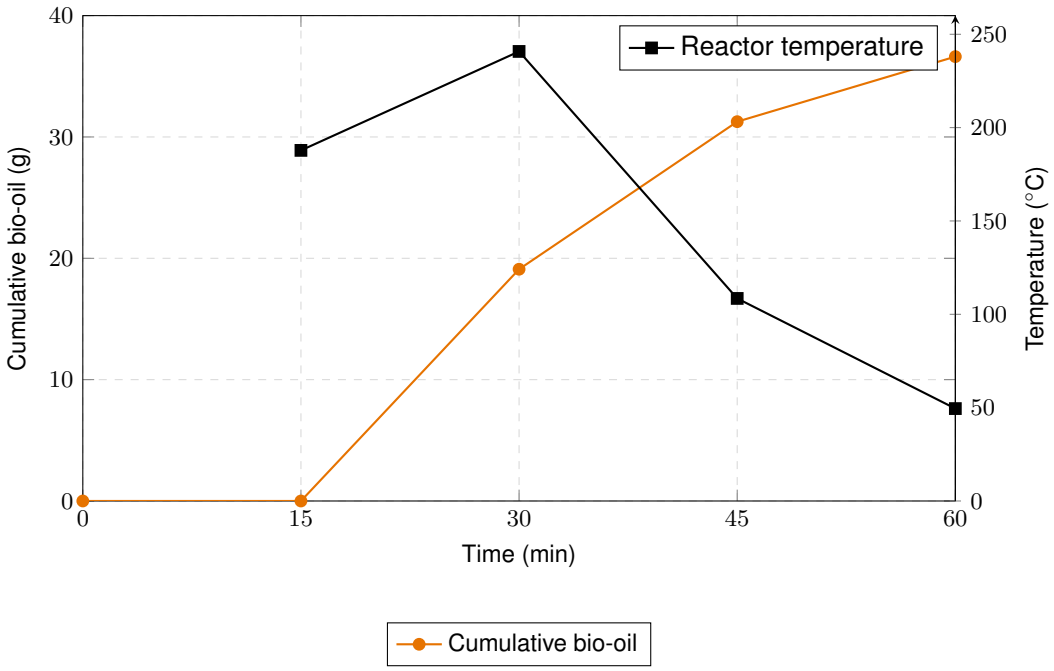

Figure 4.2: Cumulative bio-oil production and reactor temperature as a function of process time during the pyrolysis experiment.

The comparison between cumulative bio-oil production and reactor temperature shows that the main release of the liquid fraction occurs during the heating phase, when the reactor reaches its highest temperatures, while bio-oil formation progressively slows down during the cooling stage. Considering all this, given the significant contribution of the bio-oil to the overall mass balance, further analyses were conducted to investigate its chemical composition and antioxidant properties.

4.2 Chemical Characterization of Bio-oil

4.2.1 Antioxidant activity of bio-oil assessed by DPPH assay

The antioxidant activity of the bio-oil was evaluated using the DPPH radical scavenging assay. The calibration curve obtained using Trolox as reference antioxidant is shown in Figure 4.3.

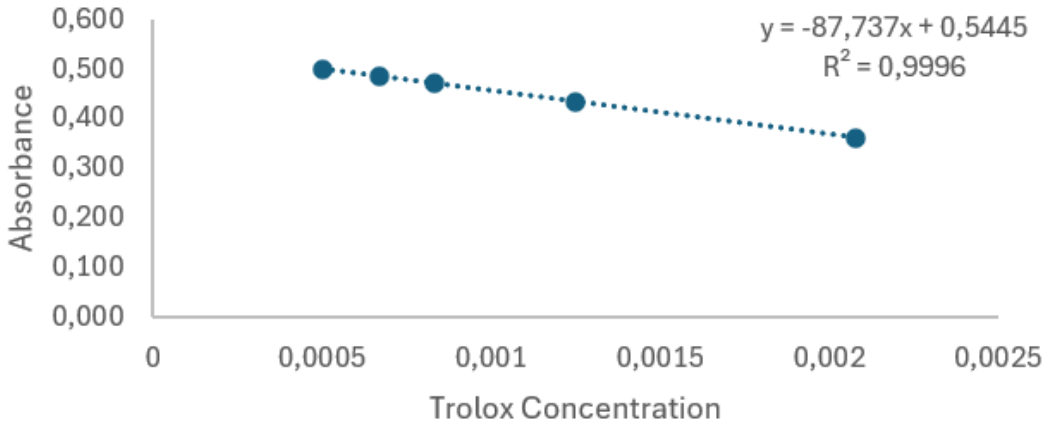

Figure 4.3: Trolox calibration curve obtained from the DPPH assay. Circular markers represent experimental absorbance values for Trolox standard solutions, while the solid line corresponds to the linear regression used for calibration ($R^2 = 0.9996$).

The experimental results show a clear linear relationship between Trolox concentration and absorbance over the investigated range. The high coefficient of determination ($R^2 = 0.9996$) confirms the reliability of the calibration curve. This was subsequently used to quantify the antioxidant activity of the bio-oil samples.

A summary of the main DPPH assay results obtained for the bio-oil sample is reported in Table 4.2.

Table 4.2: Summary of DPPH assay results for the bio-oil sample.

Sample	**Absorbance**	**DPPH inhibition (%)**	**IC_{50} (mg/mL)**
Bio-oil	0.205	61.16	0.08
Negative control	0.529	–	–

As reported in Table 4.2, the bio-oil sample exhibited a substantial reduction in absorbance compared to the negative control, indicating an intense scavenging activity toward the DPPH radical. The calculated inhibition percentage equals 61.16%, confirming the ability of the bio-oil to effectively neutralize free radicals.

Furthermore, the IC_{50} value of 0.08 mg/mL reflects a high antioxidant efficiency, as lower IC_{50} values correspond to stronger radical scavenging capacity.

4.2.2 Total Phenolic Content

The total phenolic content of the bio-oil was determined using the Folin-Ciocalteu colorimetric method, as described in the methodology section. The calibration curve obtained using gallic acid as reference standard is shown in Figure 4.4.

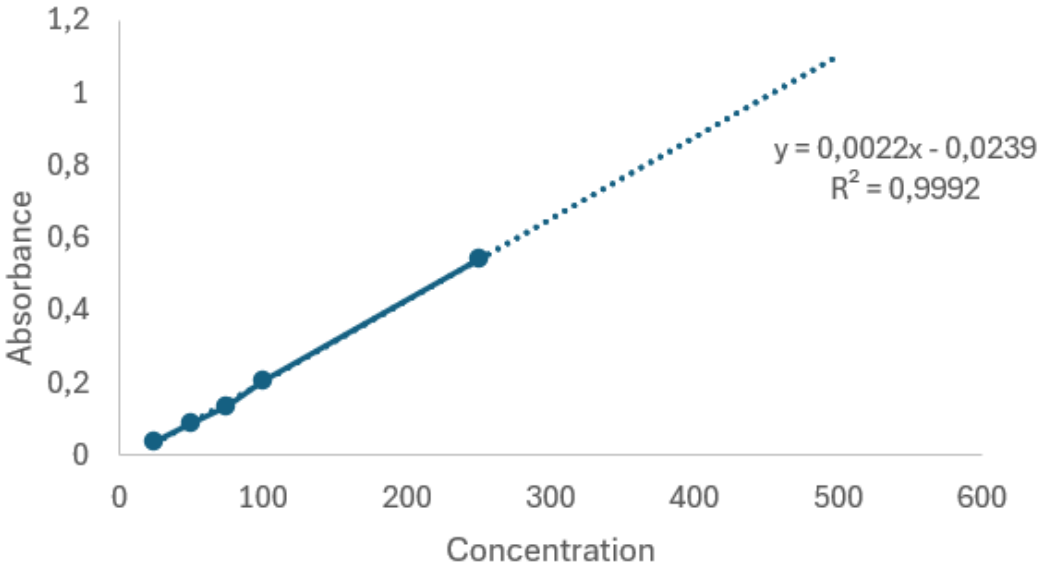

Figure 4.4: Gallic acid calibration curve obtained from the Folin-Ciocalteu assay. Circular markers represent experimental absorbance values for gallic acid standard solutions, while the dotted line corresponds to the linear regression used for calibration ($R^2 = 0.9992$).

The high coefficient of determination ($R^2 = 0.9992$) indicates an excellent linear correlation between gallic acid concentration and absorbance, confirming the reliability of the calibration curve. A summary of the total phenolic content results obtained for the bio-oil sample is reported in Table 4.3.

Table 4.3: Total phenolic content of the bio-oil determined by the Folin-Ciocalteu method.

Sample	**Total phenolic content**
Bio-oil	7.09 mg GAE/mL

As reported in Table 4.3, the bio-oil exhibited a total phenolic content of 7.09 mg GAE/mL when quantified using the Folin-Ciocalteu method. This result confirms the presence of phenolic compounds in the bio-oil derived from spent coffee grounds. These findings provide a chemical basis for the antioxidant activity observed in the DPPH radical scavenging assay and support the potential of spent coffee grounds as a source of bioactive compounds.

4.2.3 pH measurament

The bio-oil sample exhibited an acidic pH value of 3.52.

4.2.4 Chromatography analysis

The chemical composition of the sample was investigated by GC/MS analysis. The resulting chromatogram is shown in Figure 5.23. Several peaks were detected across the entire retention time range, indicating a complex mixture of volatile and semi-volatile compounds.

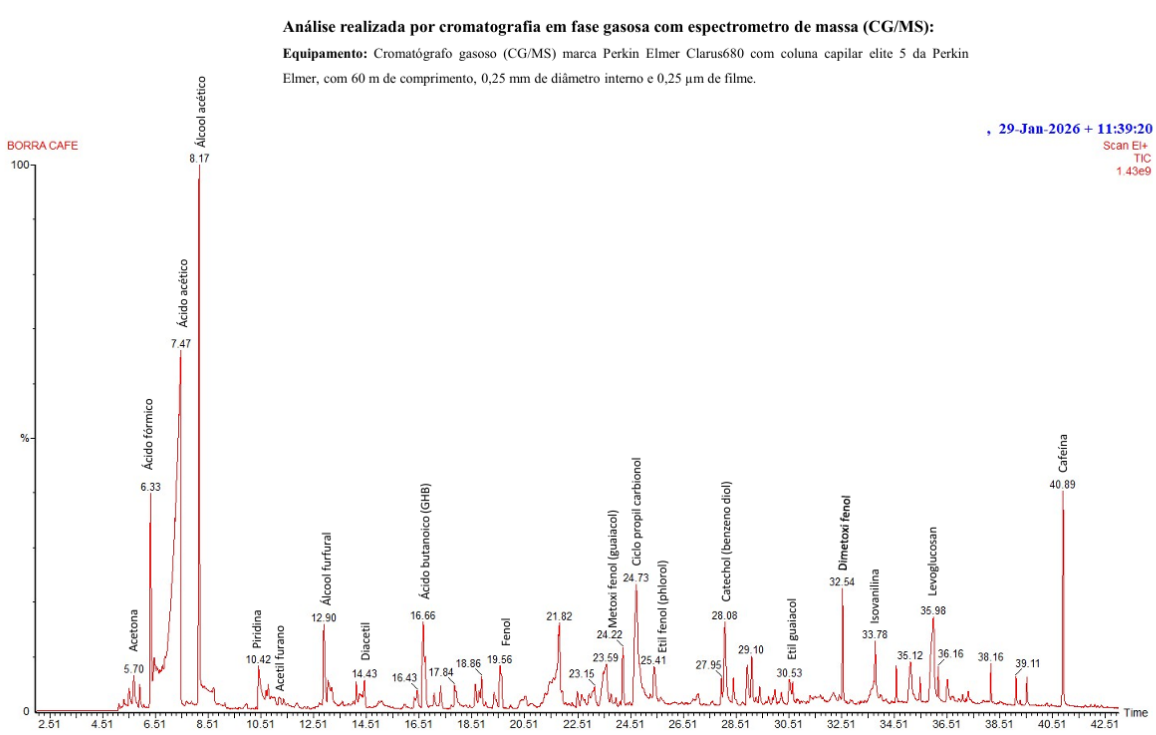

Figure 4.5: GC/MS chromatogram of the analyzed sample, showing the main identified compounds and their corresponding retention times.

The identified compounds mainly include oxygenated chemical species, such as organic acids, ketones, furans, phenolic compounds, sugar-derived species and nitrogen-containing compounds.

Light oxygenated compounds, including acetone and ethyl acetate, were observed at low retention times, followed by organic acids such as butyric acid. A significant fraction of the chromatogram corresponds to phenolic compounds, including guaiacol, ethylphenol, catechol, ethyl guaiacol, syringol and isovanillin. In addition, levoglucosan and nitrogen-containing compounds such as pyridine and caffeine were identified.

4.2.5 Thermogravimetric Analysis

Thermogravimetric Analysis (TGA) was performed to evaluate the thermal stability and volatility profile of the bio-oil samples obtained from the pyrolysis of spent coffee grounds (Duongbia et al., 2025). The TGA curve represents the evolution of the sample's mass as a function of temperature, while the derivative curve (DTG) highlights the specific temperatures at which the highest mass-loss rates occur.

The TGA test was conducted from ambient temperature to 800 °C at a heating rate of 10 °C/min. The mass loss profile of the sample shows three main stages (Figure 4.6).

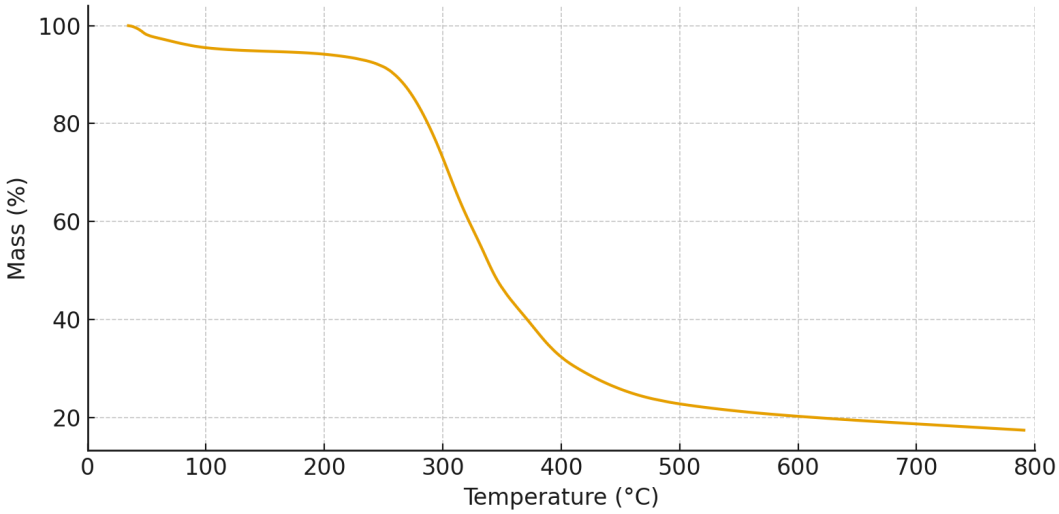

Figure 4.6: TGA of SCG. A major mass-loss event occurs between 250 ℃ and 380 ℃, followed by a gradual degradation of heavier species, leaving a residual mass of approximately 17–18 wt% at 800 ℃.

The first minor mass loss below approximately 120 ℃ corresponds to the evaporation of moisture and very light volatile compounds typically present in bio-oils. A second and much more pronounced mass-loss event occurs between 250 and 380 ℃, as confirmed by the dominant DTG peak centred near 300 ℃ (Figure 4.7). This region is associated with the thermal degradation and volatilization of medium-weight organic compounds generated during pyrolysis.

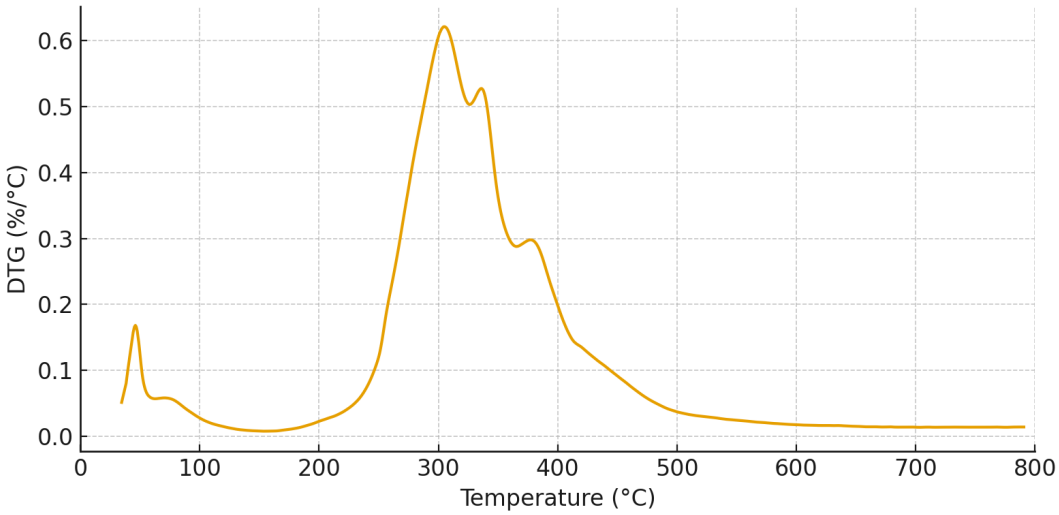

Figure 4.7: DTG curve of SCG. The main peak corresponds to the temperature at which the maximum mass-loss rate occurs during thermal decomposition.

Beyond 400 ℃, the mass decreases at a slower rate, indicating the decomposition of heavier and more thermally resistant components. At 800 ℃, the residual mass stabilizes at approximately 17–18 wt%, representing the non-volatile fraction and carbonaceous residue (Setter et al., 2020).

Overall, the TGA results indicate that the bio-oil contains a significant volatile fraction, a substantial portion of medium-weight organics and a measurable amount of heavier components that contribute

to char formation. This behaviour is consistent with bio-oils derived from lignocellulosic residues and supports further analysis of the chemical composition through complementary techniques.

4.3 Chemical Characterization of Biochar

Table 4.4 summarizes the main properties of the biochar obtained from the pyrolysis of spent coffee grounds. The reported values are derived from proximate analysis and carbon content measurements performed on replicated samples and are presented as average values.

Table 4.4: Main properties and yield of biochar obtained from the pyrolysis of spent coffee grounds

Property	**Average value (wt%)**
Biochar yield (dry basis)	30.12
Moisture content	0.09
Ash content	4.03
Carbon content	60.14

The reported properties indicate that the produced biochar is characterized by low moisture and ash contents and a carbon fraction of approximately 60 wt%. This supports its potential valorization as a co-product of the pyrolysis process.

4.4 Discussion of Chemical Results

The chemical characterization results provide an integrated overview of the products obtained from the pyrolysis of spent coffee grounds. The mass balance indicates that the process leads to the formation of a liquid bio-oil fraction as the main product, accompanied by the generation of biochar as a solid co-product and a fraction of non-condensable gases. This distribution is consistent with typical pyrolysis processes and confirms that the conversion of spent coffee grounds does not result in a single output, but rather in multiple fractions with potential value (Bridgwater, 2012; Pattiya, 2018; Jerzak et al., 2024; Barahmand et al., 2025).

The DPPH assay findings showed that the bio-oil had strong antioxidant activity. The presence of bioactive and oxygenated chemicals is responsible for the effective radical scavenging capacity indicated by an inhibition percentage of 61.16% and a low IC value of 0.08 mg/mL.(Mattos et al., 2019; Malagón-Romero et al., 2023; Ouattara et al., 2023). Since phenolic chemicals are known to be crucial to the antioxidant action of bio-oil, the total phenolic content further supports this concept. (Mohan et al., 2006; Mattos et al., 2019; Hu et al., 2022). Together with the DPPH results, the phenolic content confirms the complex chemical nature of the produced bio-oil and highlights its potential as an intermediate feedstock rather than a simple end product (Machado et al., 2022).

The acidic character of the bio-oil, reflected by a pH value of 3.52, is typical of pyrolysis-derived oils and is mainly associated with the presence of organic acids and phenolic species (Bridgwater, 2012; Lachos-Perez et al., 2023). While this acidity may pose limitations for certain direct applications due

to issues such as corrosiveness and material compatibility, it does not represent a critical drawback for energy-related uses (Rogers and Brammer, 2012).

Thermogravimetric analysis provided further insight into the thermal behavior of the bio-oil. The TGA and DTG profiles indicate a multi-step mass loss pattern, reflecting the presence of compounds with different volatilities and thermal stabilities (Mohan et al., 2006; Krause et al., 2019). This behavior is consistent with the heterogeneous composition of bio-oil and supports its suitability for thermal applications, while also highlighting the complexity that must be managed in any upgrading or fractionation process (Fonseca and Funke, 2024).

The GC/MS results confirm the heterogeneous chemical nature of the bio-oil produced from spent coffee grounds pyrolysis (Bridgwater, 2012). The presence of light oxygenated compounds and organic acids is consistent with the acidic character of the bio-oil, while the detection of phenolic compounds such as guaiacol, catechol and syringol reflects the contribution of lignin-derived products (Mohan et al., 2006). These phenolic species are known to play a key role in the antioxidant behavior of bio-oils, supporting the results obtained from the DPPH assay and total phenolic content analysis (Mattos et al., 2019). In addition, the identification of levoglucosan indicates the contribution of cellulose degradation products, whereas nitrogen-containing compounds such as caffeine highlight feedstock-specific characteristics.

In addition to bio-oil, the production of biochar represents a valuable output of the pyrolysis process. The biochar yield, equal to 30.12 wt% on a dry basis, confirms that a significant fraction of the initial biomass is converted into a solid carbon-rich product. (Segers et al., 2024; Li et al., 2017; Ferrari et al., 2025). The low moisture content (0.09 wt%) suggests good stability. The ash content of 4.03 wt% remains within a range commonly reported for biomass-derived biochars (Joseph, 2015; Cai et al., 2020). A carbon content of approximately 60 wt% further indicates the formation of a stable solid fraction, which is a desirable characteristic for most biochar applications (Pereira et al., 2022).

Overall, the chemical characterization results demonstrate that the pyrolysis of spent coffee grounds leads to the production of a chemically complex bio-oil and a solid biochar fraction.

Chapter 5

Techno-Economic Assessment and Valorization Scenarios

This chapter presents the techno-economic assessment of the proposed SCGs pyrolysis process. Two valorization scenarios are explored, evaluating capital investment, operating expenditures, revenue streams and key economic performance indicators. Particular emphasis is placed on understanding how alternative product valorization strategies influence economic outcomes.

The chapter is organized as follows:

- Section 5.1 provides an overview of the economic results for the two scenarios;
- Section 5.2 evaluates the Technology Readiness Level (TRL) of the proposed process;
- Section 5.3 discusses the techno-economic results, with particular focus on potential applications of bio-oil and biochar;
- Section 5.4 presents a comparative assessment of green coffee and coffee cherry husk as alternative feedstocks;
- Section 5.5 discusses scale-up considerations and their implications on capital and operating costs.

5.1 Economic Results Overview

The economic performance of the two valorization pathways is evaluated in the following sections, where Scenario A and Scenario B are analyzed separately using the assumptions defined in Section 3.7.

5.1.1 Scenario A

Scenario represents the simplest valorization route for the products obtained from the pyrolysis process. In this scenario, the liquid fraction generated during pyrolysis is collected and sold as crude bio-oil, without undergoing any additional procedure. The simplicity of this approach translates into low capital requirements, since only the pyrolysis unit, condensation system, and basic storage infrastructure are needed. Operating costs are primarily driven by energy consumption and general maintenance operations.

CAPEX Once the process configuration has been set, the capital expenditure (CAPEX) was estimated to represent the one-time investments required to set up and operate the system.

Regarding the equipment cost, the purchase cost of the pyrolysis reactor amounts to 1383 €, the cost of the heat exchanger was estimated based on material weight and unit material cost, resulting in a total cost of 37.90 €, The cost of the galvanized steel funnel was estimated as 3.70 €, while the gas scrubber and the vacuum pump were already available in the laboratory and were therefore not associated with a cost.

The total capital expenditure for Scenario A was estimated by summing the purchase costs of the equipment items and applying standard installation and indirect cost factors. This approach is consistent with the CAPEX estimation methodology described in Section 3.6.4.

$$\text{CAPEX} = C_{\text{inst}} + C_{\text{indirect}} \tag{5.1}$$

Based on the cost components described above, the total capital expenditure for Scenario A was estimated and is summarised in Table 5.1.1

Table 5.1: Capital expenditure (CAPEX) calculation for Scenario A

Cost item	**Symbol**	**Calculation**	**Cost [€]**
Equipment cost	$C_{\text{equipment}}$	$\sum_i C_{\text{equipment},i}$	1424.39
Installation cost	$C_{\text{installation}}$	$0.4 \times C_{\text{equipment}}$	571.76
Installed cost	C_{inst}	$C_{\text{equipment}} + C_{\text{installation}}$	2001.15
Indirect capital cost	C_{indirect}	$0.6 \times C_{\text{inst}}$	1200.69
Total CAPEX	**CAPEX**	$C_{\text{inst}} + C_{\text{indirect}}$	**3201.83**

Based on the selected equipment costs and cost factors, the total estimated capital expenditure for Scenario A amounts to 3201.83 €.

OPEX In addition to the initial investment costs, the economic performance of Scenario A is also influenced by the annual operating expenses required to run the system. These costs reflect the consumption of resources such as feedstock, electricity, cooling utilities, labour and routine maintenance.

The electricity consumption for Scenario A was calculated based on the rated power of the auxiliary equipment and the operating time per batch, as described in the methodology. The auxiliary equipment considered includes the reactor motor, the vacuum pump and the water pump.

The electrical power of each unit was calculated as:

$$P_{\text{reactor}} = 0.25 \times 0.7355 = 0.1839 \text{ kW}$$

$$P_{\text{vacuum}} = 0.25 \times 0.7355 = 0.1839 \text{ kW}$$

$$P_{\text{pump}} = 0.035 \text{ kW}$$

Assuming an operating time of $t = 1$ h per batch, the electricity consumption per batch was calculated as:

$$E_{\text{batch}} = (P_{\text{reactor}} + P_{\text{vacuum}} + P_{\text{pump}})\, t$$

$$E_{\text{batch}} = (0.1839 + 0.1839 + 0.035) \times 1 = 0.4028 \text{ kWh/batch}$$

Using the base-case electricity price of $P_{\text{el}} = 1.10$ R$/kWh, the electricity cost per batch is:

$$C_{\text{el,batch}} = E_{\text{batch}} \times P_{\text{el}}$$

$$C_{\text{el,batch}} = 0.4028 \times 1.10 = 0.44 \text{ R\$/batch}$$

The annual electricity cost was obtained by multiplying the cost per batch by the annual number of batches. Assuming $N_{\text{batch,day}} = 6$ batches per day and $N_{\text{op,days}} = 260$ operating days per year:

$$C_{\text{el,annual}} = C_{\text{el,batch}} \times N_{\text{batch,day}} \times N_{\text{op,days}}$$

$$C_{\text{el,annual}} = 0.44 \times 6 \times 260 = 686.40 \text{ R\$/year}$$

Finally, the annual electricity cost was converted to euros using the reference exchange rate for 2025 ($r_{\text{FX}} = 6.40$ R$/EUR):

$$C_{\text{el,annual}}^{\text{EUR}} = \frac{686.40}{6.40} = 107.30 \text{ €/year}$$

Additional operating costs include routine maintenance.

The total annual operating expenditure for Scenario A was calculated as the sum of all operating cost components described above.

$$OPEX_A = C_{\text{feed}} + C_{\text{energy}} + C_{\text{labour}} + C_{\text{maintenance}} + C_{\text{consumables}}$$

Based on the operating cost components described above, the total annual operating expenditure

for Scenario A was estimated and is summarised in Table 5.1.1

Table 5.2: Operating expenditure (OPEX) calculation for Scenario A

Cost item	**Symbol**	**Calculation**	**Cost [€/year]**
Feedstock Cost	C_{feed}	Assumed	0
Energy cost	C_{energy}	$E_{\text{annual}} \times P_{\text{el}}$	107.00
Labour cost	C_{labour}	Assumed	0
Maintenance cost	$C_{\text{maintenance}}$	$0.03 \times$ CAPEX	96.06
Consumables cost	$C_{\text{consumables}}$	Assumed	0
Total OPEX	**OPEX**	$C_{\text{feed}} + C_{\text{energy}} + C_{\text{labour}} + C_{\text{maintenance}} + C_{\text{consumables}}$	**203.01**

The total annual operating expenditure for Scenario A amounts to approximately 203.01 €/year.

Revenue Model In Scenario A, revenues come from the sale of crude bio-oil and biochar. The annual revenue depends on the amount of dried SCGs processed, the experimentally determined bio-oil and biochar yield and the assumed selling price of the two products. Based on the assumptions described above, the estimated annual revenue for Scenario A is summarized in Table 5.3.

Table 5.3: Annual revenue calculation for Scenario A based on crude bio-oil and biochar commercialization

Revenue item	**Symbol**	**Calculation**	**Value**
Annual processed biomass	$MSCG_{\text{annual}}$	Derived	4160 kg/year
Bio-oil yield	Y_{oil}	Experimental	36.62%
Annual bio-oil production	$m_{\text{oil,annual}}$	$MSCG_{\text{annual}} \cdot Y_{\text{oil}}$	1523.39 kg/year
Bio-oil selling price	P_{oil}	Market reference	0.55 €/kg
Bio-oil revenue	R_{oil}	$m_{\text{oil,annual}} \cdot P_{\text{oil}}$	837.87 €/year
Biochar yield	Y_{char}	Experimental	30.12%
Annual biochar production	$m_{\text{char,annual}}$	$MSCG_{\text{annual}} \cdot Y_{\text{char}}$	1253.00 kg/year
Biochar selling price	P_{char}	Market reference	0.50 €/kg
Biochar revenue	R_{char}	$m_{\text{char,annual}} \cdot P_{\text{char}}$	626.50 €/year
Total annual revenue	R_A	$R_{\text{oil}} + R_{\text{char}}$	**1464.40 €/year**

The annual revenue for Scenario A amounts to approximately 1464.40 €/year.

Economic Indicators Based on the estimated cost and revenue structure, the main economic indicators for Scenario A were calculated and are presented as follows:

- Annual Profit (Π): as reported in Table 5.4, Scenario A results in a positive annual profit of 1261.31 €/year.

Table 5.4: Annual profit calculation for Scenario A

Economic Item	**Symbol**	**Calculation**	**Value [€/year]**
Total annual revenue	R_A	From revenue analysis	1464.40
Total annual OPEX	$OPEX_A$	From OPEX analysis	203.01
Annual profit	Π	$R_A - OPEX_A$	**1261.31**

- Operating Margin (OM): the OM results to be equal to 86.10%.

Table 5.5: Operating margin calculation for Scenario A

Economic Item	**Symbol**	**Calculation**	**Value**
Annual profit	Π	From profit analysis	1261.31 €/year
Total annual revenue	R_A	From revenue analysis	1464.40 €/year
Operating margin	OM_A	$(\Pi/R_A) \cdot 100$	**86.10%**

- Payback Period (PBP): the PBP was found to be equal to 2.5 years.

Table 5.6: Payback period calculation for Scenario A

Economic Item	**Symbol**	**Calculation**	**Value**
Total capital investment	$CAPEX_A$	From CAPEX analysis	3201.83€
Annual profit	Π	From profit analysis	1261.31 €/year
Payback period	PBP_A	$CAPEX_A/\Pi$	**2.54 years**

- Unit Production Cost (UPC): the UPC was found to be equal to 0.13 €/kg.

Table 5.7: Unit production cost calculation for Scenario A

Economic Item	**Symbol**	**Calculation**	**Value**
Annual raw material processed	$M_{SCG,annual}$	Derived	4160 kg/year
Bio-oil yield	Y_{oil}	From experimental results	36.62 %
Annual bio-oil production	m_{annual}	$M_{SCG,annual} \cdot Y_{oil}$	1523.40 kg/year
Total annual OPEX	$OPEX_A$	From OPEX analysis	203.06 €/year
Unit production cost	UPC_A	$OPEX_A/m_{annual}$	**0.13 €/kg**

- Profit per Unit of Product (Π_{unit}): the profit per kilogram of crude bio-oil results to be equal to 0.83 EUR/kg.

Table 5.8: Profit per unit of product calculation for Scenario A

Economic Item	**Symbol**	**Calculation**	**Value**
Annual profit	Π	From profit analysis	1261.31 €/year
Annual bio-oil production	m_{annual}	From mass balance	1523.39 kg/year
Profit per unit of product	$\Pi_{unit,A}$	Π/m_{annual}	**0.83 €/kg**

Sensitivity Analysis This paragraph presents the results of the sensitivity analysis performed on Scenario A. The analysis evaluates the impact of ±10% variations in selected techno-economic parameters on the annual profit, while all other parameters were kept constant.

Table 5.9: Sensitivity analysis on annual profit for Scenario A (bio-oil + biochar)

Parameter varied	**Symbol**	**Profit (10%)**	**Base case profit**	**Profit (+10%)**
Bio-oil selling price	P_{oil}	1177.88	1261.31	1345.45
Bio-oil yield	Y_{oil}	1177.52	1261.31	1345.09
Biochar selling price	P_{char}	1199.01	1261.31	1324.31
Biochar yield	Y_{char}	1198.66	1261.31	1324.96
Energy cost	C_{energy}	1272.36	1261.31	1250.96
Maintenance cost factor	f_{maint}	1270.91	1261.31	1251.70
Installation cost factor	f_{inst}	1264.05	1261.31	1258.56
Indirect cost factor	f_{ind}	1264.05	1261.31	1257.70

The results reported in Table 5.9 show that the annual profit of Scenario A is primarily influenced by variations in bio-oil selling price and bio-oil yield, which represent the main revenue drivers of the process. Variations in biochar selling price and biochar yield also affect profitability, although to a lower extent compared to bio-oil-related parameters. In contrast, changes in cost-related parameters, such as energy cost and CAPEX-related factors, result in comparatively smaller variations in annual profit. Figure 5.1 provides a graphical representation of the sensitivity analysis results, showing the variation in annual profit with respect to the base case for ±10% changes in each parameter.

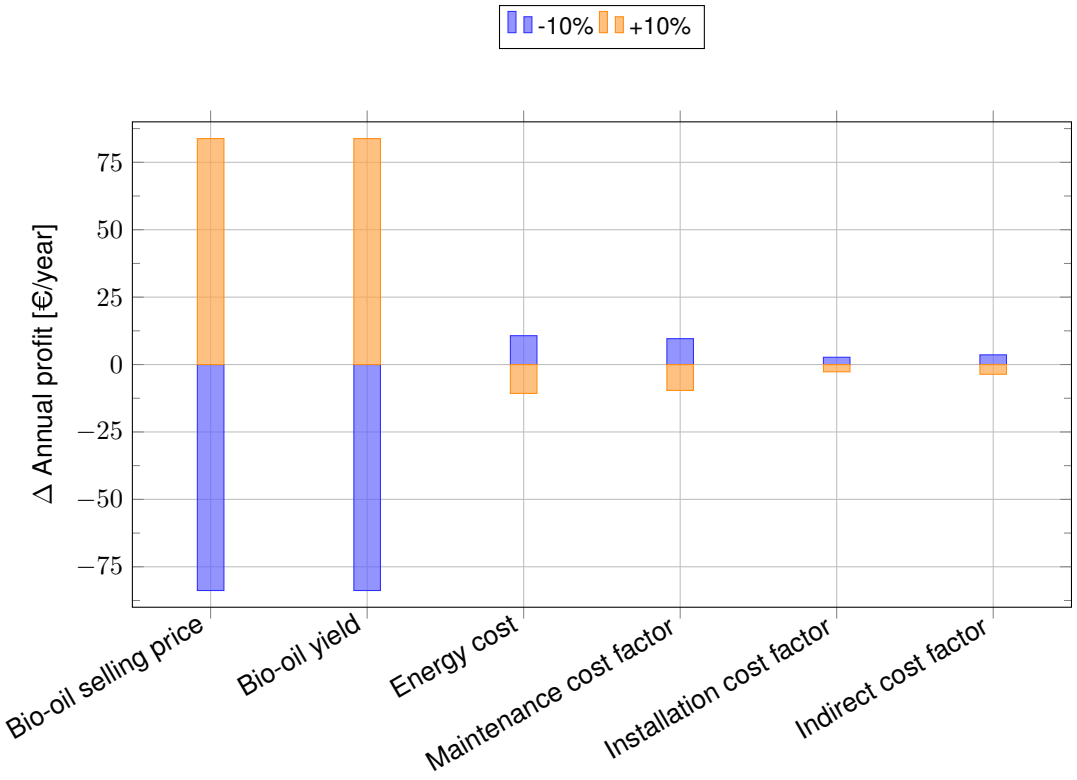

Figure 5.1: Sensitivity analysis of Scenario A: deviation of annual profit from the base case ($\Pi_{\text{base}} = 634.90$ €/year) under ±10% variations of key techno-economic parameters.

5.1.2 Scenario B

Scenario B represents a more advanced valorization pathway for the products obtained from the pyrolysis process. In this scenario, the constituents of the liquid fraction are identified and valued.

CAPEX The capital investment required for Scenario B was assumed to be equal to that of Scenario A, as the upstream pyrolysis process and the associated equipment remain unchanged. Accordingly, the total CAPEX for Scenario B was estimated at 3190.63 €.

Table 5.10: Capital expenditure estimation for Scenario B

Cost Item	**Symbol**	**Calculation**	**Value [€]**
TOTAL CAPEX	$CAPEX_B$	Same as Scenario A	3190.63

OPEX The operating expenditures for Scenario B were estimated by adding the cost of external chromatographic analyses to the operating cost structure of Scenario A.

Table 5.11: Operating expenditure estimation for Scenario B

Economic Item	**Symbol**	**Calculation**	**Value [€/year]**
Feedstock cost	C_{feed}	Assumed	0
Energy cost	C_{energy}	Same as Scenario A	107.00
Labour cost	C_{labour}	Assumed	0
Maintenance cost	C_{maint}	$0.03 \cdot CAPEX_B$	96.06
Consumables cost	C_{cons}	Assumed	0
External chromatographic analysis	C_{chrom}	Assumed annual cost	170.00
Total OPEX	$\mathbf{OPEX_B}$	$C_{feed} + C_{energy} + C_{labour} + C_{maint} + C_{cons} + C_{chrom}$	**373.06**

The total annual operating expenditure for Scenario A amounts to approximately 373,06 €/year.

Revenue Model In Scenario B, revenues originate from the sale of individual chemical fractions obtained from the bio-oil, as well as from the sale of biochar. The annual revenue depends on the amount of dried spent coffee grounds processed, the experimentally determined bio-oil and biochar yields, the relative distribution of the chemical fractions derived from chromatographic analysis, and the assumed selling prices of the individual products. Based on the assumptions described above, the estimated annual revenue for Scenario B is summarized in Table 5.12.

Table 5.12: Annual revenue estimation for Scenario B

Revenue item	Symbol	Calculation	Value
Annual processed biomass	$MSCG_{\text{annual}}$	Derived	4160 kg/year
Chemical fractions derived from bio-oil upgrading			
Acetic Acid yield	Y_{acetic}	Chromatographic analysis	0.18
Annual aceitc acid production	$m_{acetic,annual}$	$m_{oil,annual} \cdot Y_{acetic}$	274.21 kg/year
Acetic acid selling price	P_{acetic}	Market reference	0.60 €/kg
Acetic acid revenue	R_{acetic}	$m_{acetic,annual} \cdot P_{acetic}$	164.53 €/year
Formic Acid yield	Y_{formic}	Chromatographic analysis	0.04
Annual formic acid production	$m_{formic,annual}$	$m_{oil,annual} \cdot Y_{formic}$	60.94 kg/year
Formic acid selling price	P_{formic}	Market reference	0.70 €/kg
Formic acid revenue	R_{formic}	$m_{formic,annual} \cdot P_{formic}$	42.65 €/year
Phenol yield	Y_{phenol}	Chromatographic analysis	0.05
Annual phenol production	$m_{phenol,annual}$	$m_{oil,annual} \cdot Y_{phenol}$	76.17 kg/year
Phenol selling price	P_{phenol}	Market reference	0.95 €/kg
Phenol revenue	R_{phenol}	$m_{phenol,annual} \cdot P_{phenol}$	72.36 €/year
Furfural yield	$Y_{furfural}$	Chromatographic analysis	0.08
Annual furfural production	$m_{furfural,annual}$	$m_{oil,annual} \cdot Y_{furfural}$	121.87 kg/year
Furfural selling price	$P_{furfural}$	Market reference	0.90 €/kg
Furfural revenue	$R_{furfural}$	$m_{furfural,annual} \cdot P_{furfural}$	109.68 €/year
Acetone yield	$Y_{acetone}$	Chromatographic analysis	0.03

Annual acetone production	$m_{acetone,annual}$	$m_{oil,annual} \cdot Y_{acetone}$	45.70 kg/year
Acetone selling price	$P_{acetone}$	Market reference	1.10 €/kg
Acetone revenue	$R_{acetone}$	$m_{acetone,annual} \cdot P_{acetone}$	50.27 €/year
Ethil acetate yield	$Y_{ethilacetate}$	Chromatographic analysis	0.03
Annual ethil aceate production	$m_{ethilacetate,annual}$	$m_{oil,annual} \cdot Y_{ethilacetate}$	45.70 kg/year
Ethil acetate selling price	$P_{ethilacetate}$	Market reference	0.94 €/kg
Ethil acetate revenue	$R_{ethilacetate}$	$m_{ethilacetate,annual} \cdot P_{ethilacetate}$	42.96 €/year
Diacetyl yield	$Y_{diacetyl}$	Chromatographic analysis	0.02
Annual diacetyl production	$m_{diacetyl,annual}$	$m_{oil,annual} \cdot Y_{diacetyl}$	30.47 kg/year
Diacetyl selling price	$P_{diacetyl}$	Market reference	3.50 €/kg
Diacetyl revenue	$R_{diacetyl}$	$m_{diacetyl,annual} \cdot P_{diacetyl}$	106.64 €/year
Butyric Acid yield	$Y_{butyric}$	Chromatographic analysis	0.03
Annual butyric acid production	$m_{butyric,annual}$	$m_{oil,annual} \cdot Y_{butyric}$	45.70 kg/year
Butyric acid selling price	$P_{butyric}$	Market reference	2.05 €/kg
Butyric acid revenue	$R_{butyric}$	$m_{butyric,annual} \cdot P_{butyric}$	93.69 €/year
Guaiacol yield	$Y_{guaiacol}$	Chromatographic analysis	0.07
Annual guaiacol production	$m_{guaiacol,annual}$	$m_{oil,annual} \cdot Y_{guaiacol}$	106.64 kg/year
Guaiacol selling price	$P_{guaiacol}$	Market reference	5.90 €/kg
Guaiacol revenue	$R_{guaiacol}$	$m_{guaiacol,annual} \cdot P_{guaiacol}$	629.16 €/year
Ethylphenol yield	$Y_{ethylphenol}$	Chromatographic analysis	0.04

Annual ethylphenol production	$m_{ethilphenol,annual}$	$m_{oil,annual} \cdot Y_{ethilphenol}$	60.94 kg/year
Ethylphenol selling price	$P_{ethylphenol}$	Market reference	4.20 €/kg
Ethylphenol revenue	$R_{ethylphenol}$	$m_{ethilphenol,annual} \cdot P_{ethilphenol}$	255.93 €/year
Catechol yield	$Y_{catechol}$	Chromatographic analysis	0.06
Annual catechol production	$m_{catechol,annual}$	$m_{oil,annual} \cdot Y_{catechol}$	91.40 kg/year
Catechol selling price	$P_{catechol}$	Market reference	6.30 €/kg
Catechol revenue	$R_{catechol}$	$m_{catechol,annual} \cdot P_{catechol}$	575.84 €/year
Ethyl guaiacol yield	$Y_{ethylguaiacol}$	Chromatographic analysis	0.04
Annual ethyl guaiacol production	$m_{ethylguaiacol,annual}$	$m_{oil,annual} \cdot Y_{ethylguaiacol}$	60.94 kg/year
Ethyl guaiacol selling price	$P_{ethylguaiacol}$	Market reference	6.90 €/kg
Ethyl guaiacol revenue	$R_{ethylguaiacol}$	$m_{ethylguaiacol,annual} \cdot P_{ethylguaiacol}$	420.46 €/year
Syringol yield	$Y_{syringol}$	Chromatographic analysis	0.05
Annual syringol production	$m_{syringol,annual}$	$m_{oil,annual} \cdot Y_{syringol}$	76.17 kg/year
Syringol selling price	$P_{syringol}$	Market reference	7.60 €/kg
Syringol revenue	$R_{syringol}$	$m_{syringol,annual} \cdot P_{syringol}$	578.89 €/year
Isovanillin yield	$Y_{isovanillin}$	Chromatographic analysis	0.02
Annual isovanillin production	$m_{isovanillin,annual}$	$m_{oil,annual} \cdot Y_{isovanillin}$	30.47 kg/year
Isovanillin selling price	$P_{isovanillin}$	Market reference	17.20 €/kg
Isovanillin revenue	$R_{isovanillin}$	$m_{isovanillin,annual} \cdot P_{isovanillin}$	524.05 €/year
Levoglucosan yield	$Y_{levoglucosan}$	Chromatographic analysis	0.22

Annual levoglucosan production	$m_{levoglucosan,annual}$	$m_{oil,annual} \cdot Y_{levoglucosan}$	335.15 kg/year
Levoglucosan selling price	$P_{levoglucosan}$	Market reference	5.60 €/kg
Levoglucosan revenue	$R_{levoglucosan}$	$m_{levoglucosan,annual} \cdot P_{levoglucosan}$	1876.82 €/year
Caffeine yield	$Y_{caffeine}$	Chromatographic analysis	0.04
Annual caffeine production	$m_{caffeine,annual}$	$m_{oil,annual} \cdot Y_{caffeine}$	60.94 kg/year
Caffeine selling price	$P_{caffeine}$	Market reference	13.50 €/kg
Caffeine revenue	$R_{caffeine}$	$m_{caffeine,annual} \cdot P_{caffeine}$	822.63 €/year
Solid fraction			
Biochar yield	Y_{char}	Experimental	0.3012
Annual biochar production	$m_{char,annual}$	$M_{SCG,annual} \cdot Y_{char}$	1253.00 kg/year
Biochar selling price	P_{char}	Market reference	0.50 €/kg
Biochar revenue	R_{char}	$m_{char,annual} \cdot P_{char}$	626.50 €/year
Total annual revenue	$\mathbf{R_B}$	$\sum_{R\ compounds} + R_{char}$	**6993.06 €/year**

The annual revenue for Scenario B amounts apporximately 6993.06 €/year.

Economic Indicators Based on the estimated cost and revenue structure, the main economic indicators for Scenario B were calculated and presented as follows:

- Annual Profit (Π): as reported in Table 5.13, Scenario B results in a positive annual profit of 6620.00 €/year.

Table 5.13: Annual profit calculation for Scenario B

Economic Item	**Symbol**	**Calculation**	**Value [€/year]**
Total annual revenue	R_B	From revenue analysis	6993.06
Total annual OPEX	$OPEX_B$	From OPEX analysis	373.06
Annual profit	Π	$R_B - OPEX_B$	**6620.00**

- Operating Margin (OM): the OM results to be equal to 95.00%.

Table 5.14: Operating margin calculation for Scenario B

Economic Item	**Symbol**	**Calculation**	**Value**
Annual profit	Π	From profit analysis	6620.00 €/year
Total annual revenue	R_B	From revenue analysis	6993.06 €/year
Operating margin	OM_A	$(\Pi/R_A) \cdot 100$	**95.00%**

- Payback Period (PBP): the PBP was found to be equal to 0.48 years.

Table 5.15: Payback period calculation for Scenario B

Economic Item	**Symbol**	**Calculation**	**Value**
Total capital investment	$CAPEX_A$	From CAPEX analysis	3201.83€
Annual profit	Π	From profit analysis	6620.00 €/year
Payback period	PBP_A	$CAPEX_A/\Pi$	**0.48 years**

- Unit Production Cost (UPC): the UPC was found to be equal to 0.24 €/kg.

Table 5.16: Unit production cost calculation for Scenario B

Economic Item	**Symbol**	**Calculation**	**Value**
Annual raw material processed	$M_{SCG,annual}$	Derived	4160 kg/year
Bio-oil yield	Y_{oil}	From experimental results	36.62 %
Annual bio-oil production	m_{annual}	$M_{SCG,annual} \cdot Y_{oil}$	1523.40 kg/year
Total annual OPEX	$OPEX_A$	From OPEX analysis	373.06 €/year
Unit production cost	UPC_A	$OPEX_A/m_{annual}$	**0.24 €/kg**

- Profit per Unit of Product (Π_{unit}): the profit per kilogram of crude bio-oil results to be equal to 4.35 €/kg.

Table 5.17: Profit per unit of product calculation for Scenario B

Economic Item	**Symbol**	**Calculation**	**Value**
Annual profit	Π	From profit analysis	6620.00 €/year
Annual bio-oil production	m_{annual}	From mass balance	1523.39 kg/year
Profit per unit of product	$\Pi_{unit,A}$	Π/m_{annual}	**4.35 €/kg**

Sensitivity Analysis This paragraph presents the results of the sensitivity analysis performed on Scenario B. The analysis evaluates the impact of ±10% variations in selected techno-economic parameters on the annual profit, while all other parameters were kept constant.

Table 5.18: Sensitivity analysis on annual profit for Scenario A (bio-oil + biochar)

Parameter varied	**Symbol**	**Profit (10%)**	**Base case profit**	**Profit (+10%)**
Biochar selling price	P_{char}	6557.35	6620.00	6682.65
Biochar yield	Y_{char}	6557.35	6620.00	6682.65
Energy cost	C_{energy}	6630.70	6620.00	6609.30
Maintenance cost factor	f_{maint}	6629.61	6620.00	6610.40
Installation cost factor	f_{inst}	6622.75	6620.00	6617.26
Indirect cost factor	f_{ind}	6623.60	6620.00	6616.40
Compound Price	P_{como}	5983.34	6620.00	7256.66

The results reported in Table 5.18 indicate that the annual profit of Scenario B is primarily influenced by variations in compound price. Also biochar selling price and yield have a noticeable impact on profitability, although their influence is secondary compared to compound-related revenues. Moreover, cost-related parameters, including energy cost, maintenance cost factor, installation cost factor and indirect cost factor, show a significant effect on the annual profit, indicating a higher sensitivity of Scenario B to cost structure variations compared to Scenario A. Figure 5.2 provides a graphical representation of the sensitivity analysis results, illustrating the variation in annual profit relative to the base case for ±10% changes in the selected parameters.

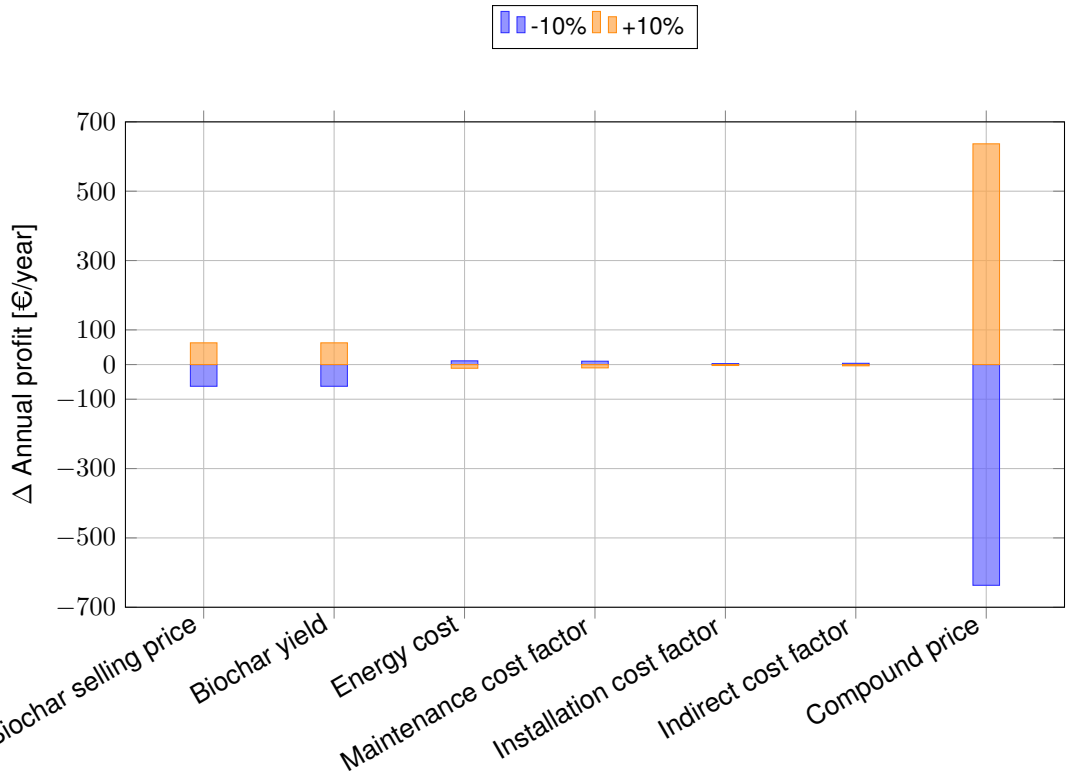

Figure 5.2: Sensitivity analysis of Scenario B: deviation of annual profit from the base case ($\Pi_{\text{base}} = 6620$ €/year) under ±10% variations of key techno-economic parameters.

5.2 Technology Readiness Level TRL

When conducing a cost analysis, it's important to define the technology readiness leves (TRL), that is, the stage of development and industrial deployment reached by the proposed system.
In this regard, the TRL scale offers a standardized metric to evaluate a technology's proximity to full commercialization. As shown in Figure 5.3, the scale comprises nine levels, ranging from TRL 1 to 9.

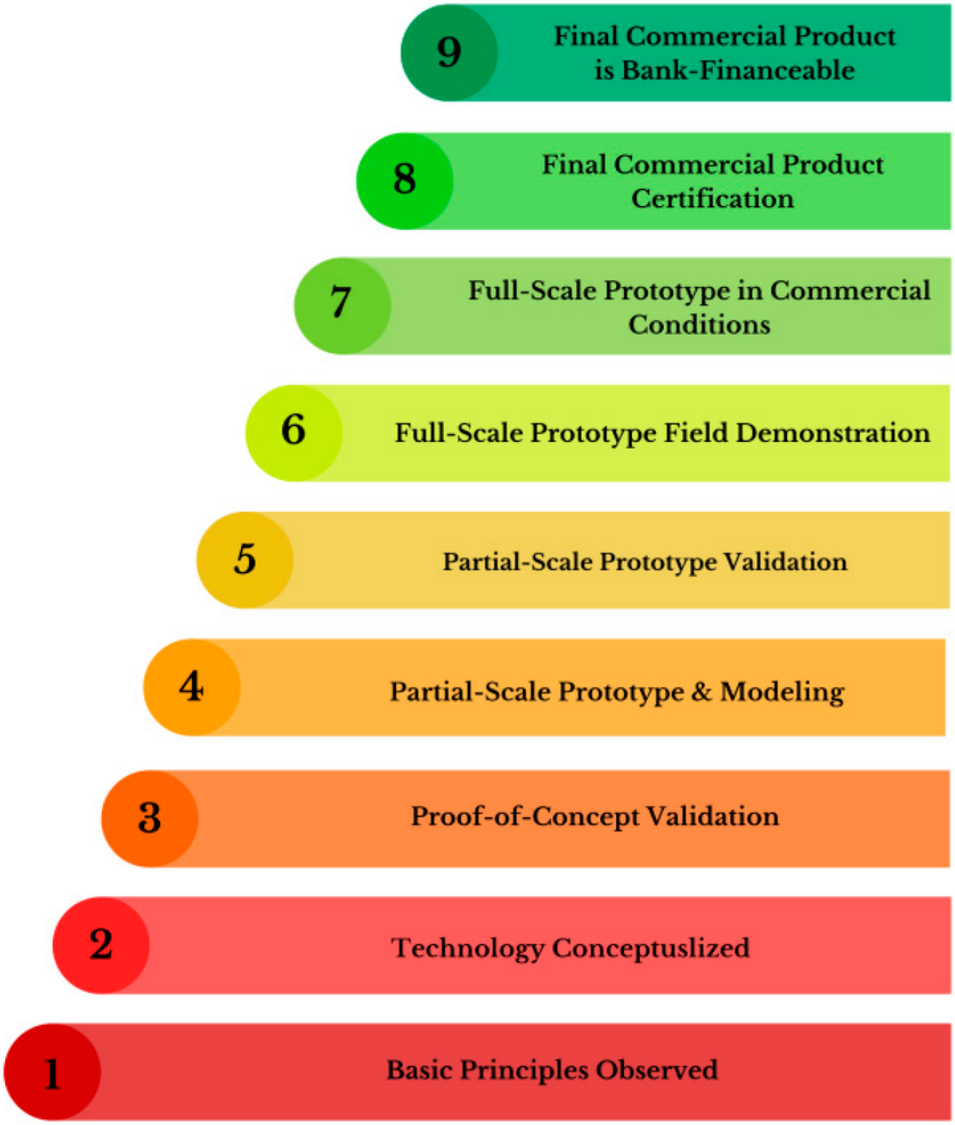

Figure 5.3: TRL scale. Credit: Grzegorz Cie´slak, Marta Gostomska, Adrian Dąbrowski, Tinatin Ciciszwili-Wyspia´nska , Katarzyna Skroban,Anna Mazurek, Edyta Wojda, Michał Głowacki, Tomasz Rygier and Anna Gajewska-Midziałek

In the context of the production of bio-oil, according to the literature, the optimal temperature range for maximizing bio-oil yield lies between 500 ℃ and 550℃, as higher temperatures promote volatilization and liquid-phase formation while minimizing secondary cracking reactions. However, the current experimental setup used in this study is capable of reaching a maximum operating temperature of approximately 400 ℃, which limits the overall conversion efficiency. This technical constraint confirms that

the process, while operational, is still in a development and optimization phase, corresponding to a TRL between 4 and 6.

To conclude, the main operating parameters of the experimental reactor are summarized in Table 5.19, together with the corresponding optimal ranges from literature. This comparison helps illustrate the technological maturity of the process and supports the TRL classification presented above.

Table 5.19: Comparison between optimal operating parameters from literature and current experimental setup.

Parameter	**Experimental setup (this work)**	**Optimal range (literature)**
Reactor type	Low-temperature batch pyrolysis unit (coffee roaster prototype)	Fast or intermediate pyrolysis reactor (fluidized-bed, auger, or fixed-bed)
Maximum temperature [℃]	400	500–550
Heating rate [℃/min]	12	20–100
Feedstock type	Spent Coffee Grounds (SCG)	SCG, wood chips, agricultural residues
Feedstock moisture [wt%]		< 10
Char yield [wt%]	30	15–25
Bio-oil yield [wt%]	37	60–70
Non-condensable gas yield [wt%]	30	10–20
Estimated TRL	4–6	7–9

5.3 Discussion of Techno-Economic Results

The economic performance of Scenario A was evaluated by considering capital and operating expenditures, revenue streams and key economic indicators. The estimated capital expenditure reflects the investment required for the laboratory-scale pyrolysis unit and associated auxiliary operations, corresponding to a total CAPEX of apporximately 3201.80 €, which represents a moderate initial cost when compared to conventional large-scale energy conversion technologies (Jerzak et al., 2024). This aspect is particularly relevant because the process relies on a waste-derived feedstock, which contributes to reducing raw material costs and improving overall economic feasibility.

Operating costs mainly derive from energy consumption and maintenance-related factors. Feedstock cost are negligible due to the waste nature of SCGs. As a consequence, the operating expanditure amounts to 203 €/year, bringing a low unit production cost of bio-oil, estimated at approximately 0.13

€/kg in Scenario A. On the revenue side, bio-oil represents the main source of income, while biochar provides an additional revenue stream. Although biochar contributes to a smaller share of total revenues, its valorization is important to the overall profitability, since it doesn't require any significant increase in operating costs. Under the assumed market conditions, the annual profit of Scenario A is on the order of 1.26 x 10^3 €/year, indicating a positive economic outcome. Considering the value on a unit basis, the profit corresponds approximately to 0.83 €/kg of bio-oil, highlighting a substantial margin between production cost and economic return.

The estimated unit production cost (0.13 €/kg) and the assumed market reference price of bio-oil (approximately 0.55 €/kg) further confirms the presence of a significant gap between production cost and selling price. This gap represents the maximum allowable cost that can be sustained while maintaining a positive outcome. Moreover, it indicates that the process could tolerate additional costs or inefficiencies. The estimated payback period is relatively short, showing that the initial investment could be recovered within a limited time period.

The sensitivity analysis of Scenario A was performed by varying the main economic and technical parameters by ±10%. The results show that annual profit is primarily influenced by bio-oil selling price and bio-oil yield. Given that Scenario A heavily depends on market circumstances and process efficiency, changes in these parameters result in the biggest changes in profitability. Changes in biochar related parameters, so biochar price and yield, result in more limited profit variations, confirming that biochar plays a secondary role in the overall revenue structure. In contrast, variations in operating and capital related parameters have a lower effect. This suggests that Scenario A is quite insensitive to small changes in CAPEX related factors and cost assumptions. All things considered, the sensitivity analysis demonstrates that Scenario A shows strong economic behavior, with profitability primarily determined by the production and market value of bio-oil. The economic performance of Scenario B was evaluated by considering the recovery of high-value compounds from bio-oil, with biochar valorization retained as a co-product. Operating expenditures in Scenario B are mainly associated with energy consumption, maintenance activities and the additional costs related to chromatographic separation. Feedstock costs remain limited due to the use of spent coffee grounds as a waste-derived raw material. Although the inclusion of chromatography leads to higher operating costs compared to the baseline configuration, these costs are relatively small (approximately 370 €/year), as the core process configuration and CAPEX remain unchaged from the previous scenario.

On the revenue side, the commercialization of individual compounds represents the dominant source of income. Under the assumed conditions, Scenario B achieves an annual profit on the order of 7.00 x 10^3 €/year, corresponding to a unit profit of about 4.35 €/kg. This indicates that advanced bio-oil valorization technologies have a great economic potential, as evidenced by the approximately five times increase in comparison with Scenario A. It should be noted that the economic assessment of Scenario B accounts explicitly for the additional costs related to chromatographic separation, while other potential downstream separation or purification steps are not included in the analysis. As a result, the obtained economic indicators should be interpreted as a preliminary estimate of the economic potential of compound recovery rather than as a detailed industrial-scale cost assessment. Despite this limitation, the

results clearly indicate that the increased revenues from compound recovery can offset the additional operating costs introduced in the advanced scenario.

Sensitivity analysis further supports this interpretation. A ±10% variation in compound selling price results in a change of approximately ±636 € in annual profit. Variations in cost related parameters produce significantly smaller profit deviations, indicating that Scenario B profitability is predominantly governed by revenue related factors rather than by capital or operating cost fluctuations.

Overall, Scenario B represents the most attractive option. The findings point to the necessity for further research focused on improving the downstream processing steps while also indicating that bio-oil upgrading can greatly increase the economic viability of SCGs pyrolysis.

The comparison between the two scenarios highlights a clear trade-off between economic robustness and profitability. Scenario A exhibits a simpler configuration with lower absolute profit but greater stability. This configuration may therefore be considered more resilient under uncertain market and operating conditions.

In contrast, Scenario B achieves a substantially higher economic return. Although this advanced configuration is more sensitive to market-related parameters, particularly compound selling prices, it offers significantly higher profitability under favorable market conditions. The comparison indicates that Scenario A represents a conservative and robust option, while Scenario B emerges as the most economically attractive strategy when higher-value valorization pathways are pursued. These economic results should however be interpreted in light of the technological maturity of the proposed system, which is discussed as follows.

The assigned TRL is relevant for the interpretation of the economic assessment. Since the proposed system has not yet reached full industrial maturity, capital and operating costs should be regarded as preliminary estimates rather than definitive values. Furthermore, additional investments may be required to improve reactor design, temperature control and thermal efficiency in order to approach the optimal operating conditions reported in the literature. Furthermore, additional investments may be required to improve reactor design, temperature control, and thermal efficiency in order to approach the optimal operating conditions reported in the literature. These technological improvements would likely affect both capital expenditure and operating expenditure, as well as key economic indicators such as payback period and return on investment.

To conclude, the TRL classification highlights that the economic results presented in this work should be interpreted within the context of a developing technology.

5.3.1 Applications

Bio-oil Bio-oil produced via biomass pyrolysis is a complex mixture of oxygenated organic compounds, whose potential applications strongly depend on its physicochemical properties and degree of upgrading (Bridgwater, 2012). From an economic perspective, the relevance of crude bio-oil lies in its flexibility as an intermediate energy carrier, which can be valorized through different pathways depending on market conditions and processing requirements (Mohan et al., 2006; Lachos-Perez et al., 2023).

One of the most established and technically mature applications of bio-oil is its use as a renewable fuel for heat and power generation (Bridgwater, 2012). Crude bio-oil is a high-volume, relatively low-value product that can be used in boilers and furnaces or co-fired with conventional fuels. (Bridgwater, 2012). Compared to heavy fossil fuels, the use of bio-oil may also provide environmental benefits in terms of reduced net greenhouse gas emissions.

However, these applications are generally associated with significant technical challenges, including corrosion, coking, ignition difficulties and increased emissions (Mohan et al., 2006). As a result, such uses typically require additional operation, which increase system complexity and costs.

Although raw bio-oil presents known limitations related to water content, acidity, and chemical instability, these characteristics do not prevent its use in stationary heat and power generation applications, where operating conditions can be adapted to the fuel properties (Bridgwater, 2012; Santos et al., 2025; Barahmand et al., 2025). In this context, crude bio-oil can be effectively valorized as a renewable fuel without the need for extensive upgrading, provided that appropriate handling and combustion strategies are adopted.

Acetic Acid It is one of the most commonly reported organic acids in biomass-derived bio-oils and is mainly formed during the thermal degradation of carbohydrate fractions such as cellulose and hemicellulose (Bridgwater, 2012; El-Sayed, 2025).

From an industrial perspective, acetic acid is a well-established bulk chemical with a large and consolidated market. Its main applications include its use as an intermediate in the production of vinyl acetate monomer, acetic anhydride, and acetate esters, which are widely employed in the manufacture of polymers, resins, adhesives, and coatings (Chadwick, 1988; Weissermel and Arpe, 2008; Sarchami et al., 2021). In addition, acetic acid is commonly used as a solvent and process reagent in several chemical and material processing industries (Weissermel and Arpe, 2008). In the context of this work, acetic acid is considered suitable for bulk industrial applications that are consistent with the assumed level of processing. No additional purification or upgrading steps beyond those included in the process design were assumed, and the selected applications therefore reflect the direct use of the compound in its current form. This assumption is adopted for all the compounds analyzed in Scenario B in order to ensure a conservative and consistent economic assessment.

Formic Acid It is a light organic acid commonly detected in biomass-derived bio-oils and is mainly formed through the thermal degradation of carbohydrate fractions during fast pyrolysis. Although it is generally present in lower concentrations compared to acetic acid, formic acid contributes to the overall acidic fraction of bio-oil obtained from spent coffee grounds and represents a relevant secondary compound for chemical valorization (Bridgwater, 2012; Zhang et al., 2007; Pereira et al., 2022; Barahmand et al., 2025). From an industrial perspective, formic acid is a well-established bulk chemical used in several sectors, including chemical manufacturing, leather processing, textile finishing, and as a reducing agent and preservative in industrial processes. Its applications are typically associated with technical- or industrial-grade specifications rather than high-purity requirements (Isocyanates, 1985; Weissermel and Arpe, 2008).

Phenolic compounds They are a broad class of oxygenated aromatic molecules commonly reported in biomass-derived bio-oils. They mainly originate from the thermal decomposition of lignin during fast pyrolysis (Lu and Gu, 2022). Typical phenolic species include phenol, alkylphenols, guaiacol, and cresols. Their presence and relative abundance strongly depend on the lignin content of the feedstock and on the operating conditions of the pyrolysis process (Bridgwater, 2012; Mohan et al., 2006). From an industrial perspective, cresols are specialty phenolic chemicals used as intermediates in the production of antioxidants, disinfectants, agrochemicals, resins, and polymer additives. Due to their aromatic structure, cresols are generally associated with higher market values compared to simple oxygenated compounds (Rinaldi et al., 2016; Weissermel and Arpe, 2008; Pereira et al., 2022; Machado et al., 2022).

Furfural It is a key furanic compound commonly reported in biomass-derived bio-oils and is primarily formed through the thermal degradation of hemicellulose fractions (Bridgwater, 2012; El-Sayed, 2025). From an industrial perspective, furfural is a well-established platform chemical with a large range of applications (Bozell and Petersen, 2010). It is widely used as an industrial solvent, as an intermediate in the production of resins and specialty chemicals, and as a precursor for the synthesis of bio-based fuels and value-added chemicals (Chadwick, 1988).

Acetone It is a low-molecular-weight ketone commonly detected in biomass-derived bio-oils and volatile fractions produced during pyrolysis. It is mainly formed through the thermal degradation of carbohydrate fractions, particularly cellulose and hemicellulose, as well as through secondary cracking reactions of oxygenated intermediates (Bridgwater, 2012; Mohan et al., 2006). Due to its high volatility, acetone is typically concentrated in the lighter fractions of bio-oil or recovered during condensation and separation stages. From an industrial perspective, acetone is a widely used commodity chemical with a well-established global market. It is primarily employed as an industrial solvent in the chemical, pharmaceutical, and coatings industries, as well as a key intermediate in the production of methyl methacrylate (MMA) and bisphenol A, both of which are precursors for polymers and resins (Bozell and Petersen, 2010).

Ethyl Acetate It is an oxygenated ester that can be identified in biomass-derived bio-oils and condensable fractions obtained from pyrolysis, particularly when alcohols and organic acids are simultaneously present. Its formation is generally attributed to esterification reactions between ethanol and acetic acid, both of which are commonly generated during the thermal degradation of cellulose and hemicellulose (Bridgwater, 2012; Mohan et al., 2006). These reactions may occur during pyrolysis or in the condensed liquid phase under suitable conditions. From an industrial standpoint, ethyl acetate is a widely used solvent characterized by low toxicity, pleasant odor, and favorable environmental properties compared to conventional petrochemical solvents. It is extensively employed in the production of paints, coatings, adhesives, inks, and pharmaceuticals, as well as in food and cosmetic applications (Bozell and Petersen, 2010).

Diacetyl It's a low-molecular-weight diketone commonly detected in biomass-derived bio-oils and volatile fractions produced during pyrolysis. It is mainly formed through the thermal degradation of carbohydrate fractions, particularly cellulose and hemicellulose, as well as through secondary reactions involving sugars and fermentation-related intermediates naturally present in biomass residues (Bridgwater, 2012; Mohan et al., 2006). Due to its high volatility, diacetyl is typically associated with the light condensable fraction of bio-oil. From an industrial perspective, diacetyl is a well-known flavor compound characterized by a distinctive buttery aroma. It is widely used in the food industry as a flavoring agent, particularly in dairy products, baked goods, and snack foods. In addition to food applications, diacetyl is employed in fragrance formulations and has niche applications in the chemical industry as a precursor for specialty chemicals (Bozell and Petersen, 2010; Clark et al., 2012).

Butyric Acid It's a short-chain carboxylic acid commonly identified in biomass-derived bio-oils produced through pyrolysis. It is mainly generated from the thermal degradation of carbohydrate fractions, particularly hemicellulose, as well as from secondary reactions involving organic acids and oxygenated intermediates formed during biomass decomposition (Bridgwater, 2012; Mohan et al., 2006). Due to its relatively high polarity, butyric acid is typically found in the aqueous or light oxygenated fraction of bio-oil. From an industrial perspective, butyric acid is an established platform chemical with applications in several sectors. It is used in the production of esters for fragrances and flavorings, as an intermediate in the manufacture of pharmaceuticals, and as a precursor for bio-based chemicals and polymers. In addition, butyric acid and its derivatives are employed in the food, feed, and agricultural industries, particularly in animal nutrition and silage additives (Werpy and Petersen, 2004) (Werpy and Petersen, 2004).

Guaiacol It is a phenolic compound commonly found in biomass-derived bio-oils. It is mainly associated with the thermal decomposition of lignin during pyrolysis (Bridgwater, 2012; Mohan et al., 2006). From an industrial perspective, guaiacol is a valuable compound that has a wide range of possible applications. It can be used as an intermediate in the synthesis of pharmaceuticals, agrochemicals, fragrances and flavoring agents. It can be employed in the production of vanillin and other aromatic compounds and in the manufacture of resins and antioxidants (Werpy and Petersen, 2004).

Ethylphenol It is an alkylated phenolic compound commonly detected in biomass-derived bio-oils, particularly within the phenolic fraction generated during pyrolysis. It is mainly formed from the thermal decomposition of lignin, through demethylation, alkylation, and side-chain rearrangement reactions of lignin-derived aromatic structures (Bridgwater, 2012; Mohan et al., 2006). From an industrial perspective, ethylphenol is a chemical with applications primarily as an intermediate in chemical synthesis. It is used in the production of resins, antioxidants, pharmaceuticals, and agrochemicals, and it can also serve as a precursor for functional materials and polymer additives. In addition, alkylphenols such as ethylphenol are employed in fragrance and flavor formulations due to their characteristic aromatic properties (Werpy and Petersen, 2004). Although its market volume is smaller compared to bulk phenols, ethylphenol's higher added value makes it a potentially attractive compound in bio-oil upgrading strategies aimed at the valorization of lignin-derived products.

Catechol It is a dihydroxybenzene compound commonly detected in biomass-derived bio-oils and is primarily associated with the thermal degradation of lignin during pyrolysis (Bridgwater, 2012; Mohan et al., 2006). From an industrial perspective, catechol has multiple applications. It is used as an intermediate in the production of pharmaceuticals, agrochemicals, antioxidants and polymer additives. Moreover, it's also employed in the synthesis of flavors, fragrances, photographic chemicals and in the manufacture of resins and rubber-processing chemicals (Werpy and Petersen, 2004).

Ethyl Guaiacol It is an alkylated phenolic compound commonly detected in biomass-derived bio-oils and is primarily associated with the thermal decomposition of lignin during pyrolysis. It is formed through alkylation and side-chain modification reactions of guaiacol-type lignin units, which originate from guaiacyl structures prevalent in lignocellulosic biomass (Bridgwater, 2012; Mohan et al., 2006). From an industrial perspective, ethyl guaiacol is a valuable specialty chemical mainly used in flavor and fragrance applications due to its characteristic smoky and spicy aroma. It is also employed as an intermediate in the synthesis of fine chemicals and specialty additives, and it has potential applications in the formulation of antioxidants and resin modifiers. Although its production volumes are relatively limited compared to bulk phenolic compounds, ethyl guaiacol's high added value and niche market relevance make it an attractive target for bio-oil upgrading strategies focused on the selective recovery of lignin-derived aromatic compounds (Werpy and Petersen, 2004).

Syringol It is a methoxylated phenolic compound commonly identified in biomass-derived bio-oils and is primarily formed through the thermal degradation of lignin during pyrolysis. It originates from syringyl-type lignin units, which are particularly abundant in hardwood biomass, and is generated through cleavage and rearrangement reactions of methoxy-substituted aromatic structures (Bridgwater, 2012; Mohan et al., 2006). From an industrial perspective, syringol is a valuable aromatic compound with applications mainly as an intermediate in the synthesis of specialty chemicals. It is used in the production of pharmaceuticals, fragrances, and agrochemicals, and it also serves as a precursor for functional phenolic derivatives and antioxidants. In addition, syringol and related compounds have potential applications in resin formulation and as bio-based alternatives to petrochemical phenols (Werpy and Petersen, 2004).

Isovanillin It's a methoxy-substituted aromatic aldehyde commonly detected in biomass-derived bio-oils and is primarily associated with the thermal degradation of lignin during pyrolysis. It is formed through the cleavage and oxidation of guaiacyl-type lignin units, similarly to vanillin, but differs in the position of the methoxy and hydroxyl substituents on the aromatic ring (Bridgwater, 2012; Mohan et al., 2006). From an industrial perspective, isovanillin is a high-value specialty chemical mainly used in the flavor and fragrance industry as an alternative to vanillin, owing to its characteristic vanilla-like aroma. It is also employed as an intermediate in the synthesis of pharmaceuticals, fine chemicals, and specialty additives. Although its market volume is smaller compared to bulk chemicals, isovanillin's relatively high market value and niche applications make it an attractive target for bio-oil upgrading strategies focused on the selective recovery of lignin-derived aromatic compounds (Werpy and Petersen, 2004).

Levoglucosan It is an anhydrosugar commonly identified in biomass-derived bio-oils and condensable fractions obtained from the pyrolysis of lignocellulosic materials. It is primarily formed through the depolymerization and dehydration of cellulose during thermal treatment, and its formation is favored under fast pyrolysis conditions and relatively moderate temperatures that limit secondary cracking reactions (Bridgwater, 2012; Mohan et al., 2006). From an industrial perspective, levoglucosan is considered a valuable platform molecule due to its potential for further chemical and biochemical conversion. It can be used as a precursor for the production of bio-based chemicals, polymers, and fuels, and it represents an attractive intermediate for fermentation processes aimed at producing organic acids, alcohols, and other value-added products. Owing to its multifunctional structure and renewable origin, levoglucosan has received significant attention as a key compound in biomass valorization strategies and bio-refinery concepts (Werpy and Petersen, 2004).

Caffeine It is a nitrogen-containing alkaloid naturally present in coffee beans and therefore represents a characteristic compound associated with spent coffee grounds. During pyrolysis, caffeine can be partially released or thermally transformed, but detectable amounts may still be found in the condensable fraction or bio-oil derived from coffee-based feedstocks, depending on operating conditions and thermal severity (Bridgwater, 2012; Mohan et al., 2006). Its presence is directly linked to the unique chemical composition of the original biomass rather than to lignocellulosic decomposition pathways. From an industrial perspective, caffeine is a high-value specialty compound with a well-established global market. It is widely used in the pharmaceutical industry as a stimulant and active ingredient in analgesic formulations, as well as in the food and beverage sector for energy drinks and functional products. In addition, caffeine finds applications in cosmetics and personal care products due to its stimulating and antioxidant properties (Werpy and Petersen, 2004).

Biochar It is a carbon-rich solid by-product generated during the pyrolysis of spent coffee grounds, characterized by a porous structure and a high carbon content (Ferrari et al., 2025). Due to these properties, biochar derived from spent coffee grounds has been widely investigated in the literature for applications in agriculture and environmental remediation (Joseph, 2015; Pereira et al., 2022).

One of the primary uses of biochar is as a soil amendment. Several studies have demonstrated that biochar can improve soil structure, increase water retention capacity, boost nutrient availability and positively contribute to long-term carbon sequestration in soils (Nascimento et al., 2023).

In addition to agricultural use, biochar has been extensively studied as a low-cost adsorbent for environmental remediation. Thanks to its porous structure and surface functional groups, biochar can be employed for the adsorption of organic pollutants, dyes, and heavy metals from wastewater streams. SCGs-derived biochar has demonstrated promising adsorption performance in several studies, particularly for low-to moderate-contamination scenarios where high-grade activated carbons are not required (Cai et al., 2020; Setter et al., 2020).

Although the properties of biochar are strongly influenced by pyrolysis conditions, the yields and basic characteristics obtained in this study indicate that the produced biochar can be reasonably compared to commercially available biochars currently used for low-grade agricultural or adsorption purposes.

Therefore, despite not being the primary focus of this work, biochar can be considered a valuable co-product of the pyrolysis process, providing an additional source of revenue and contributing to the overall economic feasibility of the system (Segers et al., 2024; Nematian et al., 2021; Barahmand et al., 2025).

5.4 SCGs positioning among coffee-derived feedstocks

Spent coffee grounds, green coffee, and coffee cherry husk represent coffee-derived feedstocks with different compositional and processing histories. A comparative chemical analysis was performed to assess how these differences affect the composition of the resulting bio-oils and to support the subsequent techno-economic evaluation.

From a chemical standpoint, the liquid products consist of complex mixtures of oxygenated organic compounds formed through the thermal degradation of carbohydrates, lignin, and minor nitrogen-containing constituents, in agreement with literature on biomass-derived bio-oils (Bridgwater, 2012; Pattiya, 2018).

Bio-oils obtained from green coffee and coffee cherry husk are characterized by a higher relative abundance of light oxygenated species, such as low-molecular-weight organic acids, ketones, and aldehydes, resulting in higher volatility and lower thermal stability. These features are consistent with the less processed nature of these feedstocks, which retain a larger fraction of thermally labile compounds (Figueiredo et al., 2017; Krause et al., 2019). Among them, coffee cherry husk generally exhibits the lightest chemical profile. In contrast, SCGs derived bio-oil displays a more chemically evolved composition, with a broader distribution of compounds including phenolics, sugar-derived species, and nitrogen-containing molecules, reflecting both the original biomass composition and the prior steps undergone by this feedstock (Jones et al., 2013; Matrapazi and Zabaniotou, 2020; Jerzak et al., 2024). Overall, SCGs bio-oil occupies an intermediate position between green coffee and coffee cherry husk in terms of volatility and molecular diversity. While green coffee and coffee cherry husk yield lighter and more volatile liquids, SCGs combines these features with a non-negligible fraction of higher-boiling and structurally diverse compounds. (Hasan et al., 2022; Rogers and Brammer, 2012).

Following the chemical comparison, this paragarph focuses on the economic implications associated with the use of different coffee-derived feedstocks. The objective of this comparison is not to optimise each feedstock-specific process, but to highlight how differences in feedstock characteristics translate into variations in operating costs within a consistent economic framework. Among the economic parameters, operating expenditures (OPEX) were identified as the most sensitive to feedstock selection, as capital investment and process configuration were assumed to be comparable across the analysed scenarios. In particular, the cost of the raw material emerges as the main distinguishing factor.

According to OPEXs analysis, SCGs and coffee cherry husk have similiar OPEX levels, consistent to their classification as waste or low-value agricultural residues. In contrast, the main difference in the green coffee context is the cost of the feedstock, which drives a higher operational cost. The economic disadvantage of using green coffee as a feedstock is made clear when normalized per unit of feedstock, even though the absolute increase in OPEX is still low. Feedstock prices were selected based on

representative literature and market values.

To support the economic comparison, tables 5.20, 5.21, 5.22 summarise the operating expenditures and the corresponding unit production costs for SCG, green coffee, and coffee cherry husk.

Table 5.20: Operating costs and economic indicators for the small-scale scenario.

Economic Cost	Cost Factor	Value [€/year]
Feedstock	0	0
Energy		107.00
Labour		0
Maintenance	0.03	96.06
Consumables		0
Chromatography		0
OPEX		**203.06**

Economic Item	Value
Raw material processed	4160 (kg/year)
Bio-oil yield	0.37
Bio-oil production	1523.39 (kg/year)
OPEX	203.06 (€/year)
UPC	0.13 (€/kg)

Table 5.21: Operating costs and economic indicators for the intermediate-scale scenario.

Economic Cost	Cost Factor	Value [€/year]
Feedstock	0.10	416.00
Energy		107.00
Labour		0
Maintenance	0.03	96.06
Consumables		0
Chromatography		0
OPEX		**619.06**

Economic Item	Value
Raw material processed	4160 (kg/year)
Bio-oil yield	0.37
Bio-oil production	1523.39 (kg/year)
OPEX	619.06 (€/year)
UPC	0.41 (€/kg)

Table 5.22: Operating costs and economic indicators for the industrial-scale scenario.

Economic Cost	Cost Factor	Value [€/year]
Feedstock	5.50	22880.00
Energy		107.00
Labour		0
Maintenance	0.03	96.06
Consumables		0
Chromatography		0
OPEX		**23083.06**

Economic Item	Value
Raw material processed	4160 (kg/year)
Bio-oil yield	0.37
Bio-oil production	1523.39 (kg/year)
OPEX	23083.06 (€/year)
UPC	15.15 (€/kg)

5.5 Scale-Up Considerations

The techno-economic analysis presented in this work is based on a small-scale configuration. When considering the assessment of the potencial industrial relevance of the process, the scale-up effect must be taken into account. This section discusses how process scale affects capital and operating costs by looking at three representative capacity scenarios. The goal is not to provide a detailed design, but rather to show general cost trends.

- Scenario 1 corresponds to the small-scale configuration analysed in this work, representative of laboratory operation. This scenario serves as the reference case for evaluating scale-up effects on capital and operating costs.
- Scenario 2 represents an intermediate configuration, characterized by higher throughput and the same general process configuration. At this scale, partial economies of scale are expected, particularly in regards with equipment sizing and specific capital costs.
- Scenario 3 corresponds to a fully industrial-scale implementation of the process. At this scale, it is expected a significant reductions in particular CAPEX and unit operating costs . This will be achieved through larger equipment sizes, better integration and more effective use of labor and utilities.

Table 5.23 summarises the effect of process scale on capital and operating costs, considering the three representative capacity scenarios.

Table 5.23: Effect of process scale on CAPEX and OPEX for the three scenarios. CAPEX values were scaled using a power-law correlation with an exponent of 0.6, while OPEX was assumed to scale linearly with process capacity.

Scenario	Scale Factor	CAPEX (€)	CAPEX Specific	OPEX (€/year)	Unit OPEX
Small Scale	1	3 201.83	1.00	203.06	1
Intermediate	10	12 746.73	0.40	2 030.55	1
Industrial	100	50 745.64	0.16	20 305.50	1

The results reported in Table 5.23 show that increasing process scale leads to a significant reduction in specific capital investment due to economies of scale, indeed total CAPEX increases sub-linearly with capacity. In contrast, operating expenditures were assumed to scale linearly with throughput, resulting in approximately constant unit operating costs across the analysed scenarios. These trends indicate that the main economic benefit of process scale-up is associated with capital cost reduction rather than operating cost savings.

Chapter 6

Conclusion

This thesis demonstrates the economic feasibility of the pyrolysis of spent coffee grounds (SCGs), and highlights how the process is primarily governed by the adopted valorization strategy, rather than by the thermochemical conversion itself. By integrating a chemical characterization with a techno-economic analysis, the work demonstrates how different uses of the same process output can lead to completely different economic results.

From an experimental perspective, low-temperature pyrolysis of SCGs led to a product distribution characterized by a dominant bio-oil fraction, approximately 37%, and a significant biochar yield, about 30%, with the remaining fraction consisting of non-condesable gases. Moreover, the chemical complexity of the bio-oil, often considered as a limitation for direct energy applications, is instead shown to be a key opportunity. Several compounds families were identified, including organic acids, ketones and esters, sugar-derived compounds such as furfural and levoglucosan, phenolic species, and nitrogen-containing molecules. They are associated with established application as industrial solvents, chemical intermediates, antioxidants, flavoring agents, and bio-based platform chemicals. These applications support the shift from low-value bulk utilization toward higher-value chemical markets.

This shift is additionaly supported by the outcomes of the techno-economic analysis. In the baseline scenario, based on the direct commercialization of bulk bio-oil and biochar, profitability remains limited, with an estimated profit of 0.83 €/kg. In contrast, the advanced valorization strategy, focused on the identification and economic assessment of individual bio-oil compounds, results in an improved economic performance, with an estimated profit of approximately 4.35 €/kg, corresponding to nearly five times the profitability of the baseline case. This substantial increase in the order of magnitude demonstrates that the economy potential of pyrolysis of SCGs is unlocked through chemical valorization. These findings are further supported by the sensitivity analysis conducted, which shows that bio-oil yield and product selling prices are the dominant driver of profitability. CAPEX and OPEX variations were found to have a comparatively smaller impact within the explored context, indicating that economic feasibility is mainly driven by experimentally determined yields and market-related assumptions.

Under the assumed operating conditions,the total capital investment results to be approximately to 3201.80 € and annual operating expenditures of 203.00 €/year for scenario A and of 373.00 €/year for

scenario B. The relatively moderate capital requirement and low annual operating costs reflect the small-scale configuration analyzed in this study and contribute to the short payback period observed. These figures indicate that the economic improvement achieved in Scenario B is not driven by reductions in investment or operating costs, but rather by enhanced revenue generation through compound-oriented valorization.

Despite the laboratory-scale of the proposed model and the simplified assumptions adopted for downstream separation, the inclusion of scale-up considerations demonstrates that increasing process scale leads to a reduction in cost in specific capital investment due to economies of scale, while unit operating costs almost remain constant. These results confirm that the positive economic trends observed are not merely artifacts of small-scale assumptions, but remain consistent when extended to larger throughputs. Further research should therefore focus on integrating detailed separation costs and upgrading technologies, enabling the transition from conceptual economic screening toward industrially oriented process design.

In conclusion, this thesis highlights spent coffee grounds as a promising feedstock for waste-to-value applications and demonstrates how the integration of experimental chemistry with techno-economic analysis can effectively guide to the identification of economically meaningful biomass valorization strategies.

Bibliography

[1] Emanuele Graciosa Pereira, Humberto Fauller, Mateus Magalhães, Bruna Guirardi, and Marcio Arêdes Martins. “Potential use of wood pyrolysis coproducts: A review”. In: *Environmental Progress & Sustainable Energy* 41.1 (2022), e13705.

[2] Kanokthip Pongsiriyakul, Peerawat Wongsurakul, Worapon Kiatkittipong, Aerwadee Premashthira, Kulapa Kuldilok, Vesna Najdanovic-Visak, Sushil Adhikari, Patrick Cognet, Tetsuya Kida, and Suttichai Assabumrungrat. “Upcycling coffee waste: Key industrial activities for advancing circular economy and overcoming commercialization challenges”. In: *Processes* 12.12 (2024), p. 2851.

[3] Zahir Barahmand, Liang Wang, Jens Bo Holm-Nielsen, and Marianne Eikeland. “Significance of pyrolysis in the circular economy: An integrative review of technologies, potential chemicals, and separation techniques”. In: *Fuel* 398 (2025), p. 135539.

[4] Maryam Nooman AlMallahi, Sara Maen Asaad, Lisandra Rocha-Meneses, Abrar Inayat, Zafar Said, Mamdouh El Haj Assad, and Mahmoud Elgendi. “A case study on bio-oil extraction from spent coffee grounds using fast pyrolysis in a fluidized bed reactor”. In: *Case Studies in Chemical and Environmental Engineering* 8 (2023), p. 100529.

[5] Britt Segers, Philippe Nimmegeers, Marc Spiller, Giorgio Tofani, Edita Jasiukaitytė-Grojzdek, Elina Dace, Timo Kikas, Jorge M Marchetti, Milena Rajić, Güray Yildiz, et al. “Lignocellulosic biomass valorisation: a review of feedstocks, processes and potential value chains and their implications for the decision-making process”. In: *RSC sustainability* 2.12 (2024), pp. 3730–3749.

[6] Muhammad Mujtaba, Leonardo Fernandes Fraceto, Mahyar Fazeli, Sritama Mukherjee, Susilaine Maira Savassa, Gerson Araujo de Medeiros, Anderson do Espírito Santo Pereira, Sandro Donnini Mancini, Juha Lipponen, and Francisco Vilaplana. “Lignocellulosic biomass from agricultural waste to the circular economy: a review with focus on biofuels, biocomposites and bioplastics”. In: *Journal of cleaner production* 402 (2023), p. 136815.

[7] Valdecir Ferrari, Mateus Torres Nazari, Nathalia Favarin da Silva, Larissa Crestani, Lucas Manique Raymundo, Guilherme Luiz Dotto, Jeferson Steffanello Piccin, Luis Felipe Silva Oliveira, and Andrea Moura Bernardes. “Pyrolysis: a promising technology for agricultural waste conversion into value-added products”. In: *Environment, Development and Sustainability* 27.8 (2025), pp. 17957–17991.

[8] Kavin Tamilselvan, Subramanian Sundarajan, Seeram Ramakrishna, Al-Ashraf Abdullah Amirul, and Sevakumaran Vigneswari. “Sustainable valorisation of coffee husk into value added product in the context of circular bioeconomy: Exploring potential biomass-based value webs”. In: *Food and Bioproducts Processing* 145 (2024), pp. 187–202.

[9] L Bartolucci, S Cordiner, A Di Carlo, A Gallifuoco, P Mele, and V Mulone. “Platform chemicals recovery from spent coffee grounds aqueous-phase pyrolysis oil”. In: *Renewable Energy* 220 (2024), p. 119630.

[10] Jawaher Al Balushi, Shamail Al Saadi, Mitra Ahanchi, Manar Al Attar, Tahereh Jafary, Muna Al Hinai, Anteneh Mesfin Yeneneh, and J Sadhik Basha. “A Comprehensive Review on Sustainable Conversion of Spent Coffee Grounds into Energy Resources and Environmental Applications”. In: *Biomass* 5.3 (2025), p. 55.

[11] Yamuna Thoppil and Sharif H Zein. “Techno-economic analysis and feasibility of industrial-scale biodiesel production from spent coffee grounds”. In: *Journal of Cleaner Production* 307 (2021), p. 127113.

[12] Dayana Nascimento Dari, Lidya Fernandes da Silva, Antônio Mairton Bezerra Lima Júnior, Isabelly Silveira Freitas, Francisco Izaias da Silva Aires, and José Cleiton Sousa dos Santos. “Spent coffee grounds: Insights and future prospects for bioenergy and circular economy applications”. In: *Green Technologies and Sustainability* (2025), p. 100213.

[13] Uyory Choe. “Valorization of spent coffee grounds and their applications in food science”. In: *Current Research in Food Science* (2025), p. 101010.

[14] Derek R Vardon, Bryan R Moser, Wei Zheng, Katie Witkin, Roque L Evangelista, Timothy J Strathmann, Kishore Rajagopalan, and Brajendra K Sharma. “Complete utilization of spent coffee grounds to produce biodiesel, bio-oil, and biochar”. In: *ACS Sustainable Chemistry & Engineering* 1.10 (2013), pp. 1286–1294.

[15] Monique Kort-Kamp Figueiredo, Beatriz Pereira de Castro Caldas Karolyne Nogueira a nd do Nascimento, Priscila Schroeder, and Gilberto Alves Romeiro. “Evaluation of the performance of bio-oil obtained through pyrolysis of coffee waste.” In: *Revista Eletrônica em Gestão, Educação e Tecnologia Ambiental* 21 (2017).

[16] Susanne Jones, Pimphan Meyer, Lesley Snowden-Swan, Asanga Padmaperuma, Eric Tan, Abhijit Dutta, Jacob Jacobson, and Kara Cafferty. *Process design and economics for the conversion of lignocellulosic biomass to hydrocarbon fuels: fast pyrolysis and hydrotreating bio-oil pathway*. Tech. rep. National Renewable Energy Lab.(NREL), Golden, CO (United States), 2013.

[17] Wojciech Jerzak, Esther Acha, and Bin Li. “Comprehensive review of biomass pyrolysis: Conventional and advanced technologies, reactor designs, product compositions and yields, and techno-economic analysis”. In: *Energies* 17.20 (2024), p. 5082.

[18] A Pattiya. “Fast pyrolysis”. In: *Direct thermochemical liquefaction for energy applications*. Elsevier, 2018, pp. 3–28.

[19] Anthony V Bridgwater. “Review of fast pyrolysis of biomass and product upgrading”. In: *Biomass and bioenergy* 38 (2012), pp. 68–94.

[20] Maurício C Krause, Adriana C Moitinho, Luiz Fernando R. Ferreira, Ranyere L de Souza, Laiza C Krause, and Elina B Caramão. “Production and characterization of the bio-oil obtained by the fast pyrolysis of spent coffee grounds of the soluble coffee industry”. In: *Journal of the Brazilian Chemical Society* 30.8 (2019), pp. 1608–1615.

[21] Carmem T Primaz, Tiago Schena, Eliane Lazzari, Elina B Caramao, and Rosângela A Jacques. “Influence of the temperature in the yield and composition of the bio-oil from the pyrolysis of spent coffee grounds: Characterization by comprehensive two dimensional gas chromatography”. In: *Fuel* 232 (2018), pp. 572–580.

[22] J Gracia-Vitoria, S Corderí Gándara, E Feghali, P Ortiz, W Eevers, KS Triantafyllidis, and K Vanbroekhoven. “The chemical and physical properties of lignin bio-oils, facts and needs”. In: *Current Opinion in Green and Sustainable Chemistry* 40 (2023), p. 100781.

[23] Henrique Machado, Ana F Cristino, Sofia Orišková, and Rui Galhano dos Santos. “Bio-oil: the next-generation source of chemicals”. In: *Reactions* 3.1 (2022), pp. 118–137.

[24] Shayan Mohammadalizadeh, Hadi Nazarpour, Seyed Sina Mousavi, and Mehdi Dehestani. “Upcycling spent coffee grounds into biochar-reinforced geopolymer mortars: sustainable structural materials with enhanced mechanical performance”. In: *European Journal of Environmental and Civil Engineering* (2025), pp. 1–32.

[25] Ícaro Vasconcelos do Nascimento, Laís Gomes Fregolente, Arthur Prudêncio de Araújo Pereira, Carla Danielle Vasconcelos do Nascimento, Jaedson Cláudio Anunciato Mota, Odair Pastor Ferreira, Helon Hébano de Freitas Sousa, Débora Gonçala Gomes da Silva, Lucas Rodrigues Simões, AG Souza Filho, et al. “Biochar as a carbonaceous material to enhance soil quality in drylands ecosystems: A review”. In: *Environmental Research* 233 (2023), p. 116489.

[26] Wenqin Li, Qi Dang, Robert C Brown, David Laird, and Mark M Wright. “The impacts of biomass properties on pyrolysis yields, economic and environmental performance of the pyrolysis-bioenergy-biochar platform to carbon negative energy”. In: *Bioresource technology* 241 (2017), pp. 959–968.

[27] VK Matrapazi and A Zabaniotou. “Experimental and feasibility study of spent coffee grounds upscaling via pyrolysis towards proposing an eco-social innovation circular economy solution”. In: *Science of the Total Environment* 718 (2020), p. 137316.

[28] JG Rogers and John G Brammer. “Estimation of the production cost of fast pyrolysis bio-oil”. In: *Biomass and bioenergy* 36 (2012), pp. 208–217.

[29] Joseph Eke, Jude A Onwudili, and Anthony V Bridgwater. “Influence of moisture contents on the fast pyrolysis of trommel fines in a bubbling fluidized bed reactor”. In: *Waste and Biomass Valorization* 11.7 (2020), pp. 3711–3722.

[30] Roel JM Westerhof, Norbert JM Kuipers, Sascha RA Kersten, and Wim PM Van Swaaij. “Controlling the water content of biomass fast pyrolysis oil”. In: *Industrial & Engineering Chemistry Research* 46.26 (2007), pp. 9238–9247.

[31] Roel JM Westerhof, D Wim F Brilman, Manuel Garcia-Perez, Zhouhong Wang, Stijn RG Oudenhoven, Wim PM Van Swaaij, and Sascha RA Kersten. “Fractional condensation of biomass pyrolysis vapors”. In: *Energy & fuels* 25.4 (2011), pp. 1817–1829.

[32] Ning Liu, Chen Dou, Xu Yang, Bohao Bai, Shujun Zhu, Jilin Tian, Zhuozhi Wang, Li Xu, and Boxiong Shen. “Effects of pretreatment procedure, compositional feature and reaction condition on the devolatilization characteristics of biomass during pyrolysis process: A review”. In: *Journal of the Energy Institute* 118 (2025), p. 101943.

[33] Frederik Ronsse, Robert W Nachenius, and Wolter Prins. “Carbonization of biomass”. In: *Recent advances in thermo-chemical conversion of biomass*. Elsevier, 2015, pp. 293–324.

[34] Daya Ram Nhuchhen, Prabir Basu, and Bishnu Acharya. “A comprehensive review on biomass torrefaction”. In: *Int. J. Renew. Energy Biofuels* 2014 (2014), pp. 1–56.

[35] C Setter, FTM Silva, MR Assis, CH Ataíde, PF Trugilho, and TJP Oliveira. “Slow pyrolysis of coffee husk briquettes: Characterization of the solid and liquid fractions”. In: *Fuel* 261 (2020), p. 116420.

[36] Hakim Abdel Aziz Ouattara, Florence Bobelé Niamké, Jean Claude Yao, Nadine Amusant, and Benjamin Garnier. “Wood vinegars: Production processes, properties, and valorization”. In: *Forest Products Journal* 73.3 (2023), pp. 239–249.

[37] Daniel Lachos-Perez, João Cláudio Martins-Vieira, Juliano Missau, Kumari Anshu, Odiri K Siakpebru, Sonal K Thengane, Ana Rita C Morais, Eduardo Hiromitsu Tanabe, and Daniel Assumpção Bertuol. “Review on biomass pyrolysis with a focus on bio-oil upgrading techniques”. In: *Analytica* 4.2 (2023), pp. 182–205.

[38] Michael Talmadge, Christopher Kinchin, Helena Li Chum, Andrea de Rezende Pinho, Mary Biddy, Marlon BB de Almeida, and Luiz Carlos Casavechia. “Techno-economic analysis for co-processing fast pyrolysis liquid with vacuum gasoil in FCC units for second-generation biofuel production”. In: *Fuel* 293 (2021), p. 119960.

[39] Luciana R Santos, Daniela R Araujo, and Marco AS Rodrigues. “Strategic techniques for upgrading bio-oil from fast pyrolysis: a critical review”. In: *Biofuels, Bioproducts and Biorefining* (2025).

[40] Sadegh Papari and Kelly Hawboldt. “A review on condensing system for biomass pyrolysis process”. In: *Fuel Processing Technology* 180 (2018), pp. 1–13.

[41] U.S. Energy Information Administration. *Biomass explained*. https://www.eia.gov/energyexplained/biomass/. Accessed: 2026-01. 2023.

[42] Rafael de Oliveira Farrapeira, Yasmine Braga Andrade, Laíza Canielas Krause, Thiago Rodrigues Bjerk, Elina Bastos Caramão, and Jaderson Kleveston Schneider. “GC$\times$ GC in the characterization of the bio-oil from Brazilian biomass: a review”. In: *Brazilian Journal of Analytical Chemistry* 8.33 (2021), pp. 19–41.

[43] Ji-Yeon Park, Md Amirul Alam Kanak, and In-Gu Lee. “Upgrading of coffee biocrude oil produced by pyrolysis of spent coffee grounds: behavior of fatty acids in supercritical ethanol reaction and catalytic cracking”. In: *Processes* 9.5 (2021), p. 835.

[44] Madhav Prasad Pandey and Chang Soo Kim. “Lignin depolymerization and conversion: a review of thermochemical methods”. In: *Chemical engineering & technology* 34.1 (2011), pp. 29–41.

[45] Xinyu Lu and Xiaoli Gu. “A review on lignin pyrolysis: pyrolytic behavior, mechanism, and relevant upgrading for improving process efficiency”. In: *Biotechnology for Biofuels and Bioproducts* 15.1 (2022), p. 106.

[46] Lokeshwar Puri, Yulin Hu, and Greg Naterer. “Critical review of the role of ash content and composition in biomass pyrolysis”. In: *Frontiers in Fuels* 2 (2024), p. 1378361.

[47] Marinos Stylianou, Agapios Agapiou, Michalis Omirou, Ioannis Vyrides, Ioannis M Ioannides, Grivas Maratheftis, and Dionysia Fasoula. “Converting environmental risks to benefits by using spent coffee grounds (SCG) as a valuable resource”. In: *Environmental Science and Pollution Research* 25.36 (2018), pp. 35776–35790.

[48] Nikoletta Solomakou, Panagiota Tsafrakidou, and Athanasia M Goula. “Valorization of SCG through extraction of phenolic compounds and synthesis of new biosorbent”. In: *Sustainability* 14.15 (2022), p. 9358.

[49] Dionisio Malagón-Romero, Andres C Torres-Velasquez, Lizeth K Tinoco-Navarro, and Juan P Arrubla-Vélez. “Pyrolysis of Colombian spent coffee grounds (SCGs), characterization of bio-oil, and study of its antioxidant properties”. In: *International Journal of Sustainable Energy* 42.1 (2023), pp. 811–829.

[50] ACM Vilas-Boas, LAC Tarelho, JMO Moura, HGMF Gomes, CC Marques, DT Pio, MIS Nunes, and AJD Silvestre. “Methodologies for bio-oil characterization from biomass pyrolysis: A review focused on GC-MS”. In: *Journal of Analytical and Applied Pyrolysis* 185 (2025), p. 106850.

[51] Annalisa Romani, Patrizia Pinelli, Francesca Ieri, and Roberta Bernini. “Sustainability, innovation, and green chemistry in the production and valorization of phenolic extracts from Olea europaea L.” In: *Sustainability* 8.10 (2016), p. 1002.

[52] Maryam Nematian, Catherine Keske, and John N Ng’ombe. “A techno-economic analysis of biochar production and the bioeconomy for orchard biomass”. In: *Waste Management* 135 (2021), pp. 467–477.

[53] Nan Cai, Huili Zhang, Jiapei Nie, Yimin Deng, and Jan Baeyens. “Biochar from biomass slow pyrolysis”. In: *IOP Conference Series: Earth and Environmental Science*. Vol. 586. 1. IOP Publishing. 2020, p. 012001.

[54] Vineet Singh Sikarwar, Ming Zhao, Peter Clough, Joseph Yao, Xia Zhong, Mohammad Zaki Memon, Nilay Shah, Edward J Anthony, and Paul S Fennell. “An overview of advances in biomass gasification”. In: *Energy & Environmental Science* 9.10 (2016), pp. 2939–2977.

[55] Joseph Zakzeski, Pieter CA Bruijnincx, Anna L Jongerius, and Bert M Weckhuysen. “The catalytic valorization of lignin for the production of renewable chemicals”. In: *Chemical reviews* 110.6 (2010), pp. 3552–3599.

[56] Nuapon Duongbia, Wassana Kamopas, Khomsan Ruangrit, Thoranis Deethayat, Attakorn Asanakham, and Tanongkiat Kiatsiriroat. “Biochar from Co-pyrolysis of Spent Coffee Ground with Leptolyngbya sp. KC 45 Biomass and Residue for Energy and Agricultural Utilization”. In: *Energy Nexus* (2025), p. 100454.

[57] C Mattos, MCC Veloso, GA Romeiro, and E Folly. “Biocidal applications trends of bio-oils from pyrolysis: Characterization of several conditions and biomass, a review”. In: *Journal of Analytical and Applied Pyrolysis* 139 (2019), pp. 1–12.

[58] Tim Schulzke, Stefan Conrad, and Jan Westermeyer. “Fractionation of flash pyrolysis condensates by staged condensation”. In: *Biomass and Bioenergy* 95 (2016), pp. 287–295.

[59] Qi Zhang, Jie Chang, Tiejun Wang, and Ying Xu. “Review of biomass pyrolysis oil properties and upgrading research”. In: *Energy conversion and management* 48.1 (2007), pp. 87–92.

[60] Zeban Shah, Renato Cataluña Veses, Rafaela Antunes Aguilhera, and Rosângela da Silva. “Bio-oil production from pyrolysis of coffee and eucalyptus sawdust in the presence of 5% hydrogen”. In: *International Journal of Engineering Research and Science. Bikaner. Vol. 2, no. 5 (May. 2016), p. 34-42* (2016).

[61] Saad A El-Sayed. “Chemical products yielded from different pyrolysis processes of rice waste residues: a comprehensive review”. In: *Biomass Conversion and Biorefinery* (2025), pp. 1–41.

[62] Bin Hu, Zhen-xi Zhang, Wen-luan Xie, Ji Liu, Yang Li, Wen-ming Zhang, Hao Fu, and Qiang Lu. “Advances on the fast pyrolysis of biomass for the selective preparation of phenolic compounds”. In: *Fuel Processing Technology* 237 (2022), p. 107465.

[63] Nasruddin A Abdullah, Nandy Putra, Imansyah Ibnu Hakim, and Raldi A Koestoer. “A review of improvements to the liquid collection system used in the pyrolysis process for producing liquid smoke”. In: *International Journal of Technology* 8.7 (2017), pp. 1197–1206.

[64] Haiqing Sui, Chao Tian, Huijing Deng, Zi Ming, Zhichao Zhang, Wen Fu, and Jian Li. “Separation of chemical groups from wood tar via sequential organic solvent extraction and glycerol-assisted distillation”. In: *Separation and Purification Technology* 357 (2025), p. 130019.

[65] Frederico Gomes Fonseca and Axel Funke. “Modeling of liquid–vapor phase equilibria of pyrolysis bio-oils: A Review”. In: *Industrial & Engineering Chemistry Research* 63.31 (2024), pp. 13401–13420.

[66] Y. Chai, A. Donnot, F. Aubriet, M. Grateau, R. Gadiou, and J. Lédé. “Fractional condensation of biomass pyrolysis vapors”. In: *Energy & Fuels* 28.1 (2014), pp. 508–520.

[67] G. Raimundo, J. Blin, and J. Lédé. “Fractional condensation of fast pyrolysis vapors using a packed column”. In: *Journal of Analytical and Applied Pyrolysis* 134 (2018), pp. 137–146.

[68] H Susanto, N Rokhati, AMI Filardli, MH Robbani, Q Anggraini, and T Istirokhatun. “Improving the quality of liquid smoke by filtration using membranes”. In: *Food Research* 8 (2024), pp. 136–144.

[69] MM Hasan, MG Rasul, and MMK Khan. “The effects of slow and fast pyrolysis on the yields and properties of produced bio-oils from macadamia nutshell”. In: *AIP Conference Proceedings*. Vol. 2681. 1. AIP Publishing LLC. 2022, p. 020014.

[70] Hong Tian, Tong Zhou, Zhangjun Huang, Jiawei Wang, Hua Cheng, and Yang Yang. “Integration of spent coffee grounds valorization for co-production of biodiesel and activated carbon: An energy and techno-economic case assessment in China”. In: *Journal of Cleaner Production* 324 (2021), p. 129187.

[71] Muhammad Ahsan Amjed, Filip Sobic, Matteo C Romano, Tiziano Faravelli, and Marco Binotti. “Techno-economic analysis of a solar-driven biomass pyrolysis plant for bio-oil and biochar production”. In: *Sustainable Energy & Fuels* 8.18 (2024), pp. 4243–4262.

[72] Denzel Christopher Makepa, Chido Hermes Chihobo, and Downmore Musademba. “Techno-economic analysis and environmental impact assessment of biodiesel production from bio-oil derived from microwave-assisted pyrolysis of pine sawdust”. In: *Heliyon* 9.11 (2023).

[73] Dinesh Mohan, Charles U Pittman Jr, and Philip H Steele. “Pyrolysis of wood/biomass for bio-oil: a critical review”. In: *Energy & fuels* 20.3 (2006), pp. 848–889.

[74] Stephen Joseph. *Biochar for environmental management: science, technology and implementation*. Routledge, 2015.

[75] Sharon S Chadwick. “Ullmann’s encyclopedia of industrial chemistry”. In: *Reference Services Review* 16.4 (1988), pp. 31–34.

[76] Klaus Weissermel and Hans-Jürgen Arpe. *Industrial organic chemistry*. John Wiley & Sons, 2008.

[77] Tahereh Sarchami, Neha Batta, and Franco Berruti. “Production and separation of acetic acid from pyrolysis oil of lignocellulosic biomass: a review”. In: *Biofuels, Bioproducts and Biorefining* 15.6 (2021), pp. 1912–1937.

[78] Organic Update Isocyanates. “Ullmann’s encyclopedia of industrial chemistry”. In: (1985).

[79] Roberto Rinaldi, Robin Jastrzebski, Matthew T Clough, John Ralph, Marco Kennema, Pieter CA Bruijnincx, and Bert M Weckhuysen. “Paving the way for lignin valorisation: recent advances in bioengineering, biorefining and catalysis”. In: *Angewandte Chemie International Edition* 55.29 (2016), pp. 8164–8215.

[80] Joseph J Bozell and Gene R Petersen. “Technology development for the production of biobased products from biorefinery carbohydrates—the US Department of Energy’s “Top 10” revisited”. In: *Green chemistry* 12.4 (2010), pp. 539–554.

[81] J. H. Clark, T. J. Farmer, A. J. Hunt, and J. Sherwood. “Opportunities for bio-based solvents created as petrochemical and fuel products transition towards renewable resources”. In: *International Journal of Molecular Sciences* 13.3 (2012), pp. 3159–3180. DOI: 10.3390/ijms13033159.

[82] T. Werpy and G. Petersen. *Top Value Added Chemicals from Biomass. Volume I: Results of Screening for Potential Candidates from Sugars and Synthesis Gas*. Tech. rep. NREL/TP-510-35523. Golden, CO, USA: U.S. Department of Energy, National Renewable Energy Laboratory, 2004.